

Dynamic Regulation of Function of the Mitochondrial TIM23 Preprotein Translocase

Dissertation
zur Erlangung des Doktorgrades
der Fakultät für Biologie
der Ludwig-Maximilians-Universität München

von
Dušan Popov-Čeleketić
aus
Belgrad, Serbien

München
2007

Ehrenwörtliche Versicherung

Diese Dissertation wurde selbstständig, ohne unerlaubte Hilfe erarbeitet.

München, den 8.11.2005

Tag der mündlichen Prüfung: 29. November 2007

1. Gutachter: Prof. Dr. Jürgen Soll

2. Gutachter: Prof. Dr. Manfred Schliwa

Sondergutachter: Prof. Dr. Dr. Walter Neupert

Дереву и нашему миру

TABLE OF CONTENTS

1. INTRODUCTION.....	1
1.1. PROTEIN TRAFFIC IN THE CELL.....	1
1.1.1. Targeting signals of organelle proteins.....	1
1.1.2. Protein translocases	2
1.2. BIOGENESIS OF MITOCHONDRIA	3
1.2.1. Mitochondrial targeting signals.....	4
1.2.2. Translocation, sorting, folding and assembly machineries in mitochondria.....	6
1.2.3. The TOM complex	6
1.2.4. Machineries for sorting β -barrel proteins in the outer membrane	9
1.2.5. MIA-ERV disulfide relay system	10
1.2.6. The TIM22 complex.....	11
1.2.7. Machineries for protein export	12
1.2.8. The TIM23 translocase.....	13
1.3. THE OBJECTIVE OF THIS WORK.....	17
2. MATERIAL AND METHODS	19
2.1. MOLECULAR BIOLOGY METHODS	19
2.1.1. Isolation of DNA	19
2.1.1.1. Isolation of yeast genomic DNA	19
2.1.1.2. Isolation of plasmid DNA from Escherichia coli	19
2.1.2. Amplification of DNA sequences by Polymerase Chain Reaction (PCR).....	20
2.1.3. DNA analysis and purification	21
2.1.3.1. Agarose gel electrophoresis of DNA	21
2.1.3.2. Isolation of DNA from agarose gels.....	21
2.1.3.3. Measurement of DNA concentration.....	21
2.1.4. Enzymatic manipulation of DNA	22
2.1.4.1. Digestion of DNA with restriction endonucleases.....	22
2.1.4.2. Ligation of DNA fragments.....	22
2.1.5. Transformation of electrocompetent E. coli cells.....	22
2.1.5.1. Overview of E. coli strains used.....	22
2.1.5.2. Preparation of electrocompetent cells.....	22
2.1.5.3. Transformation of E. coli cells by electroporation	23
2.1.6. Bacterial plasmids used and cloning strategies.....	23
2.1.6.1. Overview of constructs used for transcription/translation	23
2.1.6.2. Cloning strategy for Tim21 construct used in transcription/translation.....	24
2.1.6.3. Overview of plasmids used for protein expression in bacteria	24
2.1.6.4. Cloning strategies for plasmids used for protein expression in bacteria.....	24
2.1.7. Transformation of S. cerevisiae cells (Lithium-acetate method).....	25
2.1.8. S. cerevisiae strains used and cloning strategies.....	26
2.1.8.1. Overview of yeast strains used	26
2.1.8.2. Cloning strategies for generation of yeast strains by homologous recombination.....	27
2.1.8.3. Cloning strategies for plasmids used for the transformation of yeast.....	29
2.2. CELL BIOLOGY METHODS	32
2.2.1. E. Coli – media and growth	32
2.2.1.1. Media for E. coli	32
2.2.1.2. Cultivation of E. coli	32
2.2.2. S.cerevisiae – media and growth	32
2.2.2.1. Media for S.cerevisiae	32
2.2.2.2. Cultivation of S.cerevisiae.....	33
2.2.2.3. Growth of yeast strains where mitochondria with the TIM23 complex in different translocation modes are generated	34
2.2.3. Determination of the growth characteristics of yeast strains	34
2.2.4. Isolation of yeast mitochondria	34

2.2.4.1. Large scale isolation of yeast mitochondria.....	34
2.2.4.2. Isolation of crude yeast mitochondria (“fast mito prep”).....	35
2.2.5. Preparation of mitoplasts	36
2.2.6. Protease treatment and “clipping assay”	36
2.2.6.1. Protease treatment of mitochondria	36
2.2.6.2. Removal of the N-terminus of Tim23 exposed on the mitochondrial surface (“clipping assay”)	36
2.2.7. Carbonate extraction.....	37
2.3. PROTEIN BIOCHEMISTRY METHODS	37
2.3.1. Protein analysis.....	37
2.3.1.1. SDS-Polyacrylamide gel electrophoresis (SDS-PAGE)	37
2.3.1.2. Blue-Native gel electrophoresis (BNGE)	38
2.3.1.3. CBB staining of SDS-PAGE gels.....	39
2.3.1.4. Transfer of proteins onto nitrocellulose/PVDF membrane (Western-Blot).....	39
2.3.1.5. Protein quantification by autoradiography.....	40
2.3.1.6. Determination of protein concentration.....	40
2.3.2. Protein preparation	40
2.3.2.1. Trichloroacetic acid (TCA) precipitation of proteins	40
2.3.2.2. Purification of recombinant His-tagged proteins from E. coli.....	40
2.3.2.3. Purification of recombinant MBP-tagged Pam17 from E. coli.....	41
2.3.2.4. In vitro synthesis of radiolabeled mitochondrial preproteins.....	41
2.3.3. Protein experiments in organello	42
2.3.3.1. Import of radiolabeled preproteins into mitochondria	42
2.3.3.2. Generation of the TOM-TIM23-preprotein supercomplex in vitro	43
2.3.3.3. Pull down experiments with tagged proteins expressed in mitochondria	43
2.3.3.4. Crosslinking of mitochondrial proteins	43
2.4. IMMUNOLOGY METHODS.....	44
2.4.1. Generation of antibodies.....	44
2.4.1.1. Overview of generated antibodies	44
2.4.1.2. Generation of polyclonal antisera against Tim21 and Pam17 proteins.....	44
2.4.1.3. Affinity purification of antibodies against Tim21 and Pam17 proteins.....	45
2.4.2. Immunodecoration.....	46
2.4.3. Coimmunoprecipitation	47
3. RESULTS.....	48
3.1. IDENTIFICATION OF TIM21	48
3.2. TIM21 IS IMPORTED BY THE TIM23 TRANSLOCASE	50
3.3. LOCALIZATION AND TOPOLOGY OF TIM21	51
3.4. TIM21 IS A COMPONENT OF THE TIM23 COMPLEX.....	52
3.5. TIM21 BINDS TO THE TIM17-TIM23 CORE OF THE TIM23 COMPLEX.....	53
3.6. THE IMPORT MOTOR IS CONNECTED WITH THE MEMBRANE PART OF THE TIM23 COMPLEX IN TWO WAYS .	54
3.7. THE NATURE OF THE TAG AFFECTS THE ASSOCIATION OF TIM21 WITH THE REST OF THE TRANSLOCASE ...	56
3.8. TIM21 CONNECTS THE TIM23 AND THE TOM COMPLEXES	57
3.9. TIM21 IS NOT ESSENTIAL FOR YEAST CELL VIABILITY	59
3.10. DELETION OF TIM21 AFFECTS NEITHER THE FUNCTION NOR THE ASSEMBLY OF THE TIM23 COMPLEX ...	60
3.11. OVEREXPRESSION OF TIM21 CHANGES THE CONFORMATION OF THE TIM23 COMPLEX.....	62
3.12. PAM17 IS THE MAJOR CROSSLINKING PARTNER OF TIM23	64
3.13. BINDING OF TIM21 AND PAM17 TO THE TIM23 COMPLEX IS MUTUALLY EXCLUSIVE.....	65
3.14. OVEREXPRESSION OF PAM17 COUNTERACTS ADVERSE CHANGES OF THE TIM23 COMPLEX INDUCED BY THE INCREASED LEVELS OF TIM21	67
3.15. DELETION OF PAM17 LEADS TO A DEFECTIVE IMPORT OF MOTOR DEPENDENT PREPROTEINS	69
3.16. DELETION OF PAM17 CHANGES THE CONFORMATION OF THE TIM23 COMPLEX.....	71
3.17. ANALYSIS OF THE STRUCTURAL ORGANIZATION OF THE TIM23 COMPLEX DURING PROTEIN TRANSLOCATION	74
3.18. PREPROTEINS IN TRANSIT LEAD TO STRONGER ASSEMBLY OF THE TOM COMPLEX	76
3.19. BOTH Laterally sorted and matrix targeted precursors use the same pore in the TIM23 TRANSLOCASE.....	77
3.20. CHANGES IN STOICHIOMETRY OF THE TIM23 COMPLEX DURING IMPORT OF PREPROTEINS	79
3.21. CONFORMATIONAL CHANGES OF THE TIM23 TRANSLOCASE DURING IMPORT OF PREPROTEINS.....	81
3.22. TIM23 CHANGES ITS TOPOLOGY DURING IMPORT OF PREPROTEINS.....	85
3.23. THE TIM23 TRANSLOCASE IS A SINGLE ENTITY.....	86
3.24. THE TIM23 COMPLEX REACTS TO SPECIFIC MUTATIONAL ALTERATIONS OF THE TOM COMPLEX.....	90

4. DISCUSSION	94
5. SUMMARY	106
6. LITERATURE	108
ABBREVIATIONS	120
PUBLICATIONS RESULTING FROM THIS THESIS	123
ACKNOWLEDGEMENTS	124
CURRICULUM VITAE	125

1. INTRODUCTION

1.1. Protein traffic in the cell

Eukaryotic cells contain intracellular membranes that create specialized aqueous compartments, known as organelles. Lipid bilayers, the main component of organelle membranes, are impermeable for proteins and other solutes. The biogenesis and function of organelles therefore relies on the transport of proteins between distinct subcellular compartments.

1.1.1. Targeting signals of organelle proteins

Proteins follow specific pathways from the cytosol, where they are synthesized, to the place where they function. Proteins that function in the cytosol usually remain there after they are synthesized. All other proteins contain intrinsic signals in their amino acid sequences that are necessary and sufficient to target them to the pertinent organelle (Blobel, 1980).

Targeting and sorting signals are present as sequences at the ends of the polypeptide chain, but they can also be located internally. Signals are made up by a contiguous stretch of amino acids, usually 15–60 residues long. They are often removed from the protein by specialized signal peptidases once the transport process is initiated or completed. Signal sequences are specific for preproteins targeted to mitochondria, the endoplasmic reticulum (ER), chloroplasts, and peroxisomes, and for proteins that are exported from the nucleus to the cytosol (Horwich, 1990; Von Heijne, 1990). Internal targeting signals are made up by one or several short stretches of amino acid residues that are distant from one another. Some internal targeting signals are characterized by hydrophobic regions or by residues flanking these regions, whereas some form specific regions in the protein tertiary structure. These signals are typical for enzymes targeted to lysosomes (Breitfeld *et al.*, 1989), but they can also be present in preproteins targeted to other organelles. Signal sequences and internal targeting signals are recognized by receptors that are coupled with or are constitutive parts of protein translocases, oligomeric membrane complexes that mediate protein translocation across, or integration into, the membrane (Walter and Lingappa, 1986).

1.1.2. Protein translocases

Protein translocases or translocons translocate proteins from one compartment to another; that is from one compartment of an organelle to another or from one subcellular compartment to another. These complexes are also the ways for exporting proteins from the cell or for importing proteins into the cell from the extracellular space. All translocons contain intrinsic signal recognition sites for the targeting signals of translocation substrates that target polypeptides from their site of synthesis (*cis* compartment) to the translocon. Translocons mediate transport of polypeptides from the *cis* compartment to their destination (*trans* compartment) by formation of selectively permeable protein-conducting channels (Schatz and Dobberstein, 1996). Translocation channels usually remain impermeable for other molecules, even the smallest ones, during the translocation of polypeptides. The translocation process requires energy that is in most cases provided from electrochemical gradient and by association of molecular chaperones with the polypeptide in the *trans* compartment.

The translocons can be divided in two main groups, depending on the folded state of their protein substrates. The nuclear pore complex, protein import system in peroxisomes, and the TAT translocation systems in bacteria and chloroplast thylakoids are able to transfer fully folded proteins across the membrane. The nuclear pore complex (NPC) mediates both protein and RNA traffic between nucleus and cytosol. Although NPC is constantly assembled in the membrane, certain regions of this large complex are remodeled during this process, indicating that NPC is more dynamic than previously assumed (King *et al.*, 2006; Melcak *et al.*, 2007). On the other hand, peroxisomal import system and the TAT translocase assemble at the site of translocation in response to the size of the protein substrate docked at the membrane and disassemble upon translocation to minimize the free diffusion of molecules across the channel and to maintain the membrane permeability barrier of the organelle (Berks *et al.*, 2000; Cline and Mori, 2001; Gould and Collins, 2002). These two complexes belong to the group of signal assembled translocons (Schnell and Hebert, 2003). It was recently suggested that some other translocons that transport unfolded proteins, like the Derlin1-VIMP retrotranslocon (Ye *et al.*, 2005) and even the TIM23 translocase (Chacinska *et al.*, 2005), partially assemble upon their interaction with the protein substrate, but these challenging views are yet to be confirmed by at least one more research group.

The majority of the translocons in the cell exists in the assembled form within the membrane and translocates nascent or newly synthesized polypeptides in a largely unfolded conformation. These complexes are also termed signal-gated translocons as the translocation

occurs through a signal-gated protein conducting channel with the help of molecular chaperones (Schnell and Hebert, 2003). The paradigm of such a process is translocation across the bacterial periplasmic, ER, and thylakoid membranes by SecYEG, Sec61 and cpSec complexes, respectively (Johnson and van Waes, 1999; Manting and Driessen, 2000; Mori and Cline, 2001). The SecYEG/61 system translocates proteins in two ways: cotranslationally, when translocation is coupled with protein synthesis, and posttranslationally, when proteins are translocated after synthesis is complete (Osborne *et al.*, 2005). The most recently discovered translocation system, Derlin1-VIMP, also resides in the ER and is responsible for export of misfolded proteins (Lilley and Ploegh, 2004; Ye *et al.*, 2004). In mitochondria and chloroplasts that contain multiple membranes different translocons work in sequence to transfer and sort proteins in different organelle subcompartments (Neupert and Herrmann, 2007; Soll and Schleiff, 2004).

The vectorial translocation across the membranes is the only pathway all soluble proteins undergo. Preproteins containing hydrophobic stretches or transmembrane (TM) domains can be vectorially translocated through the channel, but, eventually, they need to be sorted in the membrane via the following or even the same translocon (Herlan *et al.*, 2003; Johnson and van Waes, 1999; Neupert and Herrmann, 2007). Some translocons, like the TIM22, the TOB, and the OXA1 complexes in mitochondria, are specialized in membrane integration of this type of proteins, but they are not able to vectorially translocate proteins across the lipid bilayer. Yet, some translocons are able to sort both the membrane and soluble proteins, thereby transferring polypeptides in more than one direction. The evidence for multifunctional nature of the translocon are delivered for the Sec61 complex (Johnson and van Waes, 1999), and the TOM and the TIM23 complexes in mitochondria (Neupert and Herrmann, 2007); membrane integration along vectorial translocation was also suggested to occur in the TIC complex in chloroplasts (Schnell and Hebert, 2003). Therefore, these translocons should have dynamic translocation channel that can oscillate between the aqueous pore for translocation of soluble preproteins and the channel laterally opened in the lipid bilayer for integration of membrane proteins. However, a clear view on how these complexes alternate between the translocation and the integration modes is not available up to date.

1.2. Biogenesis of mitochondria

Mitochondria are essential organelles involved in many cellular processes including cellular respiration and energy production, lipid metabolism, free radical production, biosynthesis of

heme and iron-sulfur (Fe-S) clusters, and apoptosis. Depending on the organism, between 800 and 1500 different proteins (Sickmann *et al.*, 2003; Taylor *et al.*, 2003; Werhahn and Braun, 2002) are specifically distributed within the four subcompartments of mitochondria: outer membrane, highly convoluted inner membrane, intermembrane space (IMS) – the compartment between the two membranes, and the matrix. Although mitochondria have a complete system for protein synthesis, almost all mitochondrial proteins are encoded in nuclear DNA and synthesized in cytosol. Upon the termination of translation precursors of mitochondrial proteins, also termed preproteins, are released from the ribosomes in the cytosol and then imported into mitochondria in a posttranslational manner (Neupert and Herrmann, 2007). There are several observations that suggest the contribution of a cotranslational import to the biogenesis of mitochondria (Karniely *et al.*, 2006; Marc *et al.*, 2002; Regev-Rudzki *et al.*, 2005), but the definite evidence is still lacking. In the cytosol, newly synthesized preproteins interact with chaperones Hsp70 and Hsp90 that prevent their degradation and aggregation (Mihara and Omura, 1996; Young *et al.*, 2003). Preproteins in complex with cytosolic chaperones are then delivered to receptors in the outer membrane of mitochondria, which recognize different signals for targeting and sorting of preproteins.

1.2.1. Mitochondrial targeting signals

A typical mitochondrial targeting signal is encoded in the N-terminal presequence that is removed upon the import of the protein into mitochondria (Roise and Schatz, 1988). The presequence is also called matrix targeting sequence (MTS) because it is a prerogative for bringing the N-terminus across the inner membrane into the matrix. MTS consists of about 10–80 amino acid residues with a number of positive and hydroxylated charges, and a few, if any, negatively charged residues. The primary sequences of MTSs show no homology even between closely related orthologs, but their conserved feature is the ability to form an amphipathic helix with one hydrophobic and one positively charged side. Several computer algorithms were developed for *in silico* analysis of mitochondrial proteins based on MTS (Habib *et al.*, 2007a).

Upon the import into the matrix, presequences are usually cleaved by the mitochondrial processing peptidase (MPP) (Braun *et al.*, 1992). Matrix proteins rhodanese, 3-oxo-CoA-thiolase, and Hsp10 are synthesized with non-cleavable MTSs, which show no obvious differences to the cleavable ones (Hammen *et al.*, 1996; Jarvis *et al.*, 1995; Waltner and Weiner, 1995). DNA helicase Hmil is so far the only identified protein with the MTS-like

targeting signal at its C-terminus (Lee *et al.*, 1999). This preprotein appears to be imported in the reverse orientation, as placing targeting signals at the C-terminus of passenger proteins leads to the import in C to N direction (Fölsch *et al.*, 1998).

Precursors of a number of proteins residing in the inner membrane and the IMS, contain N-terminal presequence followed by hydrophobic (“stop-transfer”) sorting signal that may be responsible for the arrest and the lateral insertion of these preproteins in the inner membrane (Beasley *et al.*, 1993; Glick *et al.*, 1992b; Neupert and Herrmann, 2007). In some cases these hydrophobic sorting sequences are cleaved off at the outer surface of the inner membrane by specialized peptidases, thereby releasing a mature protein in the IMS (Glick *et al.*, 1992a). Not all MTS-containing inner membrane precursors are arrested in the membrane, but instead undergo so called conservative sorting pathway. These preproteins are completely imported into the matrix, and then exported in the inner membrane (Stuart, 2002). The distinction between the proteins going via the “stop-transfer” and the conservative sorting pathway apparently lies in the presence of proline residues in hydrophobic stretches, which strongly disfavor the translocation arrest of the TM domain and favor the transfer of preproteins to the matrix (Beasley *et al.*, 1993; Meier *et al.*, 2005b). Some inner membrane proteins, like Bcs1, Tim14, and Mdj2 do not contain N-terminal presequence, but instead they have a hydrophobic sorting signal followed by an internal MTS-like sequence. It was proposed that these two stretches within the preprotein sequence form hairpin loops during import thereby mimicking the amphipatic structures of a typical MTS (Fölsch *et al.*, 1996).

Mitochondrial proteins from all mitochondrial subcompartments that do not have cleavable N-terminal presequence contain internal targeting signals present in the sequences of mature proteins. The targeting of some proteins that span the outer membrane only once is dependent on the presence of positive charges either at the N-terminus or flanking their transmembrane domains. The targeting signals of outer membrane β -barrel proteins are, however, completely unknown. Small IMS proteins do not contain MTS, but instead a specific pattern of cysteine residues that enables their trapping and folding in the IMS (Herrmann and Hell, 2005). Proteins of the metabolite carrier family of the inner membrane contain multiple signals distributed over the entire length of the preprotein, mostly in regions around the three pairs of hydrophobic transmembrane segments (Endres *et al.*, 1999; Koehler, 2004). Some other precursors of proteins in the inner membrane, like Tim17, Tim22, and Tim23, contain similar internal targeting and sorting signals that include hydrophobic segments and positively charged loops (Kaldi *et al.*, 1998; Paschen and Neupert, 2001).

1.2.2. Translocation, sorting, folding and assembly machineries in mitochondria

Correct recognition and intramitochondrial sorting of preproteins depends on a coordinated action of complex molecular machineries present in all mitochondrial subcompartments: the TOM (*translocase of the outer membrane*) and the TOB (*translocase of outer membrane β -barrel proteins*) complexes in the outer membrane, MIA-ERV system in the IMS and the TIM23, the TIM22 (*translocase of the inner membrane*), and the OXA1 (*oxidase assembly*) complexes in the inner membrane. The action of these machineries is intertwined and a protein going to its final destination may serve as a substrate for more than one of these machineries. In addition, although some of these molecular machines may be responsible for only one type of substrate, e.g. the TIM22 translocase, some import and sort preproteins in several directions, like the TOM and the TIM23 complexes. In addition, components of one system (small Tim proteins and the TOM complex) may be involved in import of proteins in both membranes. Finally, protein constituents of one translocase often demand another translocase for their own import. Thus the interplay of these molecular machines represents a translocation network responsible for the biogenesis of mitochondria (Figure 1.1).

1.2.3. The TOM complex

The TOM complex is the major translocase of the mitochondrial outer membrane responsible for initial steps of import of mitochondrial preproteins synthesized in cytosol that are targeted to all four subcompartments of mitochondria. Strongly associated subunits: the pore forming β -barrel protein Tom40, receptor Tom22, and small proteins Tom5, Tom6, and Tom7 form the general import pore (GIP) or the TOM_{core} complex. Receptors Tom20 and Tom70 loosely associate with the TOM_{core} complex forming the TOM_{holo} complex (Ahting *et al.*, 1999; van Wilpe *et al.*, 1999). The assembly of the TOM_{core} complex occurs via two assembly intermediate complexes and requires concerted action of the TOM and the TOB complexes (Model *et al.*, 2001; Sherman *et al.*, 2006).

The TOM complex accepts preproteins on the cytosolic or *cis* side of the membrane, translocates them through the hydrophilic pore, then interacts with them on the IMS or *trans* side and, in coordinated action with other protein transport machineries, mediates their sorting in the adequate mitochondrial subcompartment. The receptors on the *cis* side can interact with the cytosolic chaperones and are responsible for the specific initial recognition of preproteins with various targeting signals. Tom20 is the main receptor for preproteins with N-terminal

Upon the interaction either with Tom20 or Tom70 the preprotein is transferred to Tom22 which then, with the help of Tom5, leads the translocation on the *cis* side of the translocation pore, transferring the preprotein to the channel formed by Tom40 (Dietmeier *et al.*, 1997; van Wilpe *et al.*, 1999). The TOM complex was proposed to contain six Tom40 molecules that form two to three protein conducting channels. Each channel is formed by Tom40 dimer and, with the diameter of 22 Å, is wide enough to allow the passage of two α -helices (Ahting *et al.*, 2001; Ahting *et al.*, 1999; Kunkele *et al.*, 1998; Schwartz and Matouschek, 1999), whereas larger folded proteins like dihydrofolate reductase (DHFR) are not able to pass (Eilers and Schatz, 1986; Rassow *et al.*, 1989; Wienhues *et al.*, 1991). The vectorial translocation of the presequence containing preproteins across the outer membrane is driven by the increase in the binding affinity of the presequence for sites in the channel that, in addition, assists in unfolding of the preprotein on the *cis* side of the complex (Komiya *et al.*, 1998; Mayer *et al.*, 1995; Rapaport *et al.*, 1998). Small proteins Tom6 and Tom7 are also embedded in the membrane, and function as antagonistic regulators of the stability of the TOM complex, the role that was recently also assigned to Tom5 (Dekker *et al.*, 1998; Schmitt *et al.*, 2005). The deletion of any of the small proteins is tolerable in fungi and only triple deletion of Tom5, Tom6, and Tom7 was found to be lethal in *N. crassa*, corroborating the notion that these three proteins have partially overlapping functions (Sherman *et al.*, 2005). After its translocation through the pore, the preprotein is accepted at the *trans* binding site formed by IMS exposed domains of Tom22, Tom40, and Tom7 (Court *et al.*, 1996; Esaki *et al.*, 2004; Moczko *et al.*, 1997; Rapaport *et al.*, 1997).

There are at least six different pathways that preproteins follow after the initial interaction with the TOM complex and, with few exceptions, they all require coordinated action of the TOM complex with other mitochondrial translocation machineries. Coordinated action of the TOM complex with the TIM23 translocase leads to (i) translocation of presequence containing preproteins either into the matrix or (ii) their insertion in the inner membrane. (iii) Small IMS proteins with conserved patterns of cysteine residues are accepted on the *trans* side of the TOM complex by MIA-ERV relay system whereas (iv) polytopic proteins of the carrier family are accepted by the small Tim proteins and conveyed to the TIM22 complex that inserts them in the inner membrane. Small Tim proteins also play a role in accepting (v) precursors of the β -barrel proteins which are subsequently inserted in the outer membrane via the TOB complex. Finally, (vi) N-terminally anchored outer membrane proteins require the TOM complex, but they do not use a protein conducting channel for their insertion in the lipid bilayer. Together with reports that it distinguishes between the protein substrates destined to

the various subcompartments (Esaki *et al.*, 2003; Gabriel *et al.*, 2003), these data show that the TOM complex, although usually referred to as the GIP, is not a passive pore in outer membrane, but it has an active role in sorting and translocating preproteins through intensive coordinated actions with other translocation machineries in mitochondria.

1.2.4. Machineries for sorting β -barrel proteins in the outer membrane

Membrane proteins composed of antiparallel transmembrane β -strands connected by soluble loop regions are known as β -barrel proteins (Schulz, 2000; Wimley, 2003). In prokaryotes these proteins are found in the outer membrane of Gram-negative bacteria (Tamm *et al.*, 2001; Wimley, 2003). In eukaryotic cells β -barrel proteins are present in the outer membranes of mitochondria and chloroplasts (Rapaport, 2003; Schleiff and Soll, 2005), reflecting the endosymbiotic origin of these organelles (Margulis, 1970). The riddle of how β -barrel proteins are inserted and assembled in the outer membrane was solved recently with the discovery of the translocase of outer membrane β -barrel proteins or the TOB (SAM) complex (Paschen *et al.*, 2003; Wiedemann *et al.*, 2003).

Upon their translocation through the TOM complex precursors of β -barrel proteins interact with small Tim proteins in the IMS (Hoppins and Nargang, 2004; Wiedemann *et al.*, 2004) which guide them to the TOB complex. The TOB complex of ca. 250 kDa consists of the central component Tob55 (Sam50) (Kozjak *et al.*, 2003; Paschen *et al.*, 2003) and hydrophilic proteins Tob38 (Tom38/Sam35) (Ishikawa *et al.*, 2004; Milenkovic *et al.*, 2004; Waizenegger *et al.*, 2004) and Mas37 (Wiedemann *et al.*, 2003). Tob55 is a β -barrel protein essential for viability in yeast cells with homologous proteins, not only throughout the entire eukaryotic kingdom but also in the outer membrane of Gram-negative bacteria (Omp85/YaeT) (Gentle *et al.*, 2004; Voulhoux *et al.*, 2003; Wu *et al.*, 2005). Tob55 is anchored in the outer membrane by C-terminal domain with 14-16 transmembrane β sheets. Hydrophilic N-terminus is exposed in the IMS forming characteristic polypeptide translocation associated (POTRA) domain (Sanchez-Pulido *et al.*, 2003). This domain accepts the incoming β -barrel precursors, presumably from small Tim proteins, and transfers them to the membrane part of the complex for the subsequent sorting in the lipid bilayer (Habib *et al.*, 2007b). Tob38 and Mas37 are peripheral outer membrane proteins exposed to the cytosol. Although deletion of *MAS37* gene leads to impaired import of β -barrel proteins, it does not stop the growth of yeast cells. On the

other hand, Tob38 is an essential protein that forms the core of the complex with Tob55 even in the absence of Mas37 (Habib *et al.*, 2005; Waizenegger *et al.*, 2004).

Recently a protein that selectively affects the assembly of Tom40, but not other β -barrel proteins, was identified and named Mim1 or Tom13. Mim1 is the component neither of the TOM nor the TOB complex, but it forms a separate high molecular weight complex of 180 kDa and acts in the later stages of the assembly of the TOM complex between the assembly intermediate II and the mature TOM complex (Ishikawa *et al.*, 2004; Waizenegger *et al.*, 2005). The separation of β -barrel proteins sorting pathway on general and Tom40-specific seems to require the activity of Tom7 and proteins involved in the maintenance of mitochondrial morphology Mdm10, Mdm12, and Mmm1 (Meisinger *et al.*, 2007; Meisinger *et al.*, 2004; Meisinger *et al.*, 2006).

1.2.5. MIA-ERV disulfide relay system

MIA-ERV disulfide relay system is responsible for the import and folding of small (6 – 22 kDa) IMS proteins through oxidation of their cysteine residues. Mia40 (Tim40) was the first identified component of this system. Homologs of Mia40 are present from yeast to human with a highly conserved C-terminal domain of ca. 60 amino acid residues containing six cysteines (CPC-Cx₉C-Cx₉C) that appear to form three intramolecular disulfide bonds (Chacinska *et al.*, 2004; Hofmann *et al.*, 2005; Naoe *et al.*, 2004; Terziyska *et al.*, 2005). Only in fungi this domain is anchored in the inner membrane by N-terminal hydrophobic stretch, which is not essential for yeast cell viability. Erv1 is a sulfhydryl oxidase consisting of the flexible N-terminal domain with conserved CxxC motif and the FAD-binding domain on C-terminus, which contains another CxxC motif (Coppock and Thorpe, 2006; Hofhaus *et al.*, 2003).

All the substrates sorted via MIA-ERV system lack presequences but have conserved cysteine residues mostly presented either as twin Cx₃C motif or as Cx₉C motif. In their unfolded state small preproteins are able to diffuse through the pore of the TOM complex in both directions. When, however, they fold on the *trans* side of the outer membrane through the formation of the intramolecular disulfide bridges, they cannot go back through the pore (Lutz *et al.*, 2003). Upon traversing the outer membrane, unfolded preproteins interact with oxidized Mia40 forming mixed disulfide bonds. These bonds are then conveyed from Mia40 to the imported preproteins releasing them into the IMS in an oxidized and folded state, whereas Mia40 remains in its reduced, inactive state. Erv1 oxidizes and reactivates Mia40 which is then ready

to accept new preprotein. This way Mia40 and Erv1 form a disulfide relay system that retains small proteins in the IMS by oxidative folding mechanism (Mesecke *et al.*, 2005). In addition, two or more proteins are likely linked to this system. Hot13 influences the assembly and the activity of the small Tim proteins in the IMS (Curran *et al.*, 2004). Also, Erv1 needs to be reoxidized to reenter the relay system and this is presumably performed by cytochrome c (Allen *et al.*, 2005), which may then deliver electrons to the final acceptor, oxygen.

1.2.6. The TIM22 complex

The TIM22 complex is responsible for the insertion into the inner membrane of hydrophobic proteins with multiple transmembrane segments, such as Tim17, Tim22, Tim23, and the members of metabolite carrier proteins family. Carrier preproteins, like ADP/ATP translocator (AAC) are translocated across the outer membrane in a specific hairpin-loop conformation and are accepted on the *trans* side of the TOM complex by the small Tim proteins (Koehler *et al.*, 1999). The sequences of the small Tim proteins contain twin C_x3C motif that is required for their helix-loop-helix organization and the formation of hexameric structures. Whereas the only firmly proven substrate of non-essential 70 kDa Tim8-Tim13 complex is the precursor of Tim23, the essential 70 kDa Tim9-Tim10 complex is required for the transport of both Tim23 and precursors of carrier proteins (Davis *et al.*, 2007; Davis *et al.*, 2000; Paschen *et al.*, 2000; Vasiljev *et al.*, 2004). The small Tim proteins function in a chaperone-like manner to prevent aggregation of the hydrophobic precursors in the aqueous environment and to translocate them from the outer membrane to the TIM22 complex, similar to their role in facilitating the transfer of β -barrel preproteins from the TOM to the TOB complex. Structural analysis revealed that the Tim9–Tim10 complex has six-blade α -helical propeller structure that resembles jellyfish with 12 flexible tentacles, which may shield hydrophobic regions of carrier proteins en route from the *trans* side of the TOM complex to the TIM22 complex (Webb *et al.*, 2006).

The 300 kDa TIM22 complex consists of the core component Tim22 with associated transmembrane proteins Tim18 and Tim54, and the small proteins Tim9, Tim10, and Tim12. The peripheral part, which consists of the 70 kDa Tim9-Tim10-Tim12 subcomplex, associates with the membrane part of the complex on the IMS side (Koehler, 2004; Neupert and Herrmann, 2007). Tim22 is the central component of the complex and may insert preproteins even in the absence of Tim18 and Tim54, but with reduced efficiency (Kovermann *et al.*, 2002). Two pores formed by Tim22 molecules, each with a diameter of 16 Å, cooperate

during protein transport using the membrane potential across the inner membrane ($\Delta\Psi$) as a sole energy source (Rehling *et al.*, 2003).

1.2.7. Machineries for protein export

Insertion of all polytopic proteins encoded in mitochondrial DNA and a number of nuclear encoded proteins from matrix into the inner membrane, is usually referred to as mitochondrial protein export. Yeast mitochondrial genome encodes eight proteins, seven of which are highly hydrophobic membrane proteins: cytochrome b (Cytb) of the bc_1 -complex, Cox1, Cox2, and Cox3 of the cytochrome oxidase and Atp6, Atp8, and Atp9 of the F_1F_0 -ATPase (Borst and Grivell, 1978; Grivell *et al.*, 1999; Tzagoloff and Myers, 1986). The insertion of these proteins in the inner membrane goes via the OXA1 translocase (Hell *et al.*, 2001). Oxa1 is the mitochondrial representative of the Oxa1/YidC/Alb3 family of related proteins that mediate the insertion of substrate proteins into the membranes of bacteria, chloroplasts, and mitochondria (Kuhn *et al.*, 2003; Stuart, 2002). Oxa1 spans the inner membrane five times, exposing into the matrix a long α -helical coiled-coil C-terminal domain that binds mitochondrial ribosomes (Jia *et al.*, 2003; Szyrach *et al.*, 2003). The ability of this domain to bind mitochondrial ribosomes, as well as observed interactions of Oxa1 with newly synthesized mitochondrial proteins (Hell *et al.*, 2001) suggests the cotranslational integration of hydrophobic proteins into the lipid bilayer. Ribosomal docking is mediated both by hydrophilic C-terminus of Oxa1, and by Mba1 (Ott *et al.*, 2006). Mba1 is an additional component of the mitochondrial export machinery that shares substrate specificity with Oxa1 but can either cooperate with or function independently of Oxa1 (Preuss *et al.*, 2001). Several presequence-carrying transmembrane proteins, including Oxa1, are imported into the matrix via the TIM23 translocase from where they are inserted into the inner membrane via the export machinery (Hell *et al.*, 2001). This pathway resembles insertion reactions of polytopic membrane proteins of bacterial origin and has been termed the conservative sorting pathway (Stuart, 2002).

Two proteins, Cox18 in *Saccharomyces cerevisiae* (Souza *et al.*, 2000) and Oxa2 in *Neurospora crassa* (Funes *et al.*, 2004), are also involved in the export process coupled with the assembly of the cytochrome oxidase. Both proteins share sequence homology with Oxa1, but lack the α -helical C-terminal ribosome-binding domain. In addition, it was recently proposed that Mdm38, protein first found involved in the maintenance of mitochondrial morphology (Dimmer *et al.*, 2002) is involved in the alternative machinery for insertion of

Cytb and Atp6, proteins that are not strictly dependent on the OXA1 translocase activity (Frazier *et al.*, 2006).

1.2.8. The TIM23 translocase

The TIM23 complex is the main translocase in the inner membrane of mitochondria. It is the entrance gate for all preproteins destined for the matrix, a vast majority of preproteins targeted for the inner membrane and a number of preproteins that end up soluble in the IMS. The majority of preproteins imported via the TIM23 translocase contain cleavable N-terminal matrix targeting sequence (MTS). The import is driven by the energy of ATP and the difference in membrane potential across the inner membrane ($\Delta\psi$). $\Delta\psi$ is necessary for the translocation of the positively charged residues of the MTS on the matrix side of the translocase. Further import of the preprotein requires the energy from ATP hydrolysis by mtHsp70.

The TIM23 translocase is traditionally subdivided into two sectors: membrane embedded part and the import motor. Membrane embedded part of the complex contains the receptor Tim50 and the translocation channel formed by Tim23 and Tim17. The import motor consists of Tim44, chaperone mtHsp70 with several of its cochaperones: Tim14, Tim16, and Mge1 (Figure 1.2) (Neupert and Herrmann, 2007).

Tim50 is the main receptor for incoming polypeptides emerging from the TOM complex. It exposes its large C-terminal domain in the IMS, whereas a transmembrane domain in its N-terminal part serves as the anchor in the inner membrane. The IMS domain of Tim50 interacts with preproteins which are only partially translocated through the TOM complex, and transfers them to the translocation channel of the TIM23 complex (Geissler *et al.*, 2002; Mokranjac *et al.*, 2003a; Yamamoto *et al.*, 2002).

The membrane embedded core of the complex is formed by Tim17 and Tim23. Both proteins share the same topology with four transmembrane segments and N- and C-termini facing the IMS. Their sequences are significantly similar, yet not interchangeable (Emtage and Jensen, 1993; Ryan *et al.*, 1998; Ryan *et al.*, 1994). Tim23 contains an additional domain in the IMS. The N-terminal segment of Tim23 (amino acid residues 1-50) spans the outer membrane and is exposed at the surface of mitochondria. It was suggested that this protrusion of the outer membrane plays a role in the positioning of the TIM23 complex in proximity of the outer membrane and the TOM complex (Donzeau *et al.*, 2000), but this hypothesis was questioned

by another research group (Chacinska *et al.*, 2003). Amino acid residues 50-100 contain an essential coiled-coil domain, critical for dimerization of Tim23 and for substrate binding (Bauer *et al.*, 1996). This domain of Tim23 was also shown to interact with Tim50. This interaction seems to be crucial for exposure of the N-terminus of Tim23 on the surface of mitochondria, as in mitochondria depleted of Tim50 the N-terminus of Tim23 apparently remains in the IMS (Yamamoto *et al.*, 2002). Recombinant Tim23 is able to form cation-selective channel after reconstitution in planar bilayers, which led to speculations that the C-terminus of Tim23 forms protein conducting channel of the TIM23 translocase also *in vivo* (Truscott *et al.*, 2001). The estimated size of the channel formed by Tim23 monomer is, however, significantly smaller than diameter of DNA helix that can be imported into mitochondria if fused to MTS (Vestweber and Schatz, 1989). In addition, recent electrophysiological measurements suggest that the protein conducting channel has a twin-pore structure (Martinez-Caballero *et al.*, 2007). Hence, one cannot exclude the role of transmembrane segments of Tim17 in formation of the protein conducting channel. The N-terminal part of Tim17 exposed in the IMS is much shorter compared to Tim23 (11-14 amino acid residues), but still essential for cell viability. Conserved negatively charged residues in this stretch were proposed to be critical for channel gating at the IMS (Meier *et al.*, 2005a), possibly with the assistance of the C-terminal domain of Tim50 (Meinecke *et al.*, 2006).

The import motor is associated with the membrane embedded part on the matrix side. It consists of five proteins: Tim44, mtHsp70, Mge1, Tim14, and Tim16, which in a coordinated action facilitate vectorial threading of a preprotein into the matrix. Tim44 is a peripheral membrane protein associated with the matrix side of the import channel and can be partially coisolated with the Tim17-Tim23 core (Moro *et al.*, 1999). The association with the membrane presumably occurs via the C-terminus of Tim44 (Josyula *et al.*, 2006). Tim44 is a docking site for mtHsp70, the ATP-consuming subunit of the complex. MtHsp70 cycles between ATP and ADP bound states which correspond to its low and high affinity states for preproteins, respectively. When ATP is bound to N-terminal ATPase domain of mtHsp70, C-terminal peptide binding domain is open and the preproteins are easily bound but also released. Upon ATP hydrolysis, peptide binding domain closes and preproteins are tightly held. Binding of preprotein releases mtHsp70 from Tim44 (Liu *et al.*, 2003). Mge1, a mitochondrial homolog of the bacterial GrpE nucleotide exchange factor, mediates the release of ADP and thereby the dissociation of the mtHsp70 from the preprotein (Westermann *et al.*, 1995). Tim44 allows two mtHsp70 molecules to bind to the translocating preprotein at the

exit of the channel in a hand-over-hand manner, which leads to stepwise vectorial translocation of the whole preprotein into the matrix (Neupert and Brunner, 2002).

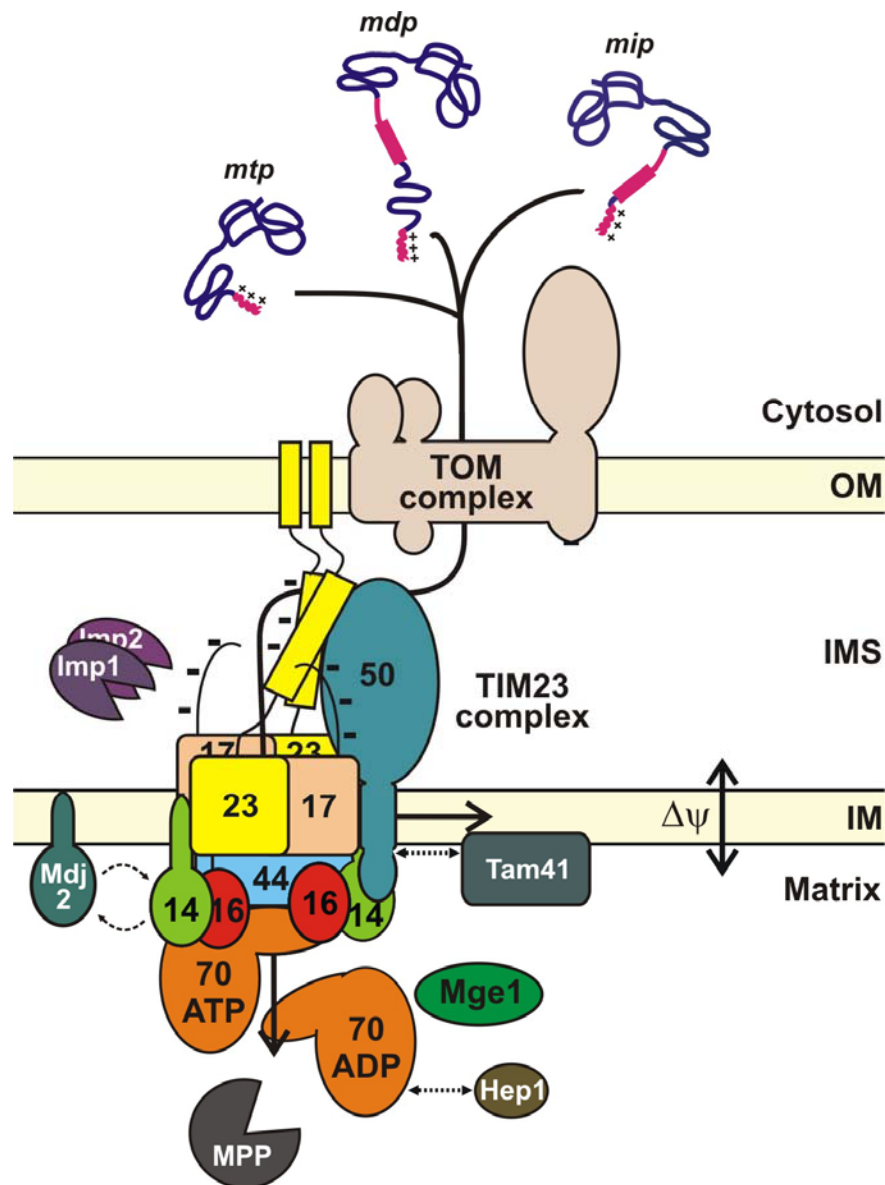


Figure 1.2. The TIM23 translocase and associated proteins. Preproteins with positively charged N-terminal presequence (magenta) synthesized in cytosol are imported into mitochondria through the concerted action of the TOM complex in the outer membrane (OM) and the TIM23 translocase in the inner membrane (IM) in a membrane-potential ($\Delta\Psi$) and ATP-dependent manner. The membrane embedded part of the TIM23 translocase contains receptor Tim50 and the channel formed by Tim23 and Tim17. The import motor formed by Tim44, mtHsp70, J-protein Tim14, J-like protein Tim16 and nucleotide exchange factor Mge1 is responsible for translocation of all matrix targeted preproteins (*mtp*) through ATP-based cycles. The TIM23 translocase also mediates the lateral insertion of preproteins containing additional hydrophobic stop-transfer signal (magenta). Some of these preproteins require the presence of ATP in the matrix for their import (motor dependent preproteins – *mdp*) and some are inserted with no apparent activity of the import motor (motor independent preproteins – *mip*). All proteins that are not components of the TIM23 complex are labeled with white letters. The maturation of preproteins requires proteolytic steps involving mitochondrial processing peptidase (MPP) and, in the case of some intermembrane space (IMS) proteins, inner membrane peptidase (Imp1-Imp2). Tam41 and Hep1 are not constituents of the TIM23 translocase but are required for its optimal functioning, whereas J-protein Mdj2 can substitute Tim14 in certain conditions.

All members of Hsp70 proteins family require J-protein cofactors for their function. Tim14 (Pam18) is a DnaJ homolog that stimulates the ATPase activity of mtHsp70 (D'Silva *et al.*, 2003; Mokranjac *et al.*, 2003b; Truscott *et al.*, 2003). Tim14 is forming a stable subcomplex with the J-like protein Tim16 (Pam16) (Frazier *et al.*, 2004; Iosefson *et al.*, 2007; Kozany *et al.*, 2004). Initial results suggest that the Tim14-Tim16 subcomplex associates with the membrane part of the TIM23 translocase via Tim44 (Kozany *et al.*, 2004), whereas more recent data point to a direct interaction of Tim14 with Tim17 (Chacinska *et al.*, 2005). The nature of association of the Tim14-Tim16 subcomplex with the Tim17-Tim23 core remains a matter of debate. Tim16 cannot stimulate the activity of mtHsp70, but in turn it acts as an antagonist of Tim14 (D'Silva *et al.*, 2005; Li *et al.*, 2004). The crystal structure of the Tim14-Tim16 subcomplex revealed the structural basis of this interaction and showed that Tim16 keeps Tim14 in a constrained conformation that is apparently not able to stimulate the ATPase activity of mtHsp70 (Mokranjac *et al.*, 2006). This crystal structure is in agreement with previously obtained biochemical data, i.e. ATP-dependent crosslinking patterns of Tim14 and Tim16 with mtHsp70 and Tim44 (Kozany *et al.*, 2004; Mokranjac *et al.*, 2003b). In addition, yeast cells contain a close homolog of Tim14, Mdj2. Mdj2 also forms a complex with Tim16, yet less stable, and stimulates the ATPase activity of mtHsp70 to the same extent as Tim14 (Mokranjac *et al.*, 2005). Cells in which the *MDJ2* gene was deleted show no obvious growth defect, yet Mdj2 is a functional J protein (Westermann and Neupert, 1997).

Two models were proposed to explain the mechanism by which mtHsp70 generates the vectorial movement of the translocating preprotein, the Brownian ratchet and the power stroke model. The Brownian ratchet mechanism suggests that a preprotein oscillates randomly in the translocation channel due to Brownian motion. After an inward sliding of a preprotein, mtHsp70 traps a segment of the polypeptide chain, at the same time blocking retrograde sliding. Complete import of the precursor is performed after a series of such events (Neupert and Brunner, 2002). According to the power stroke model, ATP hydrolysis leads to a conformational change of membrane-bound Hsp70 generating a mechanical force that pulls the preprotein into the matrix (Matouschek *et al.*, 2000). Although a large body of evidence is presented in favor of the Brownian ratchet model (Ainavarapu *et al.*, 2005; Liu *et al.*, 2003; Okamoto *et al.*, 2002; Sato *et al.*, 2005; Ungermann *et al.*, 1994), one cannot exclude the possibility that mtHsp70 can exert a minor force. This force is not sufficient to mechanically pull the preprotein into the matrix, but may reduce its conformational freedom thereby accelerating the import process (De Los Rios *et al.*, 2006; Slutsky-Leiderman *et al.*, 2007).

The structure and the function of the TIM23 translocase are directly dependent on the activity of two additional proteins. Tam41 (Mmp37) affects the assembly and maintains the functional integrity of the TIM23 complex (Gallas *et al.*, 2006; Tamura *et al.*, 2006). Hep1 (Tim15/Zim17) prevents self-aggregation of Hsp70 in the matrix, and mitochondria depleted of Hep1 show defective import of matrix targeted proteins (Burri *et al.*, 2004; Sichtung *et al.*, 2005; Yamamoto *et al.*, 2005). However, these two proteins are not constituents of the TIM23 translocase and their effect on the very process of protein import into mitochondria is not direct.

The preproteins containing MTS will be completely translocated into the matrix unless they have a sequence that is recognized by the TIM23 translocase as a signal for sorting into the inner membrane (Glick *et al.*, 1992b; van Loon *et al.*, 1986). The main part of a “stop-transfer” signal is a hydrophobic stretch that generates the transmembrane (TM) domain of the mature protein. The import of a number of precursors of membrane proteins therefore requires matrix ATP until the TIM23 translocase recognizes the stop-transfer signal. However, generation of a preprotein in which the internal hydrophobic sorting signal is placed close to the presequence by deleting a stretch of amino acid residues between the MTS and the transmembrane domain, leads to import of an inner membrane protein that is independent on the activity of mtHsp70 (Gärtner *et al.*, 1995). As some of natural preproteins do not require the activity of mtHsp70 either (Rojo *et al.*, 1998), the laterally sorted preproteins can be further subdivided into two types, motor-dependent and motor independent ones. If and how the TIM23 translocase distinguishes between the two types of laterally sorted preproteins is not known.

1.3. The objective of this work

The objective of this study was to gain new insights into the structure and function of the TIM23 translocase. Two questions were to be addressed: first, whether the TIM23 translocase contains any still unidentified components, and second, what is the nature of the process enabling the TIM23 translocase to import preproteins into two different mitochondrial subcompartments: the inner membrane and the matrix. For the first goal, the TIM23 translocase was to be purified via Protein A tag on Tim23 and its composition analyzed by SDS-PAGE and mass spectrometry. Unknown components, if any, were to be analyzed thoroughly. For the second goal, a method was to be developed to generate homogenous populations of the TIM23 translocase *in vivo* in different translocation states: the empty state

and the ones actively involved in lateral insertion and matrix translocation. Composition, topology and the conformation of the TIM23 translocase were to be analyzed in each of the states.

2. MATERIAL AND METHODS

2.1. Molecular biology methods

2.1.1. Isolation of DNA

2.1.1.1. Isolation of yeast genomic DNA

Yeast strain inoculated in 5 ml YPD medium and incubated overnight at 30°C while shaking at 140 rounds per minute (rpm). Cells were harvested by centrifugation (2500 x g, 5 min, RT), washed with 25 ml of water, resuspended in 1 ml of breaking buffer (100 µg/ml zymolyase, 1 M sorbitol, 100 mM EDTA, pH 8.0) and incubated for 1 h at 37°C. The cells were washed with 1 ml 1 M sorbitol and 100 mM EDTA, centrifuged and resuspended and incubated in 1 ml of lysis buffer (50 mM Tris·HCl, 20 mM EDTA, 1% (w/v) SDS, pH 7.5) for 30 min at 65°C. Upon addition of 400 µl 5 M K-acetate the samples were incubated on ice for 1 h and DNA was separated from cell wall and membranes by centrifugation at 20000 x g for 15 min at 4°C.

The supernatants (aqueous phase) were transferred to new tubes and DNA was precipitated by addition of the same volume of isopropanol. After centrifugation (36670 x g, 10 min, 2°C) DNA pellet was washed with 70% ethanol, dried at RT, resuspended in 100 µl H₂O and stored at -20°C.

2.1.1.2. Isolation of plasmid DNA from Escherichia coli

Plasmid DNA from *E. coli* was isolated using a “PureYield” Plasmid Midiprep System (Promega). Bacterial strain carrying plasmid of interest was inoculated in 50 ml LB-Amp medium and incubated overnight at 37°C while shaking at 140 rpm. Cells were harvested the next day by centrifugation (10000 x g, 10 min, RT) and resuspended in 6 ml of Cell Resuspension Solution. Cells were lysed by addition of 6 ml of Cell Lysis Solution. Tubes were inverted 5 times and left for 3 min at RT. After neutralization with 10 ml of Neutralization Solution, tubes were again inverted 5 times and incubated for 3 min at RT to ensure thorough clearing. Samples were centrifuged (10000 x g, 10 min, 4°C), and the supernatants immediately applied onto a clarifying column standing on top of an anion-

exchange column placed onto a vacuum manifold. After the entire volume of the sample passed under vacuum through column stack, the clarifying column was removed and the anion-exchange column was washed first with 5 ml of Endotoxin Removal Wash and then with 20 ml of the Column Wash Solution. The column was left to dry for 30 sec under vacuum and DNA was then eluted from the column with 600 μ l of sterile deionized water (ddH₂O). Plasmid DNA isolated this way was stored at -20°C .

2.1.2. Amplification of DNA sequences by Polymerase Chain Reaction (PCR)

DNA sequences were amplified by PCR as described previously (Sambrook, 1989). The DNA templates for PCR were: (i) isolated DNAs from yeast or bacteria (when the PCR product was used for subsequent cloning), (ii) commercial cassettes for deletion of specific open reading frames (ORFs) (when the PCR product was used for homologous recombination in yeast cells) and (iii) whole cell extracts from yeast or bacteria (to check the successfulness of cloning). Thermostable DNA polymerases used were *Taq* (isolated from *Thermus aquaticus*) and *Pfu* (isolated from *Pyrococcus furiosus*). As *Taq* DNA polymerase has no proofreading ability, *Pfu* DNA polymerase was added in the PCR mix when the PCR product was used for subsequent cloning.

PCR mix (total volume of 50 μ l) contained: 1 U DNA polymerase (*Taq* DNA polymerase and/or *Pfu* DNA polymerase), 5 μ l 10 x PCR-buffer (1% Triton X-100, 500 mM KCl, 15 mM MgCl₂, 100 mM Tris·HCl, pH 8.8), 2 μ l dNTPs (10 mM each), 6.25 μ l primers (20 pmol/ μ l each) and 20 ng plasmid DNA or 200 ng genomic DNA as templates. When the successfulness of cloning was checked by PCR, single *E.coli* colonies were resuspended in 15 μ l sterile H₂O or single *S. cerevisiae* colonies were resuspended in 15 μ l sterile H₂O containing 100 μ g/ml zymolyase, and 1 μ l of cell suspensions was used as a template for test PCR. The following PCR program, with small variations depending on the DNA sequence, was used:

1) 95°C, 3 min	Nuclease inactivation and complete DNA denaturation;	
2) 30-35 cycles	DNA amplification:	
	95°C, 30 s	DNA denaturation
	52°C, 45 s	Annealing of primers
	72°C, 1 min per 1 kb	Extension of primers (DNA synthesis)
3) 72°C, 10 min	Completion of the final extension reaction	

To avoid occurrence of possible non-specific PCR products in few cases, several values of annealing temperature were tested ($52 \pm 5^\circ\text{C}$) in temperature gradient PCR machine (Mastercycler gradient – Eppendorf). The PCR products were subsequently analyzed by agarose gel electrophoresis.

2.1.3. DNA analysis and purification

2.1.3.1. Agarose gel electrophoresis of DNA

DNA fragments were separated by horizontal agarose gel electrophoresis according to their molecular weights. Agarose was dissolved in TAE buffer (40 mM Tris-acetate, pH 7.5, 20 mM Na-acetate, 1 mM EDTA) at the boiling temperature in the microwave oven. When it cooled down to 65°C , ethidium-bromide was added ($0.5 \mu\text{g/ml}$) and, while still hot, it was poured in a cuboid mold to cool down to RT and solidify. DNA in solution (either isolated DNA or PCR product) was mixed in 4:1 ratio with 5 x loading dye (30% (v/v) glycerol, 0.25% (w/v) bromphenol-blue, 0.25% (w/v) xylencyanol) and loaded on a 0.8-3% (w/v) agarose gel, depending on the size of DNA fragments to be separated. Gels were run in TAE buffer at $U = 80\text{-}140 \text{ V}$ depending on the size of the gel. Separated DNA fragments were visualized under UV light (366 nm). Commercially available molecular weight markers were used in each run.

2.1.3.2. Isolation of DNA from agarose gels

DNA fragments were excised from the gel with a sterile scalpel under UV light. DNA was extracted from the gel using the “QIAquick Gel extraction kit” (Qiagen). Three volumes of QG buffer were added to the Eppendorf cup containing the agarose piece with DNA fragment of interest and the mixture was incubated for 10 min at 55°C . When the agarose was completely dissolved, solution was loaded on the DNA binding silica column. The column was washed with $750 \mu\text{l}$ of PE buffer and dried at RT. DNA was eluted with $30 \mu\text{l}$ sterile ddH_2O and $1 \mu\text{l}$ of the eluted DNA was loaded on an analytical agarose gel to check the efficiency of purification. Extracted DNA was routinely stored at -20°C .

2.1.3.3. Measurement of DNA concentration

To determine DNA concentration the absorption of DNA solutions was measured at 260 nm. One optical unit ($\text{OD} = 1.0$) corresponds to a concentration of $50 \mu\text{g/ml}$ of double stranded DNA, $33 \mu\text{g/ml}$ single stranded DNA, $40 \mu\text{g/ml}$ RNA or $20 \mu\text{g/ml}$ oligonucleotides.

2.1.4. Enzymatic manipulation of DNA

2.1.4.1. Digestion of DNA with restriction endonucleases

DNA was digested with 2-5 U of specific restriction endonucleases per 1 µg of DNA. For analytical purposes, up to 100 ng of DNA was digested in a 10 µl reaction volume. For preparative purposes up to 3 µg of DNA was digested in a 60 µl reaction volume. DNA was usually digested for 3 h at 37°C in the buffer specific for the restriction enzyme, according to the manufacturer's recommendations. Digested DNA fragments were analyzed by agarose gel electrophoresis and used for ligation reactions.

2.1.4.2. Ligation of DNA fragments

One DNA fragment (after digestion with restriction endonucleases) and a cloning vector or another DNA fragment (digested with the same or compatible enzymes) were ligated together in a buffer containing DNA ligase from bacteriophage T4. Linearized DNA vector (100-200 ng) and 5-10 fold molar excess of DNA fragment were incubated in a 10 µl reaction with 1 µl of 10 x ligation buffer (50 mM Tris·HCl, 10 mM MgCl₂, 1 mM DTT, 1 mM ATP, 5% (w/v) PEG-8000, pH 7.6) and 0.5 µl (1 U) T4 DNA ligase (Gibco-BRL). Ligation reaction was performed at 14°C for 16 h and 0.5-1 µl of the ligation mixture was transformed into electrocompetent *E. coli* cells.

2.1.5. Transformation of electrocompetent *E. coli* cells

2.1.5.1. Overview of *E. coli* strains used

Strain	Genotype	Reference
MH1	MC1061 derivative; araD139, lacX74, galU, galK, hsr, hsm ⁺ , strA	Casadaban and Cohen, 1980
XL1-Blue	supE44, hsdR17, recA1, endA1, gyrA96, thi-1, relA1, lac ⁻ , F'[proAB ⁺ , lacI ^q lacZΔM15, Tn10(tet ^r)]	commercially available from Stratagene

2.1.5.2. Preparation of electrocompetent cells

The electrocompetent *E. coli* cells (MH1 or XL1-Blue strain) were prepared as described in (Dower *et al.*, 1988). 50 ml of LB medium was inoculated with a single colony of the corresponding bacterial strain and grown overnight at 37°C while shaking at 140 rpm. Next morning 1 l of LB medium, preheated to 37°C, was inoculated with 2 ml of the overnight

culture and the cells were grown until they reached $OD_{578} \approx 0.5$. The culture was then incubated on ice for 30 min and the cells were subsequently harvested by centrifugation for 5 min at $4,400 \times g$ and at 4°C and washed sequentially with 400 ml, 200 ml and 50 ml of sterile 10% (v/v) glycerol. The competent cells were finally resuspended in 1 ml of LB medium with 10% (v/v) glycerol and stored at -80°C in 40 μl aliquots.

2.1.5.3. Transformation of *E. coli* cells by electroporation

The ligation mixture or isolated plasmid DNA (0.5-1 μl) was added on ice to 40 μl of electrocompetent cells and this transformation mixture was then transferred to ice-cold 0.2 cm electroporation cuvette. High electric voltage pulse was delivered to the cells in the cuvette through the electroporation Gene Pulser apparatus (BioRad) (settings: $U = 2.5 \text{ kV}$, $R = 400 \Omega$, $C = 25 \mu\text{F}$; time constant obtained (τ) was 7.2-8.8 ms); cell suspension treated in this way was diluted with 1 ml of LB-medium and incubated for 45 min at 37°C while shaking at 140 rpm to allow cell recovery. Cells were briefly centrifuged, most of the medium was poured off, cell pellet resuspended in the ca. 150 μl remaining medium and plated on LB-Amp plates (LB with 2% (w/v) agar supplemented with 100 $\mu\text{g/ml}$ ampicillin). Plates were incubated overnight at 37°C and the successfulness of transformation was usually checked by test PCR.

2.1.6. Bacterial plasmids used and cloning strategies

2.1.6.1. Overview of constructs used for transcription/translation

Construct	Reference
Tim21 (Sc)	This thesis
Cox5a (Sc)	Gärtner <i>et al.</i> , 1995
Cox5a Δ TM (Sc)	Gärtner <i>et al.</i> , 1995
Cox5a Δ matrix (Sc)	Gärtner <i>et al.</i> , 1995
AAC (Nc)	Pfanner <i>et al.</i> , 1987
Cytb ₂ Δ 19(167)DHFR (Sc)	Schneider <i>et al.</i> , 1994
Cytb ₂ (167)DHFR (Sc)	Schneider <i>et al.</i> , 1994
F1 β (Nc)	Rassow <i>et al.</i> , 1990
DLD(1-72)DHFR (Sc)	Rojo <i>et al.</i> , 1998

Sc – *Saccharomyces cerevisiae*; Nc – *Neurospora crassa*.

2.1.6.2. Cloning strategy for Tim21 construct used in transcription/translation

Constructs cloned for *in vitro* transcription and translation of mitochondrial preproteins comprised of cDNAs of relevant genes inserted into pGEM4 vector (Promega).

a) Cloning of Tim21 into pGEM4

Coding sequence of *TIM21* gene was amplified from yeast genomic DNA using primers BamTim21 and Tim21Hind_new. Obtained PCR product was cloned into pGEM4 vector using *Bam*HI and *Hind*III restriction sites in the primers.

BamTim21	5'– AAA GGA TCC ATG AGC TCA AGT TTG CCT AGG – 3'
Tim21Hind_new	5'– TTT AAG CTT ATC TTA ATC TTT TCT GGG GCC – 3'

2.1.6.3. Overview of plasmids used for protein expression in bacteria

Plasmid	Reference
pQE30[Tim21IMS]	This thesis
pQE30[Tim21IMSΔ14]	This thesis
pQE30[Tim21IMSΔ21]	This thesis
pMalCRI[Pam17(124-197)]	This thesis
pET21+[Cytb ₂ Δ19(167)DHFR]	This thesis

2.1.6.4. Cloning strategies for plasmids used for protein expression in bacteria

a) Cloning of C-terminal domain of Tim21 and its truncated versions into pQE30

Cloning into pQE30 vector (Qiagen) created N-terminally His-tagged versions of cDNAs encoding C-terminal domain of Tim21 [Tim21IMS(97-239)] and its truncated versions lacking 14 [Tim21IMS(97-225)] or 23 [Tim21IMS(97-216)] amino acid residues. These three nucleotide sequences were amplified from pGEM4[Tim21] vector using the same forward primer BamTim21_97 and three different reverse primers Tim21Hind_new, Tim21CD14rev and Tim21CD21rev, respectively. *Bam*HI and *Hind*III restriction sites from the primers were used to clone the obtained PCR products into pQE30 vector.

BamTim21_97	5'– CCC GGA TCC TCA GAA CTA TTT TCG CCT TCA G – 3'
Tim21CD14rev	5'– AAG CTT TTA ATT AGA AAC CGG ATG CAA TTT TGG – 3'
Tim21CD21rev	5'– AAG CTT TTA GAT CAA ATA GTA AAG CTT CTC TCC – 3'

b) Cloning of C-terminal domain of Pam17 into pMalCRI

Cloning into pMalCRI vector (New England Biolabs) created a protein construct comprising maltose-binding protein (MBP) at the N-terminus fused to C-terminal domain of Pam17. Nucleotide sequence coding for amino acids 124 to 197 of Pam17 was amplified from yeast genomic DNA using primers BamPam17_124 and Pam17Hind. *BamHI* and *HindIII* restriction sites from the primers were used to clone the obtained PCR products into pMalCRI vector.

BamPam17_124 5'– CCC GGA TCC TCG CAA GTT TTC AAA CTT TCC – 3'

Pam17Hind 5'– CCC AAG CTT TCA CAA AAA TTC TTT GGC TTT C – 3'

c) Cloning of hybrid protein Cytb₂Δ19(167)DHFR into pET21+

Nucleotide sequence coding for amino acids 1 to 167 of cytochrome b2 with an internal deletion of 19 amino acids (47-65) covering the hydrophobic stop-transfer signal fused to dihydrofolate reductase (DHFR) was amplified from pGEM4[Cytb₂Δ19(167)DHFR] vector using primers EcoRBSCytb2 and DHFRHind. *EcoRI* and *HindIII* restriction sites from the primers were used to clone the obtained PCR products into pET21+ vector (Novagen) adding His tag on the C-terminus of the hybrid protein. EcoRBSCytb2 primer contained ribosome binding site (RBS), because pET21+ is a transcription vector.

EcoRBSCytb2 5'– CCC GAA TTC AAG GAG ATA CCA TGC TAA AAT ACA AAC
CTT TAC – 3'

DHFRHind 5'– CCC AAG CTT GTC TTT CTT CTC GTA GAC TTC – 3'

2.1.7. Transformation of *S. cerevisiae* cells (Lithium-acetate method)

(Gietz *et al.*, 1992)

The yeast strain was grown overnight at 30°C while shaking at 140 rpm in YPD-medium and diluted the following morning to an OD₅₇₈ ≈ 0.2 in 50 ml medium. When the culture reached OD₅₇₈ ≈ 0.5, cells were harvested by centrifugation (1500 x g, 3 min, RT); washed with 25 ml sterile ddH₂O and resuspended in 1 ml 100 mM Li-acetate. Cells were centrifuged again (7500 x g, 15 sec, RT) and resuspended in 400 µl 100 mM Li-acetate. For each transformation 50 µl of this suspension was centrifuged (3000 x g, 5 min, RT), supernatant was removed and the pellet was overlaid in this particular order: 240 µl PEG 3350 (50% v/v), 36 µl 1 M Li-

acetate, 5 µl single stranded salmon sperm DNA (10 mg/ml; previously incubated for 5 min at 95°C and then cooled down on ice), 70 µl H₂O containing 0.1-10 µg of plasmid DNA or PCR product to be transformed. Mixture was vigorously vortexed for 1 min, moderately shaken at 30°C for 30 min and then incubated at 42°C for 20-25 min. Cells were pelleted by centrifugation (15 s, 6000 x g, RT), resuspended in 150 µl sterile ddH₂O and plated on selective medium. The plates were incubated for 2-4 days at 30°C until the appearance of single colonies.

2.1.8. *S. cerevisiae* strains used and cloning strategies

2.1.8.1. Overview of yeast strains used

Yeast strain	Reference
<i>Wild type strains</i>	
YPH499	Sikorski and Hieter, 1989
W303-1A/-1B	R. Rothstein, Department of Human Genetics, Columbia University, New York
<i>Strains generated by homologous recombination</i>	
Tim21-HA	This thesis
Tim21-ProtA	This thesis
Tim21-His ₆	This thesis
<i>TIM21::HIS3</i>	This thesis
<i>PAM17::HIS3</i>	This thesis
<i>TIM21::HIS3/PAM17::KANMX4</i>	This thesis
<i>TOM7::HIS3</i>	This thesis
GAL-Tim17	Meier <i>et al.</i> , 2005a
GAL-Tim23	Terziyska <i>et al.</i> , 2007
GAL-Tim50	Mokranjac <i>et al.</i> , 2003a
GAL-Tim44	As described in Mokranjac <i>et al.</i> , 2003a
GAL-Tim14	Mokranjac <i>et al.</i> , 2003b
GAL-Tim16	Kozany <i>et al.</i> , 2004

GAL-Mia40	Terziyska <i>et al.</i> , 2005
<i>TOM5::HIS3</i>	Dietmeier <i>et al.</i> , 1997
<i>TOM6::KANMX4</i> (BY4743)	Huntsville (AL, USA)
<i>TOM20::URA3</i>	Ramage <i>et al.</i> , 1993
<i>TOM70:: KANMX4</i> (BY4743)	Euroscarf (Frankfurt)

Strains generated by transformations with yeast vectors

<i>TIM23::HIS3</i> + pRS315[ProtATim23]	This thesis
YPH499 + pVT-102U[Tim23Δ50His ₉]	This thesis
GAL-Tim17 + pVT-102U[Tim23Δ50His ₉]	This thesis
<i>PAM17::HIS3</i> + pRS314[His ₆ Pam17]	This thesis
YPH499 + pVT-102U[Tim21]	This thesis
YPH499 + pVT-W[Pam17]	This thesis
YPH499 + pVT-102U[Tim21] + pVT-W[Pam17]	This thesis
YPH499 + pVT-102U[Cytb ₂ Δ19(167)DHFR]	This thesis
YPH499 + pVT-102U[Cytb ₂ (167)DHFR]	This thesis
YPH499 + pYX143[Cox5aDHFR]	Gift from S. Meier
YPH499 + pYX143[Cox5aΔTMDHFR]	Gift from S. Meier
Tom40-2	Kassenbrock <i>et al.</i> , 1993
Tom40-3	Kassenbrock <i>et al.</i> , 1993
Tom40-4	Kassenbrock <i>et al.</i> , 1993
Tom22-3	Moczko <i>et al.</i> , 1997

2.1.8.2. Cloning strategies for generation of yeast strains by homologous recombination

a) Tagging of Tim21 on the chromosome

Tim21 was HA-, ProtA- and His-tagged on the chromosome by homologous recombination of the corresponding PCR products in the haploid yeast strain YPH499. As DNA templates for PCR reactions pYM3, pYM7 and pYM9 vectors (Knop *et al.*, 1999), respectively, were used; amplified PCR products contained auxotrophic marker cassette *HIS3* and sequences

homologous to the last 42 bp of *TIM21* gene and first 42 bp of its 3' UTR. PCR products for HA- and ProtA-tagging of Tim21 were obtained using forward primer Tim21pYMfor and reverse primer Tim21pYMrev; for His-tagging the same reverse primer was used, whereas forward primer was Tim21hispYMfor. PCR products were transformed in yeast and stably integrated into the chromosome via the regions homologous to the *TIM21* gene. To isolate positive clones, yeast transformants were grown on selective medium lacking histidine and homologous recombination was checked by PCR.

Tim21pYMfor	5'– AAT TCG AAG GGC TTT CTG GGA ATT AGA TGG GGC CCC AGA AAA GAT CGT ACG CTG – 3'
Tim21hispYMfor	5'– AAT TCG AAG GGC TTT CTG GGA ATT AGA TGG GGC CCC AGA AAA GAT CAT CAC CAT – 3'
Tim21pYMrev	5'– CAT TTA CGA ATA TTT AAA ACC TGA GCA ACT CCG TCA AAT TTG ATC ATC GAT GAA – 3'

b) Deletions of TIM21 and PAM17 genes

TIM21 and *PAM17* genes were deleted by homologous recombination of the corresponding PCR products in the haploid yeast strain YPH499. PCR products contained an auxotrophic-marker-cassette *HIS3* and short sequences homologous to the flanking regions of the *TIM21* and *PAM17* loci. Primers Tim21deltafor and Tim21deltarev were used for deletion of *TIM21* gene, and primers Pam17deltafor and Pam17deltarev were used for deletion of *PAM17* gene. For mutants with deletion of only one of the proteins, constructs were amplified from pFA6HIS3MX6 (Wach *et al.*, 1997) and these PCR products were transformed in yeast and stably integrated into the corresponding chromosome via the regions homologous to the *TIM21* or *PAM17* gene. To isolate positive clones, yeast transformants were grown on selective medium lacking histidine and homologous recombination was checked by PCR and fast mito prep. For generation of the strain where both proteins were deleted, construct was amplified from pFA6KANMX4 (Wach *et al.*, 1997) using Pam17deltafor and Pam17deltarev primers and transformed in *TIM21::HIS3* strain. To isolate positive clones, yeast transformants were grown on selective medium lacking histidine and containing kanamycin. Homologous recombination was checked by PCR and fast mito prep.

Tim21deltafor	5'– GGT AAA ATC ATT CGT ATA TTA TTT TCC TGA CTC CAA GTT TAA ACA CGT ACG CTG – 3'
Tim21deltarev	5'– CAT TTA CGA ATA TTT AAA ACC TGA GCA ACT CCG TCA AAT TTG ATC ATC GAT GAA – 3'

Pam17deltafor	5'– AAG AAG TGT TAA AAA CAT TCA GAA AAC ATT GTC CGC CTC TTC AAA CGT ACG CTG CAG GTC GAC – 3'
Pam17deltarev	5'– GTA TAT ATA CAG AGT CTG AGA AGA AGG AAA AGA TCA CAC GTT CAA ATC GAT GAA TTC GAG CTC – 3'

c) Deletion of *Tom7*

TOM7 gene was deleted by homologous recombination of a PCR product in the haploid yeast strain YPH499. PCR product contained an auxotrophic-marker-cassette *HIS3* and short sequences homologous to the flanking regions of the *TOM7* locus. Primers Tom7deltafor and Tom7deltarev were used to amplify the construct from pFA6HIS3MX6 (Wach *et al.*, 1997) and this PCR product was transformed in yeast and stably integrated into the chromosome via the regions homologous to the *TOM7* gene. To isolate positive clones, yeast transformants were grown on selective medium lacking histidine and homologous recombination was checked by PCR.

Tom7deltafor	5'– CTT ATC TCT CAA TAT TTG CCA AAA TTA GCT TTT AAC AAA TAA ACC CGT ACG CTG CAG GTC GAC – 3'
Tom7deltarev	5'– AAT ATG GGC TTC CTC TCT CAC CCA AGT TGT ATC GAA CTG ATG TTT ATC GAT GAA TTC GAG CTC – 3'

2.1.8.3. Cloning strategies for plasmids used for the transformation of yeast

a) pRS315[ProtATim23]

Promoter region 400 bp upstream of *TIM23* gene was amplified from yeast genomic DNA using primers SacTim23p and Tim23pKpn. Protein A with TEV cleavage site was amplified from pYM9 vector using primers KpnProtA and ProtATEVBam. These two PCR products were simultaneously cloned in pGEM4 vector. Coding sequence of *TIM23* gene was amplified from yeast genomic DNA using primers BamTim23 and Tim23Hind and cloned in the abovementioned pGEM4 plasmid using *Bam*HI and *Hind*III restriction sites. It was not possible to clone all three PCR products simultaneously due to the presence of *Kpn*I restriction site within the coding sequence of *TIM23* gene. The entire construct was cut out from pGEM4 vector and subcloned in pRS315 vector using *Sac*I and *Hind*III restriction sites. The obtained plasmid was transformed in *TIM23::HIS3* + pVT-102U[*TIM23*] yeast strain that was subsequently grown on selective medium lacking leucine and containing 5-fluoro-orotic acid (5-FOA), that allows growth of *URA3* mutants. This led to the removal of plasmid pVT-

102U[TIM23] and generation of the strain expressing only Protein A-tagged version of Tim23 (plasmid shuffling). Yeast transformants were checked by fast mito prep.

SacTim23p	5'– CCT GAG CTC ACT GTG ACG TCG – 3'
Tim23pKpn	5'– CCC GGT ACC GAT TGT GTG TGA TCT GTT AAA C – 3'
KpnProtA	5'– AAA GGT ACC ATG CCT CAA CAA AAC AAA ACC GCG – 3'
ProtATEVBam	5'– AAA GGA TCC CTG AAA ATA AAG ATT CTC AAG AGC CGC GGA ATT CGC C – 3'
BamTim23	5'– AAA GGA TCC ATG TCG TGG CTT TTT GGA GA – 3'
Tim23Hind	5'– CCC AAG CTT TCA TTT TTC AAG TAG TCT TTT CTT GAC AC – 3'

b) pVT-102U[Tim23Δ50His₉]

Coding sequence of *TIM23* gene lacking first 150 bp was amplified from yeast genomic DNA using primers BamTim23_51new and Tim23His9Hind and cloned in pRS315 vector. The construct was then cut out and subcloned in pVT-102U vector using *Bam*HI and *Hind*III restriction sites. The obtained plasmid was transformed in YPH499 and GAL-Tim17 yeast strains that were subsequently grown on selective medium lacking uracil and containing glucose (YPH499) or galactose (GAL-Tim17). Yeast transformants were checked by fast mito prep.

BamTim23_51new	5'– CCC GGA TCC ATG CAT GTC GAC ACC GCT AGG CTG – 3'
Tim23His9Hind	5'– GGG AAG CTT TCA ATG GTG ATG GTG ATG GTG ATG GTG ATG TTT TTC AAG TAG TCT TTT CTT GAC – 3'

c) pRS314[His₆Pam17]

Promoter region 400 bp upstream of *PAM17* gene containing sequence coding for its mitochondrial targeting signal followed by hexahistidyl tag at its 3' end was amplified from yeast genomic DNA using primers BamPam17p and Pam17preHis6Pst. Coding sequence of *PAM17* gene lacking the sequence coding for mitochondrial targeting signal was amplified from yeast genomic DNA using primers PstPam17m Pam17fXho. These two PCR products were cloned in pRS314 vector that was transformed in *PAM17::HIS3* yeast strain. Yeast transformants were subsequently grown on selective medium lacking tryptophan and checked by fast mito prep.

BamPam17p	5'– CCC GGA TCC ATG TTT ACC AGT GCC ATT AGA TTG – 3'
Pam17preHis6Pst	5'– TTT CTG CAG GTG ATG GTG ATG GTG ATG ATA TGA TCT TAA GGG TAA GGT TG – 3'
PstPam17m	5'– AAA CTG CAG TCT CAG CCC GCA TCC CTT CAA G – 3'
Pam17fXho	5'– GGG CTC GAG CAA ATG CGC ATA AAG GAA ATG C – 3'

d) pVT-102U[Tim21]

Coding sequence of *TIM21* gene was cut out from pGEM4[Tim21] and subcloned in pVT-102U vector using *BamHI* and *HindIII* restriction sites. The obtained plasmid was transformed in YPH499 yeast strain. Yeast transformants were subsequently grown on selective medium lacking uracil and the levels of overexpression of Tim21 in the transformants were checked by fast mito prep.

e) pVT-W[Pam17]

Coding sequence of *PAM17* gene was amplified from yeast genomic DNA using primers BamPam17 and Pam17Hind. The same reverse primer was previously used for generation of pMalCRI[Pam17(124-197)] plasmid. The construct was cloned in pVT-W vector using *BamHI* and *HindIII* restriction sites. The obtained plasmid was transformed in YPH499 yeast strains with and without pVT-102U[Tim21] plasmid. Yeast transformants were subsequently grown on selective medium lacking tryptophan or tryptophan and uracil and the levels of overexpression of Pam17 in the transformants were checked by fast mito prep.

BamPam17	5'– CCC GGA TCC ATG TTT ACC AGT GCC ATT AGA TTG – 3'
----------	------------------------------------------------------

f) pVT-102U[Cytb₂Δ19(167)DHFR] and pVT-102U[Cytb₂(167)DHFR]

Coding sequences for hybrid proteins Cytb₂Δ19(167)DHFR and Cytb₂(167)DHFR were amplified from plasmids pGEM4[Cytb₂Δ19(167)DHFR] and pGEM4[Cytb₂(167)DHFR], respectively, using primers HindCytb2 and DHFREco. The obtained PCR products were cloned in pVT-102U vector using *HindIII* and *EcoRI* restriction sites. The obtained plasmids were transformed in YPH499 yeast strains. Yeast transformants were subsequently grown on selective medium lacking uracil and the levels of overexpression of hybrid proteins and their arrest within the TIM23 complex in the transformants were checked by fast mito prep upon cell growth in medium containing galactose and 0.2 mM aminopterin.

HindCytb2	5'– CCC AAG CTT ATG CTA AAA TAC AAA CCT TTA C – 3'
DHFR _{Eco}	5'– TTT GAA TTC TTA GTC TTT CTT CTC GTA GAC – 3'

2.2. Cell biology methods

2.2.1. *E. Coli* – media and growth

2.2.1.1. Media for *E. coli*

LB-medium: 0.5% (w/v) yeast extract, 1% (w/v) bacto-tryptone, 1% (w/v) NaCl.

LB-Amp medium: LB-medium supplemented with 100 µg/ml of ampicillin.

Described media were used for preparing liquid cultures. For preparation of solid media (LB or LB-Amp plates) 2% (w/v) bacto-agar was added to the liquid media solutions and autoclaved (120°C, 20 min). The ampicillin was added after the media had been cooled down to 50°C.

2.2.1.2. Cultivation of *E. coli*

Liquid medium (usually 50 ml of LB-Amp) was inoculated with the single colony from the plate and grown overnight at 37°C while shaking at 140 rpm. If necessary, cells were grown for up to 24h at lower temperatures (30 or 24°C).

2.2.2. *S.cerevisiae* – media and growth

2.2.2.1. Media for *S.cerevisiae*

Non-selective media:

YP-medium: 10 g yeast extract, 20 g bacto-peptone, H₂O to 930 ml, pH 5.0 (adjusted with HCl).

YPD-medium: YP-medium supplemented with 2% glucose.

YPG-medium: YP-medium supplemented with 3% glycerol.

YPGal-medium: YP-medium supplemented with 2% galactose.

Lactate medium: 3 g yeast extract, 1 g KH_2PO_4 , 1 g NH_4Cl , 0.5 g $\text{CaCl}_2 \times 2\text{H}_2\text{O}$, 0.5 g NaCl , 1.1 g $\text{MgSO}_4 \times 6\text{H}_2\text{O}$, 0.3 ml 1% FeCl_3 , 22 ml 90% lactic acid, H_2O to 1 l, pH 5.5 (adjusted with KOH) and supplemented with 0.1% glucose or 0.5% galactose.

Selective media:

SD medium: 1.7 g yeast nitrogen base, 5 g $(\text{NH}_4)_2\text{SO}_4$, 20 g glucose, H_2O to 1 l.

SLac medium: 1.7 g yeast nitrogen base, 5 g $(\text{NH}_4)_2\text{SO}_4$, 22 ml 90% lactic acid, H_2O to 1 l, pH 5.5 (adjusted with KOH).

For selective media, stock solutions: histidine (10 mg/ml, 500 x stock), leucine (10 mg/ml, 333 x stock), lysine (10 mg/ml, 333 x stock), uracil (2 mg/ml, 100 x stock) and adenine (2 mg/ml, 100 x stock) were separately autoclaved for 20 min at 120°C , whereas tryptophan (10 mg/ml, 500 x stock) was filter sterilized.

The above described media were used for preparing liquid cultures. For preparation of plates with solid media, 2% w/v bacto-agar was added. Bacto-agar, glucose, and media were autoclaved separately. The amino acid solutions were added to the selective media just before pouring the plates.

2.2.2.2. *Cultivation of S.cerevisiae*

Liquid cultures were inoculated with yeast strains from the glycerol stocks or from the agar plates and were grown in the appropriate liquid medium at 30°C while shaking at 140 rpm. Prior to the isolation of mitochondria cells were passaged for approximately 60 h in the way that OD_{578} never exceeded 1. Temperature-sensitive mutants were grown at 24°C for the same period of time. For the generation of mitochondria depleted of one its essential proteins a yeast strain having the corresponding gene under *GAL* promoter was grown for 48-60 h on galactose-containing media after which cells were collected, washed with water, resuspended in glucose-containing media and grown in the latter media for 8-18 h depending on the strain. For the generation of mitochondria with increased levels of one its proteins encoded on the gene under *GAL* promoter, the corresponding yeast strain was grown on lactate medium supplemented with 0.5% galactose. For the generation of mitochondria with increased levels of one its proteins encoded on the gene under *ADH* promoter, the corresponding yeast strain was grown on selective lactate medium supplemented with 0.1% glucose.

2.2.2.3. Growth of yeast strains where mitochondria with the TIM23 complex in different translocation modes are generated

For the generation of mitochondria with the empty translocases, wild type cells (YPH499) were grown on lactate media supplemented with 0.1% glucose. In the exponential growing phase, 100 µg/ml puromycin or cycloheximide was added one hour before the isolation of mitochondria. For the generation of mitochondria containing arrested preproteins, wild-type cells transformed with the corresponding plasmids were grown on selective lactate medium supplemented with 0.1% glucose. Two hours prior to isolation of mitochondria yeast cells were collected, washed with sterile water and resuspended in medium containing 0.5% galactose and aminopterin was added in drops from 100 x stock solution until the final concentration of 0.2 mM.

2.2.3. Determination of the growth characteristics of yeast strains

To determine the growth phenotype of a specific yeast strain, the growth assays were performed either on solid media, i.e. dilutions assay on agar plates, or in liquid media. For dilution assays, the strains were grown in liquid culture for 24-36 h, diluted to identical $OD_{578} \approx 0.5$ and then a series of 1:10 dilutions were made for each strain. 4 µl of each dilution were loaded as drops on plates with the adequate medium, previously dried for 45 min at RT under sterile conditions. Plates were incubated for 2-4 days at designated temperatures. For determination of growth phenotype in liquid medium, the strains were grown in liquid culture for 18-24 h, diluted to identical $OD_{578} \approx 0.5$ and then grown at designated temperatures for 24-48 h. Cell growth was measured spectrophotometrically every 1.5-2 h. At time zero the cell number was calculated as one.

2.2.4. Isolation of yeast mitochondria

2.2.4.1. Large scale isolation of yeast mitochondria

(Herrmann *et al.*, 1994)

Yeast cells were grown to OD_{578} of 0.8-1.2, collected by centrifugation (3000 x g, 5 min, RT), washed with water and resuspended in a buffer containing 10 mM DTT, 100 mM Tris, pH not adjusted, to a concentration of 0.5 g/ml (2 ml of buffer per gram of cell wet weight). Cells were incubated for 15 min at 30°C while shaking at 140 rpm, followed by the repeated

centrifugation step and washed in 200 ml of 1.2 M sorbitol solution. Cells were harvested by centrifugation and resuspended to a concentration of 0.15 g/ml in buffer containing 1.2 M sorbitol, 20 mM $\text{KH}_2\text{PO}_4\cdot\text{KOH}$, pH 7.4 and 4 mg zymolyase per 1 g cell wet weight. Addition of zymolyase leads digestion of the cell wall and formation of spheroplasts. The cell suspension was incubated for 30-60 min at 30°C while shaking at 140 rpm. Efficiency of cell wall digestion was checked after 30 min by diluting 25 μl of suspension in either 1 ml water or 1 ml 1.2 M sorbitol. Cell wall digestion was stopped if the OD_{578} of the water suspension was 10-20% of the sorbitol one. All following steps were performed at 4°C.

The spheroplasts were isolated by centrifugation (3000 x g, 5 min), resuspended (0.15 g/ml) in homogenization buffer (0.6 M sorbitol, 10 mM Tris·HCl, 1 mM EDTA, 0.2% (w/v) fatty acid free BSA, 1 mM PMSF, pH 7.4), and dounced 10 times in a cooled douncer (homogeniser) on ice. Cell debris, intact cells and nuclei were removed as pellets by centrifugation performed twice (2000 x g, 5 min). The supernatant was centrifuged for 12 min at 17400 x g to pellet down mitochondria. Mitochondria were resuspended in 25 ml SH buffer (0.6 M sorbitol, 20 mM HEPES·KOH, pH 7.3). After two centrifugation steps (2000 x g, 5 min), mitochondria were isolated from the supernatant by centrifugation (17400 x g, 12 min). Final mitochondrial pellet was resuspended in 0.5-1 ml SH buffer and the protein concentration determined by Bradford assay. Mitochondria were usually diluted to 10 mg/ml, distributed into 50 μl aliquots, frozen in liquid nitrogen and stored at -80°C.

2.2.4.2. Isolation of crude yeast mitochondria (“fast mito prep”)

Yeast cells were usually inoculated in 50 ml YPD medium and incubated overnight at 30°C while shaking at 140 rpm. Cells corresponding to 10 OD units were collected by centrifugation (3000 x g, 5 min, RT), washed with water and resuspended in 300 μl SH buffer containing 80 mM KCl and 1 mM PMSF. Upon addition of 0.3 g glass beads (diameter 0.3 mm) the samples were vortexed four times for 30 sec each, with 30 sec intervals on ice. After centrifugation (1000 x g, 3 min, 4°C), the supernatants were transferred to a new tube and mitochondria were sedimented by centrifugation (17400 x g, 10 min, 4°C). Cytosolic proteins from the supernatants (50 μl) were precipitated using trichloroacetic acid, while the crude mitochondrial pellets were resuspended in 25 μl 2 x sample (Laemmli) buffer, shaken for 5 min at 95°C, and analyzed by SDS-PAGE and immunodecoration.

2.2.5. Preparation of mitoplasts

Mitoplasts are prepared by resuspending mitochondria in a hypotonic buffer which leads to their swelling and to disruption of the outer membrane whereas the inner membrane remains intact. Mitochondria in SH buffer were diluted 1:10 in a hypotonic buffer containing 20 mM HEPES·KOH and 1 mM ATP, pH 7.3 and incubated on ice for 20 min. As a control, mitochondria were diluted in SH buffer in the same manner. If necessary, mitoplasts and control mitochondria were reisolated by centrifugation (17400 x g, 10 min) and resuspended in a desired buffer.

2.2.6. Protease treatment and “clipping assay”

2.2.6.1. Protease treatment of mitochondria

After the import reaction, 50 µg/ml proteinase K was added to the import mix to digest nonimported and partially imported preproteins. Samples were incubated on ice for 15 min after which the digestion was stopped by addition of 2 mM PMSF. Mitochondria were reisolated, resuspended in 2 x sample buffer and analyzed by SDS-PAGE and autoradiography.

Protease digestion was also directly performed in mitochondria and in mitoplasts enabling submitochondrial localization of the mitochondrial proteins of interest.

2.2.6.2. Removal of the N-terminus of Tim23 exposed on the mitochondrial surface (“clipping assay”)

In vivo saturated mitochondria were incubated for 10 min on ice with 500 µg/ml PK. Increasing amounts of recombinant preprotein b₂(167)Δ19DHFRHis₆ ranging from 0-170 µg were incubated for 20 min at 25°C with 100 µg energized mitochondria pretreated with puromycin. Samples were washed in SH buffer containing 80mM KCl, solubilized in SH buffer and treated with or without 500 µg/ml proteinase K. Samples were analyzed by SDS-PAGE and immunodecoration with affinity-purified antibodies against the C-terminal peptide of Tim23.

2.2.7. Carbonate extraction

For the analysis of the association of a protein with the membrane, 50 µg of precipitated mitochondria were resuspended in 100 µl of 0.1 M Na₂CO₃, pH 11.5 and incubated for 30 min on ice. That was followed by centrifugation (183254 x g, 20 min, 2°C). Soluble proteins in the supernatant were precipitated using TCA, whereas the pellet containing integral membrane proteins was resuspended directly in 2 x sample buffer. The samples were then analyzed by SDS-PAGE and immunodecoration.

2.3. Protein biochemistry methods

2.3.1. Protein analysis

2.3.1.1. SDS-Polyacrylamide gel electrophoresis (SDS-PAGE)

(Laemmli, 1970)

The proteins were separated according to their molecular weights under denaturing conditions using one-dimensional vertical SDS-polyacrylamide gel electrophoresis (SDS-PAGE). The concentrations of acrylamide and bis-acrylamide in the separating gel were chosen according to the molecular sizes of proteins of interest. The volume of the protein solution loaded per lane was between 5 and 50 µl, and the amount of loaded protein was between 25 and 150 µg. The samples were resuspended in 5-50 µl sample buffer and incubated at 95°C for 5 min before loading.

The electrophoresis was performed at 35 mA for 100 min for large gels of dimensions of approximately 14 cm x 9 cm x 0.1 cm and at 25 mA for 50 min for 1 h for small gels (Mini-PROTEAN II, Bio-Rad) of dimensions of approximately 10 cm x 5.5 cm x 0.075 cm. Protein molecular weight markers of 116, 66, 45, 35, 25, 18 and 14 kDa (PepLab) were usually used.

Buffers for SDS-PAGE:

Running gel: 8-16% (w/v) acrylamide, 0.16-0.33% (w/v) bis-acrylamide, 375 mM Tris·HCl (pH 8.8), 0.1% (w/v) SDS, 0.05% (w/v) APS, 0.05% (v/v) TEMED.

Stacking gel: 5% (w/v) acrylamide, 0.1% (w/v) bis-acrylamide, 60 mM Tris·HCl (pH 6.8), 0.1% (w/v) SDS, 0.05% (w/v) APS, 0.05% (v/v) TEMED.

Electrophoresis buffer: 50 mM Tris base, 384 mM glycine, 0.1% (w/v) SDS, pH 8.3 without adjustment.

1 x sample (Laemmli) buffer: 60 mM Tris·HCl, pH 6.8, 2% (w/v) SDS, 10% glycerol, 5% (v/v) β-mercaptoethanol, 0.05% (w/v) bromphenol-blue.

Separated proteins were either stained with Coomassie-Brilliant-blue (CBB) or transferred onto a nitrocellulose membrane.

2.3.1.2. Blue-Native gel electrophoresis (BNGE)

Blue-Native gel electrophoresis (BNGE) was applied for separation of proteins under native (non-denaturing) conditions (Schagger *et al.*, 1994). 50-150 µg of pelleted mitochondria were resuspended in 15-45 µl of solubilization buffer (20 mM Tris·HCl, 80 mM KCl, pH 8.0) containing 1% digitonin and 1 mM PMSF and incubated at 4°C for 15 min. After a clarifying spin (36670 x g, 10 min, 4°C), 5 µl of sample buffer (5% (w/v) Coomassie-Brilliant-blue G-250, 100 mM bis-Tris, 500 mM 6-amino-n-capronic acid, pH 7.0) were added to the soluble fraction and loaded onto a 6-13% or 6-16.5% gradient gel. The electrophoresis was performed at 4°C. For the first step of electrophoresis, cathode buffer (15 mM bis-Tris, 50 mM Tricine, pH 7.0) containing 0.02% Coomassie-Brilliant-blue G250 and anode buffer (50 mM bis-Tris, pH 7.0) were used and the voltage was set at 100V and after 1 h shifted to 500V. When the blue front had migrated to about two thirds of the separation distance, the cathode buffer was replaced by a cathode buffer without Coomassie-Brilliant-blue. Marker proteins: apoferritin (440 kDa), alcohol dehydrogenase (ADH) (monomer: 50 kDa, dimer: 100 kDa, trimer: 150 kDa), and bovine serum albumin (BSA) (monomer: 66 kDa, dimer: 136 kDa) were used.

Buffers for BN-PAGE:

Stacking gel: 3.8% (w/v) acrylamide, 0.12% (w/v) bis-acrylamide, 0.5 M 6-amino-n-capronic acid, 50 mM bis Tris·HCl, pH 7.0, 0.08% (w/v) APS, 0.08% (v/v) TEMED.

Running gel: 6-16.5% (w/v) acrylamide, 0.15-0.3% (w/v) bis-acrylamide, 5% (v/v) glycerol, 0.5 M 6-amino-n-capronic acid, 50 mM bis-Tris·HCl, pH 7.0, 0.04% (w/v) APS, 0.04% (v/v) TEMED.

Bottom gel: 20% (w/v) acrylamide, 0.13% (w/v) bis-acrylamide, 0.5 M 6-amino-n-capronic acid, 50 mM bis-Tris·HCl, pH 7.0, 0.05% (w/v) APS, 0.025% (v/v) TEMED.

2.3.1.3. CBB staining of SDS-PAGE gels

After SDS-PAGE separating gel was incubated in aqueous solution containing 30% (v/v) methanol, 10% (v/v) acetic acid, and 0.1 (w/v) Coomassie-Brilliant-blue G-250 at RT for 30 min. The staining was occasionally speeded up by heating the gel in the solution for 1 min in the microwave oven. The gel was then destained with aqueous solution containing 30% (v/v) methanol and 10% (v/v) acetic acid until the protein bands were clearly visible, which required several washing steps with fresh destaining solutions. Heating in the microwave oven speeded up this process also. The gel was dried overnight between two gel-drying films (Promega).

2.3.1.4. Transfer of proteins onto nitrocellulose/PVDF membrane (Western-Blot)

Proteins separated by SDS-PAGE were transferred onto nitrocellulose membranes using a modified semi-dry method (Khyse-Anderson, 1984). Proteins separated by BNGE were transferred onto PVDF membranes.

The nitrocellulose membrane was incubated for three minutes in water and subsequently in blotting buffer (20 mM Tris base, 150 mM glycine, 20% (v/v) methanol, 0.08% SDS) prior to the transfer procedure. A respective membrane was placed onto three sheets of Whatman 3MM filter paper that were previously soaked in the blotting buffer, lying on the graphite anode electrode. The gel was placed on the membrane and then covered with another three soaked filter papers. The cathode graphite electrode was placed on top creating the “blotting sandwich”. The electrotransfer was performed at 2 mA/cm² for 1 h for big and for 45 min for small gels (for big gels of dimensions of approximately 14 cm x 9 cm x 0.1 cm it translates to 250 mA for 1 h and for small gels of dimensions of approximately 10 cm x 5.5 cm x 0.075 cm it translates to 110 mA for 45min). Only in the case of the cross-linking experiments that were analyzed on big gels the time of transfer was increased to 75 min.

PVDF membrane was activated before blotting through short incubation (up to 5 min) in methanol. It was then thoroughly washed, first with water, and then 5 min (or longer) with transfer buffer. Prior to blotting, separating part of the blue native gel, freed from the stacking and bottom gel parts, was equilibrated in blotting buffer by shaking for 15 minutes at RT or 4°C. Electrotransfer onto PVDF membranes was generally performed at 220 mA for 1 h at 4°C.

To verify transfer efficiency, and to visualize and label the marker proteins' bands, the nitrocellulose membranes were reversibly stained with Ponceau S solution (0.2% (w/v)

Ponceau S in 3% (w/v) TCA), and the PVDF membranes with Coomassie solution. The PVDF membrane were destained with methanol, which was then removed by excessive washing with TBS buffer (150 mM NaCl, 10 mM Tris-HCl, pH 7.5). The membranes were then immunodecorated, or the radioactive material visualized by autoradiography.

2.3.1.5. Protein quantification by autoradiography

Radiolabeled proteins were detected by autoradiography. Dry nitrocellulose membrane was exposed to an X-ray film (Kodak Bio Max MM) and, after a desired period of exposure, film was developed in a developing machine (Gevamatic 60, AGFAGEvaert). Period of exposure depended on signal intensities. The films were scanned and the intensity of bands of interest quantified by densitometry using Image Master 1D Elite software (Amersham).

2.3.1.6. Determination of protein concentration

Protein concentration was determined according to Bradford assay (Bradford, 1976). Protein solutions (1-10 μ l) were diluted with 1 ml of 1:5 dilution of commercially available “Bio-Rad-Proteinassay” reagent and incubated for 10 min at RT. The absorbance was measured at 595 nm using a 1 cm path length microcuvette. Protein concentration was determined from a calibration curve obtained using the known amounts of the commercially available bovine IgG proteins (BioRad) as a standard.

2.3.2. Protein preparation

2.3.2.1. Trichloroacetic acid (TCA) precipitation of proteins

Proteins from aqueous solutions were precipitated by adding 72% TCA to a final concentration of 12%. The samples were incubated for 30 min at -20°C , and then centrifuged (36670 x g, 20 min, 2°C). The precipitated proteins were washed with acetone (kept at -20°C), and centrifuged (36670 x g, 12 min, 2°C). Protein pellet was shortly dried at RT and dissolved in sample buffer.

2.3.2.2. Purification of recombinant His-tagged proteins from E. coli

Recombinant proteins with N-terminal hexahistidine tagged were expressed in *E. coli* from pQE-30 vector (Qiagen). Overnight *E. coli* culture (10 ml) was diluted into 500 ml LB-Amp and grown at 37°C while shaking at 140 rpm until OD_{578} reached 0.5 units. Expression of the recombinant protein was induced by 0.5 mM IPTG and the culture was grown for additional 2

h at 37°C. Cells were harvested by centrifugation for 10 min at 4424 x g. The cell pellet was transferred on ice and resuspended in 40 ml buffer containing 50 mM NaH₂PO₄, 300 mM NaCl, 10 mM imidazole, pH 8.0), supplemented with 1 mM PMSF and 1 mg/ml lysozyme and stirred for ca. 45 min at 4°C. Cells were completely broken by sonication (10 x 12 s, Branson sonifier, setting 4, 80% duty cycle). After centrifugation for 15 min at 27216 x g, clear supernatant was loaded on 1-1.5 ml NiNTA-agarose column, preequilibrated with resuspension buffer. The column was connected to a peristaltic pump and all subsequent steps were performed at a flow rate of 1 ml/min. Column was washed with 10 ml resuspension buffer and bound proteins were eluted with 10 ml resuspension buffer with 300 mM imidazole. Expression and purification were monitored by SDS-PAGE and CBB staining.

2.3.2.3. Purification of recombinant MBP-tagged Pam17 from *E. coli*

C-terminal domain of Pam17 (124-197 amino acid residues) fused to maltose binding protein (MBP) was expressed in *E. coli* from pMAL-cRI vector (New England Biolabs). Overnight *E. coli* culture (25 ml) was diluted into 1 l LB-Amp and grown at 37°C while shaking at 140 rpm until OD₅₇₈ reached 0.5 units. Expression of the recombinant protein was induced by 0.5 mM IPTG and the culture was grown for additional 2 h at 37°C. Cells were harvested by centrifugation for 10 min at 4424 x g and resuspended in 40 ml buffer containing 20 mM HEPES·NaOH, 200 mM NaCl, 10 mM β-mercaptoethanol, 1mM PMSF, pH 7.4. Lysozyme was added to concentration of 1 mg/ml and bacterial cell wall was digested for 45 min at 4°C. Cells were completely broken by sonication (10 x 12 s, Branson sonifier, setting 4, 80% duty cycle). After centrifugation for 15 min at 27216 x g, clear supernatant was loaded on a 7 ml Amylose column (New England Biolabs) preequilibrated in buffer for resuspension. Column was washed with 35 ml of the same buffer and bound proteins were eluted with resuspension buffer containing 10 mM maltose. Expression and purification were monitored by SDS-PAGE and CBB staining.

2.3.2.4. *In vitro* synthesis of radiolabeled mitochondrial preproteins

Mitochondrial preproteins projected for radiolabeling with [³⁵S] were cloned into pGEM4 vector under the control of *Sp6* promoter. These proteins were synthesized either by separate transcription followed by translation reaction in the presence of [³⁵S] methionine or by coupled TNT system that combines transcription and translation in the same reaction mixture.

In the first case, coding sequences for these proteins were transcribed into mRNA using SP6 RNA polymerase (Melton DA, 1984; Sambrook, 1989). Transcription mixture (100 μl)

contained: 20 μ l 5x transcription buffer (200 mM Tris·HCl, 50 mM NaCl, 30 mM MgCl₂, 10 mM spermidine, pH 7.5), 10 μ l 0.1 M DTT, 4 μ l RNasin (40 U/ μ l), 20 μ l NTPs (10 mM each), 5.2 μ l 2.5 mM m⁷G(5')ppp(5')G, 3 μ l Sp6 polymerase, 27 μ l H₂O and 10 μ l plasmid DNA. After incubation for 1 h at 37°C followed by addition of 10 μ l 10 M LiCl and 300 μ l absolute ethanol, reaction was cooled down at -20°C for 30 min and RNA precipitated by centrifugation at 36670 x g for 20 at 2°C. RNA pellet was washed with ice-cold 70% (v/v) ethanol, dried and resuspended in 100 μ l H₂O with 1 μ l RNasin and used for *in vitro* translation or stored at -80°C.

Mix for *in vitro* translation (Pelham and Jackson, 1976) contained 50 μ l rabbit reticulocyte lysate, 20 U RNasin, 1.75 μ l amino acid mix (1mM each, without methionine), 6 μ l [³⁵S] methionine, 3.5 μ l 15 mM Mg-acetate and 12.5 μ l RNA. After 1 h at 30°C, incorporation of labeled methionine was stopped by addition of 6 μ l 58 mM non-labeled methionine. Upon the addition of 12 μ l 1.5 M sucrose, ribosomes and aggregated proteins were removed by centrifugation (90700 x g, 45 min, 2°C) and 12 μ l aliquots of the supernatant were frozen at -80°C.

2.3.3. Protein experiments *in organello*

2.3.3.1. Import of radiolabeled preproteins into mitochondria

Mitochondria were resuspended at 0.5 mg/ml in SI import buffer containing 600 mM sorbitol, 50 mM HEPES·KOH, 80 mM KCl, 0.05% (w/v) fatty acid free BSA, 10 mM Mg-acetate, 2.5 mM EDTA, 2 mM KH₂PO₄ and 1 mM MnCl₂, pH 7.2. Upon further addition of 2 mM NADH, 1 mM ATP, 10 mM creatine phosphate and 100 μ g/ml creatine kinase and incubation for 3 min at RT, 1-3% (v/v) of radiolabeled preproteins was added in suspension of mitochondria. Import reactions were performed for different time periods at various temperatures (10-25°C). Import was stopped by dilution 1:10 in ice cold SH buffer with or without 50 μ g/ml proteinase K. Protease treatment was stopped after 15 min of incubation on ice by addition of 2mM PMSF. Upon centrifugation (26500 x g, 12 min), mitochondrial pellets were resuspended in 20 μ l 2 x sample buffer, shaken for 5 min at 95°C and analyzed by SDS-PAGE and immunodecoration.

For two step import reactions, mitochondria were incubated with radiolabeled preprotein for 15 min in the absence of mitochondrial membrane potential ($\Delta\Psi$). The first step presumes the transfer of the preprotein through the outer membrane and its accumulation at the *trans* side

of the TOM complex. To dissipate $\Delta\Psi$, 1 μM valinomycin, 20 μM oligomycin and 10 μM CCCP were added to mitochondria prior to the addition of preprotein. Mitochondria were reisolated by centrifugation and $\Delta\Psi$ was restored by addition of SI buffer containing 2 mM NADH, 1 mM ATP, 10 mM creatine phosphate and 100 $\mu\text{g/ml}$ creatine kinase, leading to the second step of the import reaction.

2.3.3.2. Generation of the TOM-TIM23-preprotein supercomplex in vitro

Recombinant preprotein $b_2(167)\Delta 19\text{DHFRHis}_6$ was preincubated with 1 μM methotrexate (MTX) and 3 mM NADPH and then imported into energized mitochondria in the presence of 2 μM MTX and 5 mM NADPH, leading to formation of a two-membrane spanning intermediate, i.e. the TOM-TIM23-preprotein supercomplex. Following the import reactions, samples were either subjected to protease treatments (“clipping assay”) or the supercomplex was purified by Ni-NTA-agarose chromatography and subsequently analyzed by SDS-PAGE and immunodecoration.

2.3.3.3. Pull down experiments with tagged proteins expressed in mitochondria

Isolated mitochondria were centrifuged (17400 x g, 10 min, 4°C) and the mitochondrial pellet was solubilized at 2 mg/ml in 20 mM Tris·HCl, 80 mM KCl, pH 8.0 containing 1% (w/v) digitonin and 1 mM PMSF for 20 min at 4°C. After a clarifying spin (90700 x g, 20 min, 2°C), mitochondrial extract was added either to IgG beads (Amersham Biosciences), in the case of Protein A-tagged proteins, or to NiNTA beads (Qiagen), in the case of His-tagged proteins. The beads (20-60 μl) were previously washed with 3 x 1 ml TBS (150 mM NaCl, 10 mM Tris·HCl, pH 7.5) and 200 μl solubilization buffer containing 0.05% instead of 1% digitonin. IgG beads were additionally washed with 200 μl glycine, pH 2.5, after the third round of washing with TBS. Mitochondrial extract was incubated with the beads at for 1 h at 4°C. The beads were then washed three times with 200 μl solubilization buffer containing 0.05% digitonin, and the bound proteins were eluted either with glycine, pH 2.5, in the case of Protein A-tagged proteins, or with sample buffer containing 300 mM imidazole, in the case of His-tagged proteins. Upon incubation at 95°C for 5 min, samples were analyzed by SDS-PAGE and immunodecoration.

2.3.3.4. Crosslinking of mitochondrial proteins

For the crosslinking analysis of interactions between mitochondrial proteins, reisolated mitochondria were resuspended in the SI buffer (without BSA) and energized by addition of 2

mM NADH, 1 mM ATP, 10 mM creatine phosphate and 100 µg/ml creatine kinase, After incubation for 3 min at 25°C, the crosslinker was added from a 100-fold stock in DMSO. In this work two membrane permeable and lysine-specific chemical crosslinkers were used: DSG (disuccinimidylglutarate) and DSS (disuccinimidylsuberate). After 30 min incubation on ice, excess crosslinker was quenched for 10 min on ice with 100 mM glycine, pH 8.8. Mitochondria were reisolated and analyzed by SDS-PAGE and immunodecoration.

When crosslinking adducts were purified via His tag from one of the crosslinked proteins on the NiNTA-agarose beads, 250 µg of reisolated mitochondria were solubilized in buffer containing 1% SDS (v/v), 50 mM Na₂HPO₄, 100 mM NaCl, 10% glycerol, 10 mM imidazole, 1 mM PMSF, pH 8.0 for 15 min with vigorous shaking at 25°C. Samples were diluted 20 fold in the same buffer containing 0.2% Triton X-100 instead of SDS and, after a clarifying spin, added to 50 µl NiNTA-agarose beads. After 1 h of incubation at 4°C while slowly rolling, beads were washed and bound proteins eluted with 2 x sample buffer containing 300 mM imidazole during incubation for 5 min at 95°C.

2.4. Immunology methods

2.4.1. Generation of antibodies

2.4.1.1. Overview of generated antibodies

Antibody	Antigen
αTim21FL	His ₆ -Tim21
αTim21C	His ₆ -Tim21(97-239)
αPam17	MBP-Pam17(124-197)

2.4.1.2. Generation of polyclonal antisera against Tim21 and Pam17 proteins

Polyclonal antisera were generated in rabbits. Recombinant proteins were expressed in bacteria, purified using a specific tag (see 2.3.2.2. and 2.3.2.3.) and used as antigens. After the purification on the column remaining contaminants were separated from the proteins of interest by SDS-PAGE. Upon Western blotting, the bands corresponding to the proteins of interest were excised from nitrocellulose membranes. Up to 200 µg of proteins (10 bands) were dissolved in 300 µl DMSO by vortexing for 3 min (Knudsen, 1985). TiterMax adjuvant (300 µl) was added and the emulsion injected subcutaneously into rabbits (Harlow and Lane,

1988). The antigen was injected twice within ten days before the first bleeding was taken. All subsequent injections took place every four weeks. Freund's incomplete adjuvant was used instead of TiterMax adjuvant for all the injections except the first one. The rabbits were bled 10-12 days after each injection cycle. Approximately 30-40 ml of blood was taken from the ear vein and left to coagulate at RT for 2 h. Coagulated blood was centrifuged twice (5 min at 3000 x g and 15 min at 20000 x g, RT), and the supernatant was incubated at 56°C for 20 min to inactivate complement. The antisera prepared this way were then aliquoted and frozen at -20°C.

2.4.1.3. Affinity purification of antibodies against Tim21 and Pam17 proteins

Affinity purification was performed in order to reduce the cross-reactivity of the antisera. Antibodies against Tim21 and Pam17 were purified on the affinity columns made by coupling the proteins that served as antigens to the CNBr-activated Sepharose 4B (Amersham) via their -NH₂ groups. To remove all other amino group containing substances from protein in the solution prior to coupling, the buffer was exchanged with a bicarbonate one on the PD-10 column (Amersham). The column was equilibrated with 30 ml 0.1 M NaHCO₃, 0.5 M NaCl, pH 8.3 and 2.5 ml of solution containing 4-8 mg protein was loaded on the column by the gravity flow. First 2.5 ml of the eluate was discarded and the protein was collected from the column in the following 3.5 ml. During equilibration of the PD-10 column, CNBr-Sepharose was prepared in a way that 0.4 g of the beads was placed in 5 ml 1 mM HCl to swell. After 45 min the beads gave rise to ca. 1.5 ml gel. Gel was washed on a sintered glass filter with 200 ml 1 mM HCl and transferred into a column (max. volume 10 ml). Remaining HCl solution was allowed to pass through and the column was closed at the bottom. Upon addition of 3.5 ml of protein solution column was closed at the top and gently mixed by slow revolving around vertical axis for 1 h at RT. The column was put in the vertical position; buffer was allowed to pass through and it was quickly analyzed for protein content with Ponceau S staining to check the efficiency of coupling. Remaining active groups were blocked by loading 6 ml 0.1 M ethanolamine, pH 8.0; 2 ml were allowed to pass through before the column was closed and gently mixed by slow revolving for additional 2 h at RT. Subsequently, the column was put in the vertical position; ethanolamine was allowed to pass through and all nonspecifically bound proteins were removed by 3 washing cycles of alternating pH. Each cycle consisted of 6 ml 0.1 M Na-acetate, 0.5 M NaCl, pH 4.5 followed by 6 ml 0.1 M Tris·HCl, 0.5 M NaCl, pH 8.0. Column was finally washed with 10 ml 10 mM Tris·HCl, pH 7.5, and it was ready for affinity purification of antibodies. If the antibodies

were not purified the same day, 3 ml 0.05% NaN₃ water solution was added and the column was stored at 4°C.

Before purification, the column was left at RT for 45 min and then equilibrated with 10 ml of 10 mM Tris-HCl, pH 7.5. Antiserum (6 ml) was diluted with 24 ml 10 mM Tris-HCl, pH 7.5 and loaded on the corresponding affinity column under gravity flow. The column was washed with 10 ml 10 mM Tris-HCl, pH 7.5 followed by 10 ml 10 mM Tris-HCl, 0.5 M NaCl, pH 7.5. For the elution, column was subjected to alternating pH through application of 10 ml of each of the following buffers in given order: 10 mM Na-citrate, pH 4.0, 100 mM glycine-HCl, pH 2.5 and 100 mM Na₂HPO₄, pH 11.5. Fractions of 1 ml were collected and neutralized immediately with 200 µl 1 M Tris-HCl, pH 8.8 in the case of the first two buffers, and with 100 µl glycine, pH 2.2 in the case of the phosphate one. Several fractions eluted with each of the elution buffers were checked for specificity by immunodecoration on nitrocellulose membrane carrying yeast mitochondrial proteins. The majority of the specific antibodies were eluted with the glycine buffer in fractions 2-6. These fractions were usually pooled and 150 µl aliquots were stored at -20°C.

2.4.2. Immunodecoration

Proteins blotted onto nitrocellulose or PVDF membranes were visualized by immunodecoration with specific antibodies. After Western blotting membranes were incubated for 30 min in 5% (w/v) milk powder in TBS (150 mM NaCl, 10 mM Tris-HCl, pH 7.5) to block all nonspecific binding sites. The membranes were then incubated with specific primary antibody (1:100 to 1:20000 dilutions in 5% milk in TBS) for 1-2.5 h at RT, or overnight at 4°C. The membranes were then washed for 5 min in TBS, 10 min in TBS containing 0.05% Triton X-100 and again 5 min in TBS and subsequently incubated with goat Anti-rabbit antibodies coupled to horseradish peroxidase (diluted 1:10.000 in 5% milk in TBS) for 1-2 h at RT. The membrane was then washed as already described, treated with the chemiluminescent substrate of peroxidase (ECL reagents 1 and 2) and the signals were detected on X-ray films (Fuji New RX).

For detection of HA-tagged Tim21, anti-HA antibody (Roche) was used. The membranes were blocked in the supplied blocking solution. Secondary antibody (goat anti-mouse) was diluted 1:5000 in the same solution and the membranes were treated as described above.

ECL reagent 1: 3 ml Tris·HCl, pH 8.5 (1M stock), 300 µl luminol (440 mg/10 ml DMSO), 133 µl p-coumaric acid (150 mg/10 ml DMSO), H₂O to 30ml.

ECL reagent 2: 3 ml Tris·HCl, pH 8.5 (1M stock), 18 µl H₂O₂ (30%), H₂O to 30ml.

Solutions are stable for 7-10 days if kept in light-protected bottles at 4°C. Chemiluminescent substrate of peroxidase was made by mixing equal volumes of ECL reagents 1 and 2.

2.4.3. Coimmunoprecipitation

Desired amount of Protein A Sepharose CL-4B (PAS) (Amersham Biosciences) beads slurry was washed with water, followed by 3 x 5 min TBS, and then the appropriate amounts of purified antibodies (enough antibodies to immunodeplete the corresponding antigen from the extract) were added and incubated for 2 h at 4°C, while rotating the cups overhead. The beads were then washed from the unbound antibodies and were ready for incubation with proteins from the mitochondrial extract. While the PAS beads were incubating with the desired antibodies, isolated mitochondria were centrifuged (17400 x g, 10 min, 4°C) and the mitochondrial pellet was resuspended at 2 mg/ml in 20 mM TrisHCl, 80 mM KCl, pH 7.5, containing 1% (w/v) digitonin and 1 mM PMSF for 20 min at 4°C. After a clarifying spin (90700 x g, 20 min, 2°C), mitochondrial extract was added to antibodies prebound to PAS and the mixture was incubated overhead for 2 h at 4°C. Beads were washed twice with 20 mM TrisHCl, 80 mM KCl, pH 7.5, containing 0.05% (w/v) digitonin and 1 mM PMSF. Specifically bound proteins were eluted with either reducing or nonreducing Laemmli buffer (5 min at 95°C). Samples were analyzed by SDS-PAGE and immunodecoration.

3. RESULTS

The TIM23 complex is the major translocase in the mitochondrial inner membrane which translocates protein precursors synthesized in the cytosol into the matrix or sorts them into the inner membrane. For more than a decade the only known components of the TIM23 translocase were Tim23, Tim17, Tim44, mtHsp70 and the nucleotide exchange factor Mge1 (Neupert, 1997). Then, within only a few years, the field of mitochondrial protein import literally exploded, when several research groups reported discovery of three new components of the TIM23 complex: Tim50, Tim14 and Tim16 (D'Silva *et al.*, 2003; Frazier *et al.*, 2004; Geissler *et al.*, 2002; Kozany *et al.*, 2004; Mokranjac *et al.*, 2003a; Mokranjac *et al.*, 2003b; Truscott *et al.*, 2003; Yamamoto *et al.*, 2002). The question at the beginning of the present work was whether there are some more components of the TIM23 translocase missing.

3.1. Identification of Tim21

To analyze the composition of the yeast *S. cerevisiae* TIM23 complex and identify additional components, the complex was purified via a Protein A tag at the N-terminus of Tim23.

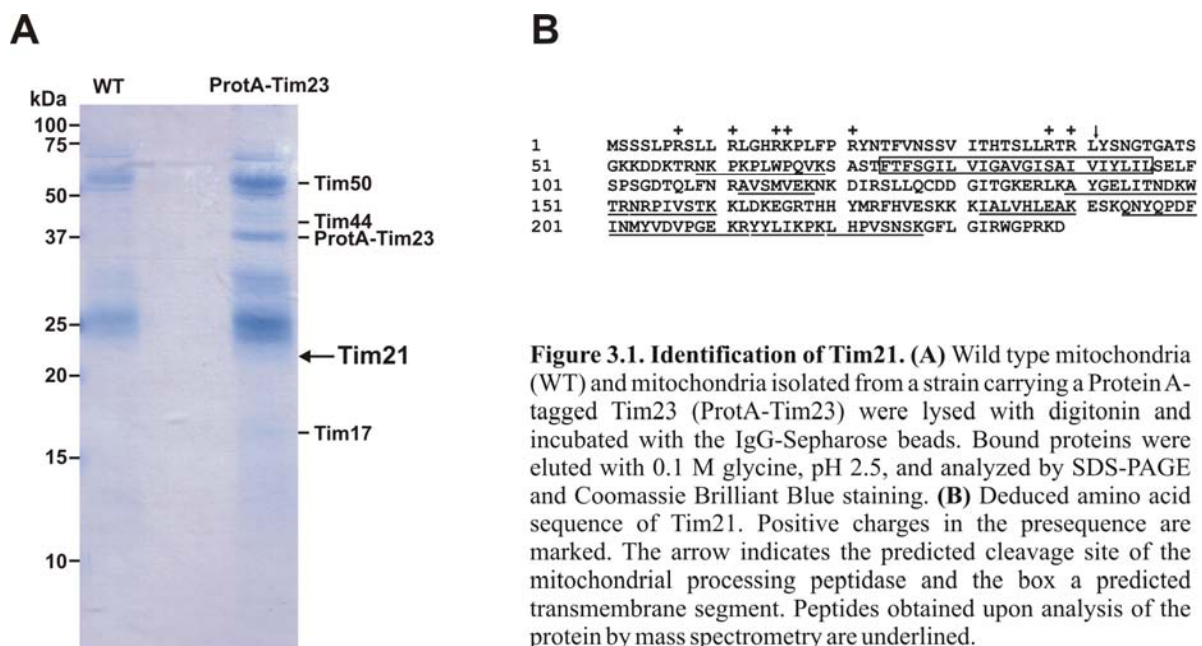


Figure 3.1. Identification of Tim21. (A) Wild type mitochondria (WT) and mitochondria isolated from a strain carrying a Protein A-tagged Tim23 (ProtA-Tim23) were lysed with digitonin and incubated with the IgG-Sepharose beads. Bound proteins were eluted with 0.1 M glycine, pH 2.5, and analyzed by SDS-PAGE and Coomassie Brilliant Blue staining. (B) Deduced amino acid sequence of Tim21. Positive charges in the presequence are marked. The arrow indicates the predicted cleavage site of the mitochondrial processing peptidase and the box a predicted transmembrane segment. Peptides obtained upon analysis of the protein by mass spectrometry are underlined.

The YPH499 strain containing ProtA-Tim23 as the only version of Tim23 showed no growth defect compared to wild type yeast (*wt*) under all conditions tested. Mitochondria were isolated, lysed with digitonin, and the TIM23 complex was isolated by IgG-Sepharose affinity chromatography. Samples were analyzed by SDS-PAGE and Coomassie Brilliant Blue staining. Mass spectrometric analysis of the proteins specifically eluted together with Protein A-Tim23 revealed a protein of previously unknown function (open reading frame *YGR033c*) along the known components of the TIM23 complex (Figure 3.1A).

A

CeMTPLSKLCAGAVTQNVLSYF...LTPSQFRSFSRTITALEKSQKSPSKQEHALQR	53
DmMSRLALLRNLTQQRNLLPTNFARLKC...AAAMHWSPHLRQEASRDGGGS	48
XtMMLPRCLRRAVLCSRALGSPRSLTVP...CYRNLSC...LLSQQRALAVPTSRFCAERPISTGSALLQVKD	67
Hs	MICTFLRAVQYTEKLRSSAKRLLLPYIVLNKACLKTEPSLRCLG...YQKKTLP...RCILGVTQKTIWTQGPSRKAEDGS	80
ScMSSSLPRSLRLGHRKPLFP...RYNTFVNSSVITHTSLRLTRLYSNGTG	47
Ce	SILEEVLVHEKAKPTTFGGKVAEKASNTFMYTAVVAGI...GLIGAFIYV...LAGEFFA...QDS...PQT...IFNKALALVRDDGRCQE	130
Dm	LQRSQDNTQVSTDV...RPIGEKIKENTKTASYTAI...IAGLGVTCVMFFAIFRELFSSES...PNN...IYADALRRVVEDPRVQD	125
Xt	KRVSVQSRGDGAS...PQTASHKVKEAGRDFTYFTV...LIGIGVTGGLFYV...VEELFSSSS...PSK...IYGEALEKCRSHPEVIG	144
Hs	KQVSVHRSQRGGTAV...PTSQKVKEAGRDFTYLI...VLFGLISITGGLFYTI...FKELFSSSS...PSK...IYGRAL...EKCRSHPEVIG	157
Sc	ATSGKKDDKTRNKPKLW...PQVKSASTFTFSGLVIGAVGISAVI...VILSEL...SPSGDTQLFNRAVSMVEKNKDIRS	124
Ce	IFGASLAGFGEETS...RGRRRHV...AHKYEK...DGMQIRIVL...FHVK...DRDEGIAQAEMEQRD...GDWQWRFLYVENKRRPKTT	206
Dm	AI...GAPIKGFGETSR...RGRRRQHV...AHSSYERN...GKPHMRM...QFYV...QGLRNKATVQLESRRSD...SGKLEYRYLFVQLDHYPRTT	202
Xt	AFGPEIKGYGETTR...RGRRRQHV...SHMEYK...DGIKCMRLK...FYIEGLEPRKQGTVHTEV...KENPESG...KYEFOYIFVEIDTYPRRT	224
Hs	VFGESV...KGYGETTR...RGRRRQHV...RFTEYK...DGLKHTCVK...FYIEGSEPGKQGTVYAQV...KENPGS...GEYDFRYIFVEIESYPRRT	237
Sc	LLQCDDGITGKERL...KAYGELITNDK...WTRNRPIVSTK...KLDKEGRTHH...YMRPHVESK...KIALVHLEAKESKQNYQPDFI	201
Ce	HVLIDNR.....	213
Dm	IILEDNRAFDP...TPEPASAGSSFGNLALMSNSRDK.....	236
Xt	I...VIEDNRRQS.....	234
Hs	IIIEDNRSQDD.....	248
Sc	NMYVDV...PGEKRYL...IKPKLHPVSN...SKGFLGIRWGPRKD.....	239

B

ScMSSSLPRSLRLGHRKPLFP...RYNTFVNSSVITH...TSLRLTRLYSNGTGATSGKKD	54
AgMLAFGSICGRLRAPAGAGLRVNVGKMPGRAWQVANGQP...YSTFYAPPEQAG	50
Ca	MHMIQVRVSSIGLRLTLRSSNIGSIRSLIVL...PILSIKPTYIR...QTQAINLKPQALLNLL...HHHHHHHHYYSTKTAPPPPP	80
NcMMKMLTGTSAGVRL...LLSPAVVRQATITTAASRALPPTAASVILVSSRRQYATTQESSKRRSVTP	65
Sc	DKTRNKPKPLW...PQVKSAS...TFTFSGLVIGAVGISAVI...VILSEL...FSPSGDTQLFNRAVSMVEKNKDIRSLLQCDD	130
Ag	NROKERRVTAWK...KVRAAA...TFSASGMLV...LGAAGVAGIV...LVYV...LILSEL...FSPSGDTQIFNRAVSTVEGD...AVARSLLQCED	126
Ca	PQPPQDKNAK...KKILNLRINRAFT...SLSLTLVWGAAGIS...VLV...SELSEL...FLPSGDT...TRTFNKAVK...LIEKNEAQK...ANFQS	160
Nc	FNDGDHVPWTR...LSTGEKAGRAVQQT...FNFLVILGVVLTGGIAY...LFTDVES...PEK...TAYFNRAVDRI...RADPRCVALLSPGD	145
Sc	GITGKERL...KAYGELITNDK...WTRNRPIVSTK...KLDKEGRTHHYMR...SHVESK...KIALVHLEAKESKQNYQPDFINMYVDV...PGE	210
Ag	GVHRSERL...KAYGDSV...GDDRWTRNRPISS...TRRLDASGREHYMR...SHVETGRRRGV...SLEAQ...QSDDSYQPEFVRMYLDV...PGE	206
Ca	GQ...RLKAYGIVSAD...KVV...RNRPVQSVKTRK...DGDHLIMK...FOVESDNGKYGV...SLEQIDNSMWNTEFEYISL...DVP...GFG	235
Nc	PKKIAAH...GEETHN...KWRRA...RPIAATVEK...DNRGVEHLKMH...SHVEGPRGSGV...VGLHLTKQPGHWEHEYQTFYVDV...RGRH	220
Sc	KRYYL...IKPKLHPVSN...SK...GFLGIRWGPRKD.....	239
Ag	KRHYL...IRPEPSVAKP...K...GFLGLNWGPRKD.....	234
Ca	KRIYI...IEEPKNQLIPKIGGSG...FLGLNWGPKKD.....	268
Nc	QRIY...LENKEAEVAAAKGGNKE...KFLGVKWN.....	251

Figure 3.2. Sequence alignment of Tim21 proteins. (A) Multiple sequence alignment of predicted Tim21 proteins from the worm *C. elegans* (Ce), fruit fly *D. melanogaster* (Dm), frog *X. tropicalis* (Xt), human *H. sapiens* and baker's yeast *S. cerevisiae* (Sc). (B) Multiple sequence alignment of predicted Tim21 proteins from the fungi *S. cerevisiae* (Sc), *A. gossypii* (Ag), *C. albicans* (Ca) and *N. crassa* (Nc). Sequence similarity of: 100% (dark blue), 75% (magenta), 50% (cyan).

This protein was named Tim21 according to its size. The primary sequence predicts a protein of 239 amino acid residues with a typical N-terminal mitochondrial targeting signal (presequence) and a transmembrane α -helical segment between amino acid residues 74 and 96. Cleavage by the mitochondrial processing peptidase is predicted after amino acid residue 41 (Figure 3.1B).

Tim21 is conserved throughout the eukaryotic kingdom (Figure 3.2A), with a high degree of sequence similarity among fungi (Figure 3.2B). Regions with particularly high conservation are present in the predicted transmembrane and in the C-terminal domain.

3.2. Tim21 is imported by the TIM23 translocase

The deduced amino acid sequence of Tim21 predicts an amphipathic helix at the N-terminus with positive residues on one and hydrophobic residues on the other side of the helix, a hallmark of the mitochondrial targeting signal (presequence). To confirm the presence of a cleavable presequence the import of [³⁵S] radiolabeled precursor of Tim21 into isolated mitochondria was performed in the presence or absence of a membrane potential ($\Delta\Psi$) across the inner membrane. Upon incubation with energized mitochondria in the presence of $\Delta\Psi$ preprotein was processed to the mature form confirming that Tim21 is synthesized as a precursor protein with a cleavable presequence, that is removed upon import into mitochondria. The difference in size between the precursor and the mature form is in agreement with the size of the predicted (MPP) cleavage site. When $\Delta\Psi$ was dissipated before the addition of the radiolabeled Tim21 preprotein, no import was observed, confirming that Tim21 is a substrate for the TIM23 translocase (Figure 3.3).

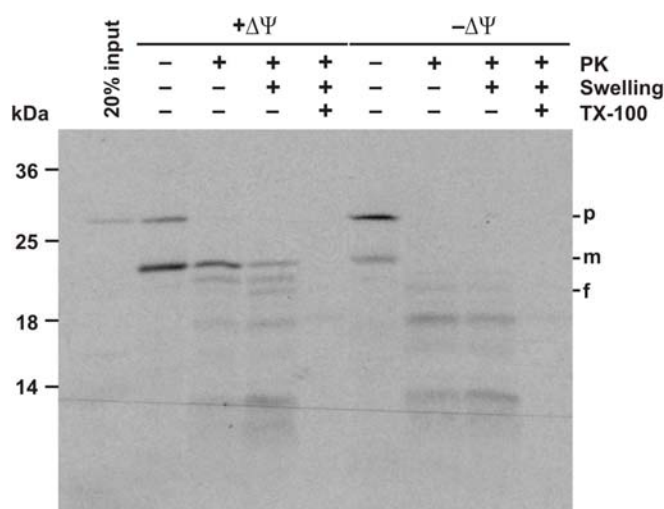


Figure 3.3. Import of Tim21 is dependent on the presence of a membrane potential ($\Delta\Psi$). Tim21 was synthesized in rabbit reticulocyte lysate in the presence of [³⁵S] methionine and imported into WT mitochondria in the presence and in the absence of $\Delta\Psi$ across the inner membrane. After 20 min. of import mitochondria were divided into two fractions each and diluted in isotonic (Sorbitol-HEPES buffer) or hypotonic solution (HEPES buffer) that led to swelling of mitochondria and formation of mitoplasts. Mitochondria and mitoplasts were treated with proteinase K (PK) and/or 1% Triton X-100. Samples were analyzed by SDS-PAGE and autoradiography. p, precursor; m, mature form of Tim21; f, 20 kDa fragment of Tim21.

After Tim21 was imported in the presence of $\Delta\Psi$, mitochondria were diluted either in isotonic or in hypotonic solution. Incubation in the hypotonic solution induced swelling of mitochondria leading to the formation of mitochondria with ruptured outer membranes, i.e. mitoplasts. Imported Tim21 was not accessible to the added Proteinase K in intact mitochondria, but only in mitoplasts. However, addition of Proteinase K generated the fragment of unexpected size of ca. 20 kDa, suggesting that either a small portion of the C-terminal domain of Tim21, predicted to be exposed in the intermembrane space, is susceptible to the protease activity or that the submitochondrial localization of Tim21 is different to that expected from its amino acid sequence. Upon addition of detergent Triton X-100 in mitoplasts, the inner mitochondrial membrane was solubilized and Tim21 was completely degraded by Proteinase K. This suggests that Tim21 spans the inner membrane with its hydrophobic α -helix, and has regions in both IMS and matrix.

3.3. Localization and topology of Tim21

To determine the orientation of Tim21 in the inner membrane a strain with an HA tag at the C-terminus of Tim21 was generated. Mitochondria and mitoplasts prepared by hypotonic swelling were treated with Proteinase K and analyzed by SDS-PAGE and immunodecoration with Anti-HA antibodies (Figure 3.4A). As a control, proteins from different mitochondrial subcompartments were tested for their accessibility to protease. Treatment of mitochondria with Proteinase K left the HA-tagged Tim21 intact, whereas the outer membrane protein Tom70 was completely degraded. In mitoplasts Tim21 was accessible to the added protease in the same manner as the intermembrane space protein cytochrome b_2 , demonstrating that the C-terminus of Tim21 indeed is located in the intermembrane space. The inner membrane in mitoplasts was intact as the matrix protein Mge1 was digested only after solubilization of mitochondria in Triton X-100. Thus, the generation of the 20 kDa fragment of the imported Tim21 upon Proteinase K treatment suggests that the C-terminus of Tim21 contains a folded domain resistant to protease activity.

Integration of Tim21 with the membrane was analyzed by incubating mitochondria at high pH (Figure 3.4B). Tim21 was recovered in the membrane fraction along with proteins from the outer membrane, Tom70, and from the inner membrane, Tim50, while the matrix protein Hep1 was recovered in the soluble fraction.

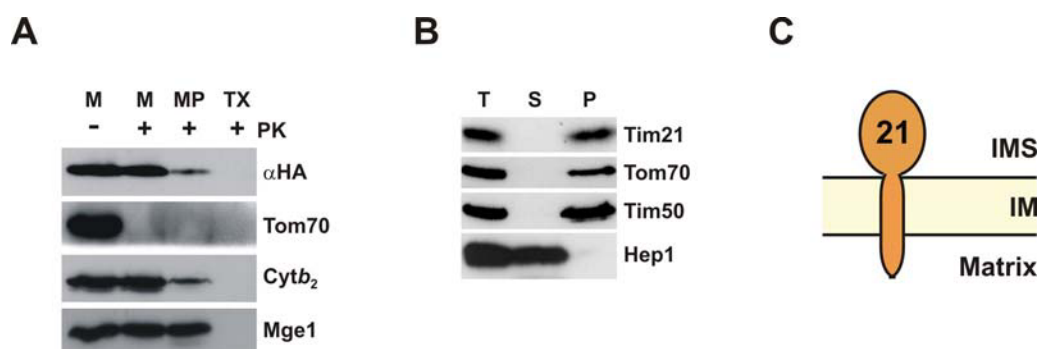


Figure 3.4. Localization and topology of Tim21. (A) Mitochondria isolated from the strain expressing Tim21 with HA tag on the C-terminus were solubilized in isotonic or hypotonic buffer. Mitochondria and mitoplasts prepared by hypotonic swelling were incubated with or without proteinase K (PK). Samples were analyzed by SDS-PAGE and immunodecoration with indicated antibodies. M, mitochondria; MP, mitoplasts; TX, mitochondria solubilized in 1% solution of Triton X-100. (B) WT mitochondria were subjected to carbonate extraction, and the supernatant (S) and pellet (P) fractions were separated by centrifugation. Samples were analyzed by SDS-PAGE and immunodecoration with the indicated antibodies. (C) Schematic representation of the localization and the topology of Tim21.

Taken together, these data demonstrate that Tim21 is spanning the inner membrane with its C-terminus located in the intermembrane space (Figure 3.4C).

3.4. Tim21 is a component of the TIM23 complex

To characterize the interaction of Tim21 with the components of the TIM23 complex wild type mitochondria were lysed with digitonin and subjected to immunoprecipitation with affinity purified antibodies against Tim17, Tim23, Tim16 and preimmune serum as a control. Antibodies against Tim17, Tim23 and Tim16 were previously shown to precipitate all known components of the translocase with different efficiencies due to the reported instability of the complex upon solubilization (Kozany *et al.*, 2004). After immunoprecipitation supernatant and pellet fractions were subjected to SDS-PAGE and analyzed by immunodecoration (Figure 3.5). Antibodies against Tim17 precipitated over 80% of the entire Tim21 from the supernatant, while they depleted both Tim17 and Tim23. The same result was obtained when antibodies against Tim23 were used for precipitation. A small amount of Tim21 was precipitated with antibodies against Tim16. Thus, the same pattern of immunoprecipitation was observed in case of Tim21 as in case of Tim17 and Tim23.

In summary, Tim21 is a novel subunit of the TIM23 translocase, more specifically a component of the membrane part of the complex that also interacts with the components of the import motor.

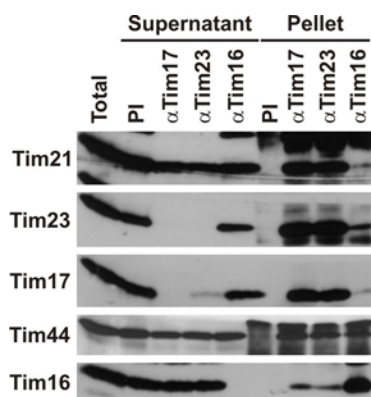


Figure 3.5. Coimmunoprecipitation of Tim21 with the TIM23 complex. Wild type yeast mitochondria were solubilized with digitonin and incubated with antibodies against Tim17, Tim23, Tim50 and preimmune IgGs (PI) prebound to Protein A-sepharose beads. Supernatants were separated, beads were washed and bound proteins directly eluted with Laemmli buffer. Total and supernatants were diluted with Laemmli buffer and represent 20% of the materials present in pellets. All the fractions were analyzed by SDS-PAGE and immunodecoration with the indicated antibodies.

3.5. Tim21 binds to the Tim17-Tim23 core of the TIM23 complex

To analyze the nature of association of Tim21 with the translocase in more detail, a series of coimmunoprecipitation experiments were performed in different types of mitochondria depleted of each of the essential subunits of the TIM23 complex. In mitochondria lacking Tim17 (Figure 3.6A), association of Tim21 with the other parts of the TIM23 complex was lost. The same result was obtained in mitochondria depleted of Tim23 (Figure 3.6B). Interestingly, removal of Tim50, another subunit of the membrane part of the translocase, affected neither the association of Tim21 with the complex, nor the binding of the import motor to the membrane part (Figure 3.6C), indicating that only Tim17 and Tim23, but not the entire membrane part of the complex, are the binding partners for Tim21. In contrast, no difference in the association of Tim21 with the TIM23 complex was seen when any of the import motor components was depleted from the complex (Figures 3.6D-F). This excludes the existence of a binding site for Tim21 in the import motor of the TIM23 translocase.

On the other hand, the disruption of the Tim17-Tim23 core led to dissociation of the motor components (Tim44 and Tim16) from the membrane sector. Complete dissociation of the import motor from the membrane part of the complex was also observed in mitochondria depleted of Tim44, whereas in mitochondria depleted of Tim16 or Tim14, the association of Tim44 for the Tim17-Tim23 core was not affected. Taken together, these observations are in accordance with the already reported association of the motor with the membrane part of the complex via Tim44 (Kozany *et al.*, 2004). However, direct interaction of the Tim14-Tim16 subcomplex with the Tim17-Tim23 core of the complex cannot be excluded.

Recently a new component of the TIM23 complex was discovered and named Pam 17 (van der Laan *et al.*, 2005). When coimmunoprecipitation as described above was applied to investigate the association of Pam17 with the TIM23 complex, the same result was obtained

as in case of Tim21 (Popov-Čeleketić *et al.*). Apparently, both Tim21 and Pam17 bind to the Tim17-Tim23 core of the TIM23 complex and this association is not dependent on any other known essential component of the complex.

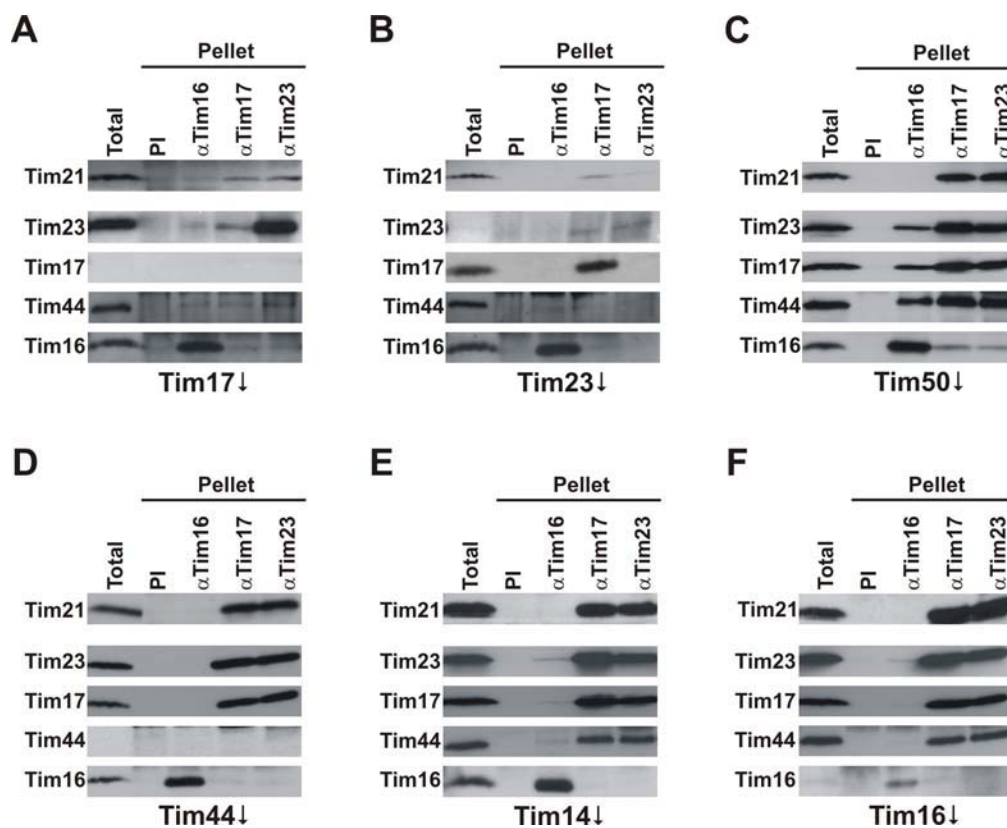


Figure 3.6. Tim21 interacts with the Tim17-Tim23 core of the TIM23 complex. Mitochondria isolated from cells depleted of the TIM23 components Tim17 (A), Tim23 (B), Tim50 (C), Tim44 (D), Tim14 (E) or Tim16 (F) were solubilized with digitonin and incubated with the affinity purified antibodies against Tim16, Tim17, Tim23 or antibodies from preimmune serum (PI) as a control. The beads were centrifuged, washed and bound proteins eluted with Laemmli buffer. Samples were analyzed by SDS-PAGE and immunodecoration with the indicated antibodies. Total fractions represent 20% of the material used for immunoprecipitations.

Taken together, both Tim21 and Pam17 are members of the membrane part of the TIM23 translocase that associate with the Tim17-Tim23 core of the complex.

3.6. The import motor is connected with the membrane part of the TIM23 complex in two ways

A truncated version of Tim23 protein lacking the first 50 amino acid residues and having a His₉ tag on its C-terminus was cloned in a single copy plasmid and used for transformations of *wt* YPH499 and *Tim17*↓ yeast cells to confirm the binding of both Tim21 and Pam17 to Tim17-Tim23 core of the TIM23 complex. The strains generated contained both full length

and a His-tagged truncated version of Tim23 protein. Mitochondria isolated from these strains were solubilized in digitonin, incubated with Ni-NTA agarose and proteins retained on the beads were eluted with imidazole in high concentrations (Figure 3.7). The vast majority of total Tim21 in WT mitochondria was specifically eluted with Tim23 Δ 50His₉, while only minor amounts of Pam17 were found associated with the TIM23 complex. However, both Tim21 and Pam17 were both virtually absent in the elution fraction from mitochondria depleted of Tim17, demonstrating that the disruption of Tim17-Tim23 core leads to dissociation of both Tim21 and Pam17 from the TIM23 complex.

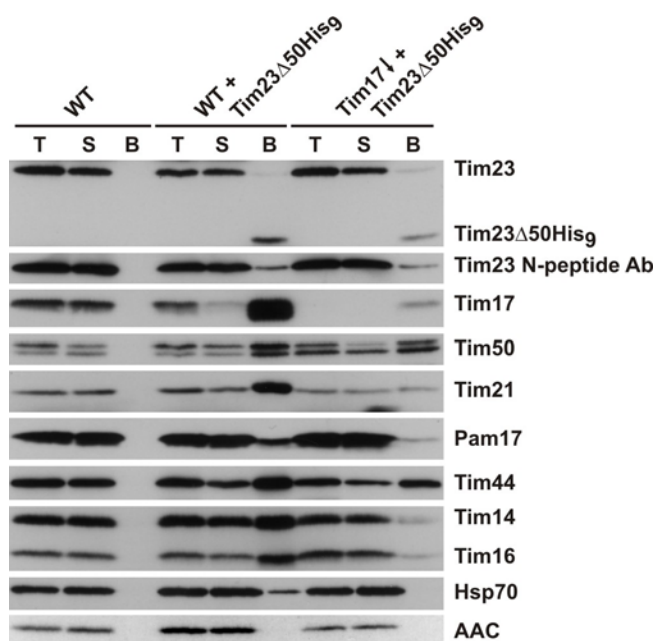


Figure 3.7. The import motor is connected with the membrane part of the complex via Tim17. Mitochondria isolated from wild type cells and cells expressing a version of Tim23 lacking the first 50 amino acid residues and containing the C-terminal His₉ tag either in the wild type or Tim17 \downarrow background were solubilized in digitonin containing buffer and incubated with NiNTA agarose. Bound material was eluted with Laemmli buffer containing 300mM imidazole. Samples were analyzed by SDS-PAGE and immunodecoration with antibodies against the N-terminal peptide of Tim23. Total (T) and supernatant (S) represent 5% of the material bound to NiNTA beads (B).

The amounts of full length Tim23 eluted together with its truncated version remained the same irrespective of the depletion of its major interacting partner Tim17. While Tim23 dimerization in the TIM23 complex was reported to be dependent on the membrane potential across the inner membrane and the binding of preprotein in transit for the TIM23 translocase (Bauer *et al.*, 1996), removal of Tim17 from the complex apparently does not affect the intensity or the stability of this dimerization. Also, the levels of Tim50 remained the same in both types of mitochondria. In contrast, the amounts of eluted Tim44 were slightly reduced in mitochondria depleted of Tim17, whereas Tim14 and Tim16 were virtually absent in the

elution fraction from Tim17↓ mitochondria. Thus it seems that Tim14 and Tim16 are connected with the membrane part of the translocase directly via Tim17 in addition to the already reported association involving Tim44 (Kozany *et al.*, 2004). This result was substantiated by the observed lack of association of mtHsp70 with the membrane part of the complex in Tim17↓ mitochondria.

Taken together, the import motor components are associated with the Tim17-Tim23 core of the TIM23 complex in two ways, via Tim44 and via the Tim14-Tim16 subcomplex. In contrast, the binding site for Tim21 and Pam17 is limited to the core of the translocase.

3.7. The nature of the tag affects the association of Tim21 with the rest of the translocase

To verify the association of Tim21 with the TIM23 complex, two yeast strains having C-terminally tagged Tim21 were generated, one with a His₆ tag and the other one with a Protein A tag. Mitochondria were isolated, solubilized with digitonin, and incubated with Ni-NTA-Agarose or IgG-Sepharose beads, respectively. Beads were washed and bound proteins were eluted with high imidazole or H⁺ concentrations (Figure 3.8).

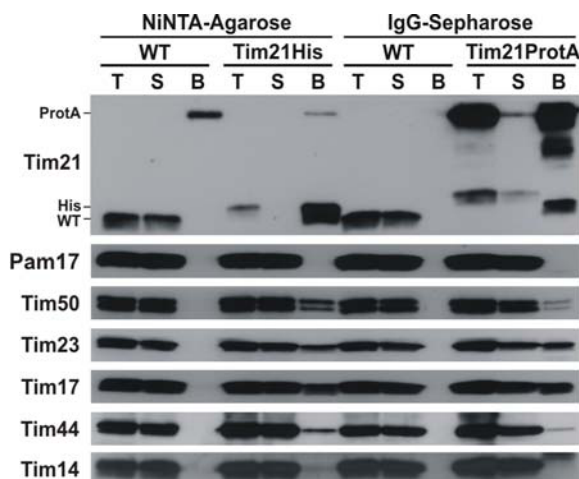


Figure 3.8. Protein A tagging of Tim21 could lead to false negative results. Mitochondria isolated from wild type and cells expressing Tim21 with C-terminal His₆ or Protein A tag were solubilized with digitonin and incubated with Ni-NTA-Agarose or IgG-Sepharose beads, respectively. Samples were analyzed by SDS-PAGE and immunodecoration with the indicated antibodies. Total (T) and supernatant (S) fractions contain 5% of the material present in the bound (B) fraction.

Tim21His₆ could coisolate Tim50, Tim23, and Tim17, but also Tim44, an import motor component, in significant amounts. Pull down on Protein A tag in Tim21 gave the same result

as far as Tim17 and Tim23 are concerned. However, the amounts of coprecipitated Tim50 and Tim44 were considerably reduced compared to the precipitation done with Tim21His. This result suggests that the nature of the tag on Tim21 may have adverse effects on the coisolation of other components of TIM23 translocase, leading to false negative results as in the case of the Protein A tag on its C-terminus. Interestingly, no coisolation of Pam17 with Tim21 could be observed. When Ni-NTA pull down was performed with mitochondria isolated from a yeast strain expressing His-tagged Pam17, Tim50, Tim23 and Tim17 were coisolated, but no significant amounts of Tim21, Tim44, Tim16 and Tim14 were recovered in the bound fraction (Popov-Čeleketić *et al.*).

Taken together, Tim21 is present in the TIM23 complex with all the essential components both of the import motor and of the membrane part. On the other hand, copurification of Tim21 and Pam17 could not be observed under all conditions tested.

3.8. Tim21 connects the TIM23 and the TOM complexes

As Tim21 is a conserved protein with a clear sequence similarity in its C-terminal domain that is located in the intermembrane space (IMS), this domain might be important for the role of Tim21 within the TIM23 complex. To identify the interacting partners of Tim21 in the IMS, its C-terminal domain carrying an N-terminal His₆ tag was expressed in *E. coli* cells, purified to homogeneity and bound to Ni-NTA agarose (Figure 3.9A). Mitochondria isolated from *wt* strain were lysed with digitonin and incubated with Ni-NTA-agarose beads with or without immobilized Tim21_{IMS} (Figure 3.9B). Surprisingly, only a small portion of Tim50 was bound to Tim21_{IMS} whereas the other components of the TIM23 complex were barely present, if at all, in the bound fraction. This indicates that the IMS exposed domain of Tim21 is not involved in the association of Tim21 with the TIM23 complex. Instead, the components of the TOM complex, Tom40 and Tom22, were specifically enriched in the bound fraction, demonstrating that C-terminus of Tim21 directly interacts with the TOM complex. Importantly, this is the first direct interaction between the TIM23 and the TOM complex observed so far.

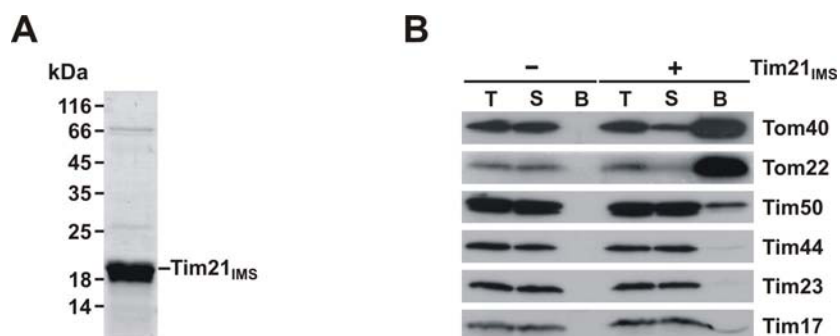


Figure 3.9. The intermembrane space domain of Tim21 interacts with the TOM complex. (A) Coomassie Brilliant Blue stained gel of the recombinantly expressed and purified intermembrane space domain of Tim21 (Tim21_{IMS}). **(B)** Ni-NTA-agarose with or without immobilized Tim21_{IMS} was incubated with solubilized wild type mitochondria. Bound proteins were eluted with Laemmli buffer containing 300mM imidazole. Samples were analyzed by SDS-PAGE and immunodecoration with the indicated antibodies. 5% of total (T) and supernatant (S) fractions and 100% of the bound (B) material were loaded.

To determine the minimal domain of Tim21 which can still interact with the TOM complex, two truncated versions of Tim21 IMS domain were made. A version of IMS domain lacking the last 14 amino acid residues (Tim21_{IMSΔ14}) and another one lacking the last 23 amino acid residues of the C-terminus (Tim21_{IMSΔ23}) and containing an N-terminal His₆ tag each were expressed in *E. coli* cells and purified to homogeneity. Equimolar amounts of these purified domains together with full length Tim21_{IMS} were immobilized on Ni-NTA-agarose. Wild type mitochondria were lysed with digitonin and incubated with beads with or without immobilized IMS domains of Tim21 (Figure 3.10A). Tom40 was present in both Tim21_{IMS} and Tim21_{IMSΔ14} elution fractions, but not in the case when 23 amino acid residues were deleted from the C-terminus of Tim21. In contrast, Tim50 was bound to all three types of immobilized beads.

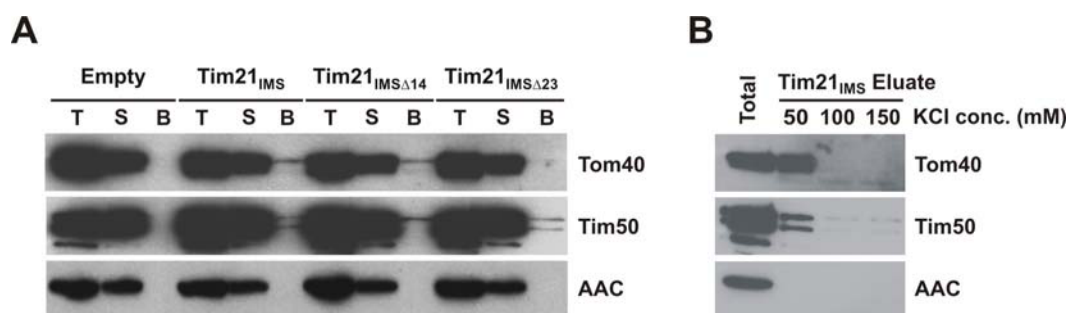


Figure 3.10. Tim21_{IMS}-TOM interaction is more sensitive than Tim21_{IMS}-Tim50 interaction. (A) Empty or Ni-NTA-agarose immobilized with intact or truncated versions of Tim21_{IMS} was incubated with wild type mitochondria solubilized in Tris buffer with 10mM imidazole pH 7.5 and 80 mM KCl. **(B)** Ni-NTA-agarose with immobilized Tim21_{IMS} was incubated with wild type mitochondria solubilized in Tris buffer with 10mM imidazole pH 7.5, containing different concentrations of KCl. In both experiments bound proteins were eluted with Laemmli buffer containing 300mM imidazole. Samples were analyzed by SDS-PAGE and immunodecoration with the indicated antibodies. 10% of total fractions and 100% of the eluted material were loaded.

In addition, binding experiments were performed in the presence of various salt concentrations to investigate the nature of Tim21_{IMS} interactions with the TOM and the TIM23 complexes (Figure 3.10B). The interaction of Tim21 with the TOM complex is very salt sensitive and it is lost already at the 100mM NaCl concentration. Although TIM23 complex shows much lower affinity to for Tim21_{IMS} than the TOM complex, this interaction persists at higher salt concentrations.

To conclude, the intermembrane space domain of Tim21 interacts with the protein components of the TOM complex *in vitro*, presumably with its *trans* binding site and this interaction is salt dependent. This result suggests that Tim21 has a role in tethering TIM23 and TOM complexes together.

3.9. Tim21 is not essential for yeast cell viability

To establish the importance of Tim21 for the growth of yeast cells, a strain was made in which *TIM21* gene was deleted by homologous recombination. When the cells from $\Delta tim21$ strain were grown on both fermentable and nonfermentable solid media no growth defect was visible. Shifting cells at to elevated temperatures induced no growth defect either (Figure 3.11A). When these strains were transferred in to liquid media, $\Delta tim21$ cells grew normally at 30°C in both YPD and YPG medium. Surprisingly, when cells grown in nonfermentable medium YPG were shifted to 37°C $\Delta tim21$ grew faster than *wt* strain (Figure 3.11B).

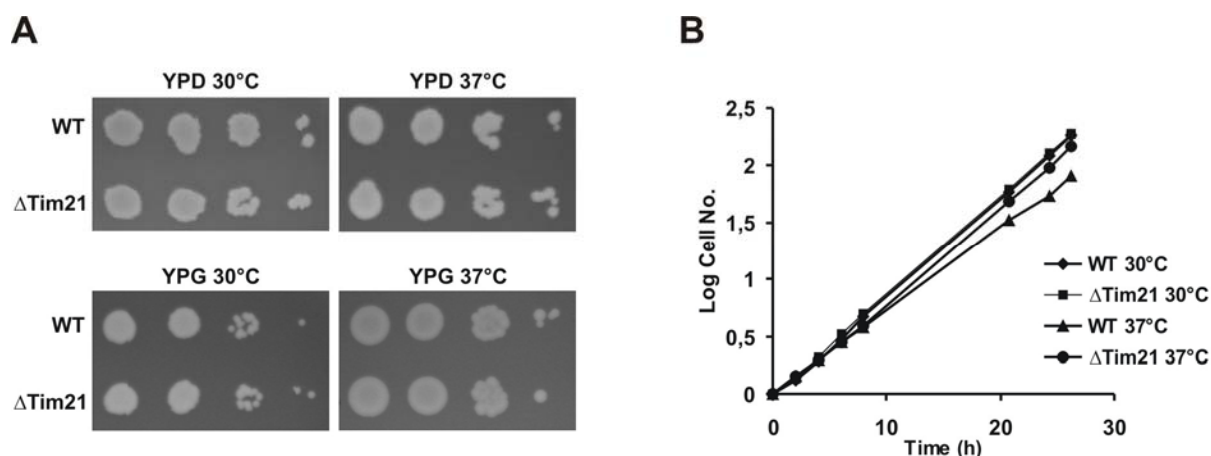


Figure 3.11. Phenotype of $\Delta tim21$ strain. (A) Yeast cells of *wt* and $\Delta tim21$ strains were grown for 24h in YPGal medium, diluted to identical $OD_{578} = 0,489$ and then, a series of 1:10 dilutions were made for each strain. 4 μ l of each dilution were loaded as drops on previously dried plates and incubated for two (YPD) or three days (YPG medium) at designated temperatures. (B) Yeast cells from *wt* and $\Delta tim21$ strains were grown for 18h in YPGal medium at 30°C, then washed with sterile water and transferred to either YPD or YPG liquid medium, diluted to $OD_{578} = 0,11-0,12$ and grown at indicated temperatures for 26h. Cell growth was measured spectrophotometrically, whereas at time zero cell number was calculated as one.

Thus, Tim21 is the first component of the TIM23 complex that is not essential for viability of yeast cells. In addition, the absence of Tim21 seems to have positive effect on cell growth at elevated temperatures.

3.10. Deletion of Tim21 affects neither the function nor the assembly of the TIM23 complex

As all the other known components of the TIM23 complex are essential for cell viability and protein import into mitochondria, the relevance of Tim21, as the first nonessential component of the TIM23 complex, for the process of protein import was questioned. To analyze the influence of Tim21 on import of preproteins via the TIM23 complex, different preprotein substrates were imported into mitochondria isolated from $\Delta tim21$ and *wt* yeast strains prepared in parallel.

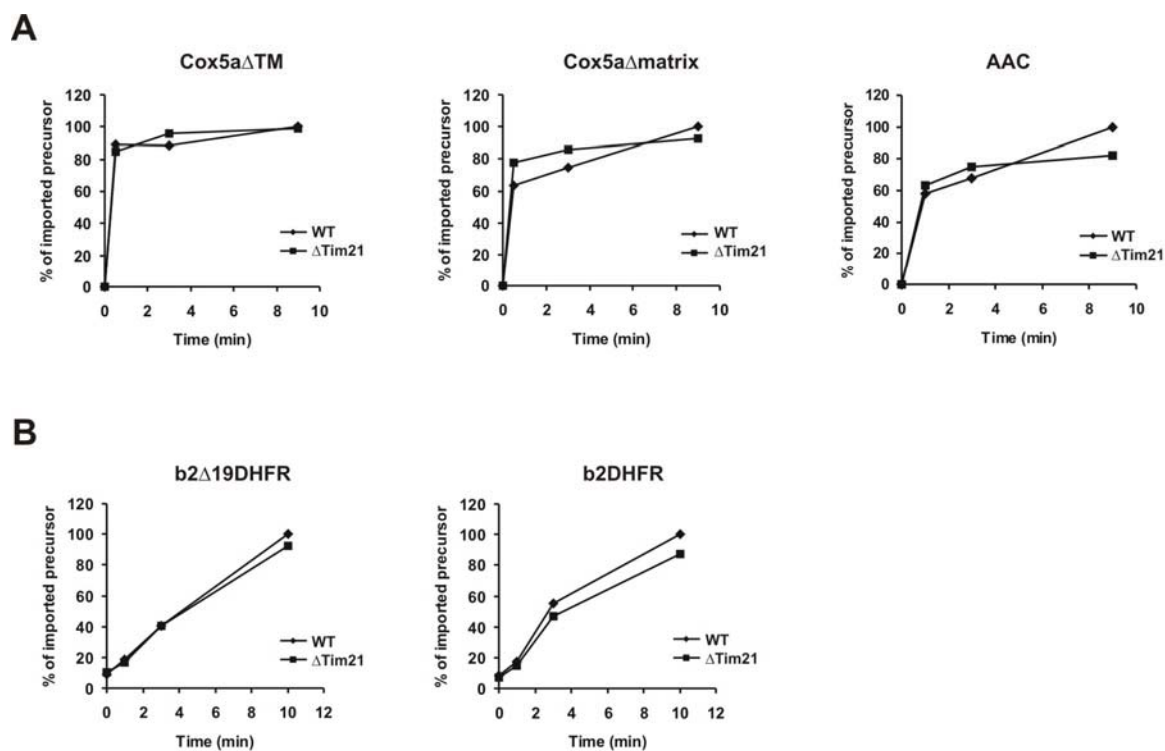


Figure 3.12. Imports of different precursors in WT and Δ Tim21 mitochondria. (A) Cox5a Δ TM and Cox5a Δ matrix [35 S] radiolabeled precursors were imported in *wt* and Δ Tim21 mitochondria at 10°C. After 30 sec., 3 and 9 min. import was stopped with 10 times the amount of ice cold SH buffer. (B) Two step import of [35 S] radiolabeled precursors b₂ Δ 19DHFR and b₂DHFR. Mitochondria were incubated for 15 min. at 25°C in the absence of $\Delta\Psi$, subsequently centrifuged, washed with SH buffer containing 80mM KCl, reisolated and then $\Delta\Psi$ was restored. After 0 sec., 1, 3 and 10 min. import was stopped with 10 times the amount of ice cold SH buffer. In A and B samples were analyzed by Urea-SDS-PAGE and SDS-PAGE, respectively and autoradiography.

Mitochondria lacking Tim21 imported all the substrates with the same efficiency as mitochondria isolated from the *wt* strain, irrespective of the final destination of the substrates, i.e. whether they end up in the matrix, like Cox5a Δ TM, the precursor to yeast cytochrome c oxidase subunit Va with a deleted transmembrane domain (amino acid residues 101-118), or they get laterally sorted in the inner mitochondrial membrane without the help of the import motor, like Cox5a Δ matrix, the precursor to yeast cytochrome c oxidase subunit Va with deleted amino acid residues 26-89. Import of AAC, a precursor of ATP-ADP carrier, which uses TIM22 complex for import, served as a control (Figure 3.12A). To confirm the absence of import defect of mitochondria lacking Tim21 in a more sensitive manner, precursors were imported in two steps. In this assay, WT and Δ Tim21 mitochondria were incubated with radiolabeled preprotein for 15 min. in the absence of $\Delta\Psi$. Upon traversing the outer membrane, precursor was accumulated at the *trans* side of the TIM23 translocase. Mitochondria were then reisolated and the $\Delta\Psi$ across the inner membrane was restored enabling the passage of the precursor through TIM23 pore. Mitochondria isolated from Δ *tim21* strain showed no difference in import function compared to WT mitochondria for both laterally sorting precursor b₂DHFR consisting of the N-terminal 167 amino acid residues of yeast cytochrome b₂ fused to mouse full length dihydrofolate reductase (DHFR) and matrix destined precursor b₂ Δ 19DHFR differing from the previously described one in deletion of its hydrophobic sorting signal (Figure 3.12B). Taken together, the absence of Tim21 does not affect the efficiency of import of any type of mitochondrial preproteins which use the TIM23 translocase.

To investigate the effect of the deletion of Tim21 on the assembly of the TIM23 complex mitochondria isolated from both *wt* and Δ *tim21* strains were lysed with digitonin and subjected to immunoprecipitation with the antibodies against Tim16, Tim17, and the preimmune serum as a control (Figure 3.13). All the components of the TIM23 complex were precipitated in the same amounts in both types of mitochondria, demonstrating that the absence of Tim21 does not affect the stoichiometry of the translocase.

To conclude, in addition to the lack of negative effect of the deletion of Tim21 on the cell growth, mitochondria lacking Tim21 import all types of preproteins with the same rate and the assembly of the TIM23 complex does not seem to be affected in these mitochondria.

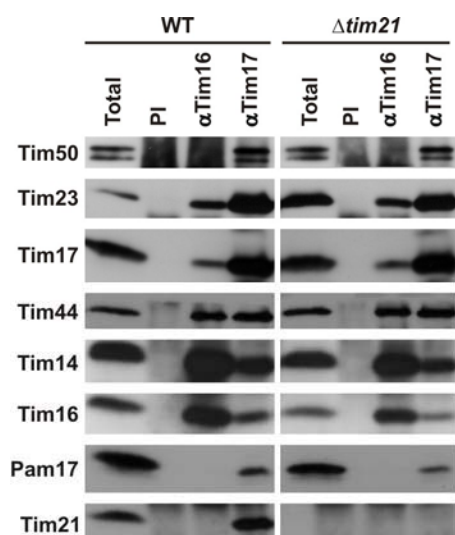


Figure 3.13. Deletion of Tim21 does not affect the stoichiometry of the TIM23 complex. Mitochondria were solubilized with digitonin and incubated with antibodies against Tim16, Tim17 and preimmune IgGs (PI) prebound to Protein A-sepharose beads. Beads were washed and bound proteins directly eluted with Laemmli buffer. Total fractions were diluted with Laemmli buffer and represent 20% of the materials present in pellets. All the fractions were analyzed by SDS-PAGE and immunodecoration with the indicated antibodies.

3.11. Overexpression of Tim21 changes the conformation of the TIM23 complex

Although deletion of Tim21 does not affect the assembly of the TIM23 complex, the role of Tim21 in the conformational organization of the translocase could not be excluded. Before addressing this issue it was necessary to establish the adequate assay for the analysis of the conformational state of the TIM23 complex in different conditions. The crosslinking approach was already used to show conformational reorganization in import motor induced by depletion of one of its components (Kozany *et al.*, 2004, Mokranjac *et al.*, 2003b). As Tim21 is the member of the membrane part of the translocase, an optimization of a crosslinking assay based on one of the membrane embedded components of the complex was the tool of choice for the analysis of the possible conformational changes of the TIM23 complex induced by various amounts of Tim21 present in mitochondria.

It was previously published that incubating WT mitochondria with small amounts of chemical crosslinker disuccinimidylglutarate (DSG) gives a defined pattern of Tim23 crosslinking adducts (Bauer *et al.*, 1996). However, only Tim23-Tim23 dimer was identified, whereas a smaller crosslinking adduct of ca. 44 kDa remained uncharacterized. Since Tim23 crosslinks were the best candidate for investigating conformational changes in the membrane part of the TIM23 complex it was important to optimize these experiments. Different amounts of added crosslinker gave the same crosslinking pattern, with the increase in intensity of the crosslinking adducts with higher concentrations of DSG. Three crosslinking adducts were observed: the highest one of ca. 54 kDa that corresponded to the previously reported Tim23-Tim23 dimer (Bauer *et al.*, 1996), the major one of ca. 44 kDa and the weakest and the lowest

one of ca. 33 kDa (Figure 3.14). Final concentration of 150 μ M DSG was estimated to be optimal as the sensitivity of the assay was increasing with lower concentrations of DSG and nonspecific bands that might occur upon the addition of higher concentrations of chemical crosslinking reagent were excluded. Lowering DSG concentration below 150 μ M, however, might lead to false negative results as the crosslinking products disappeared.

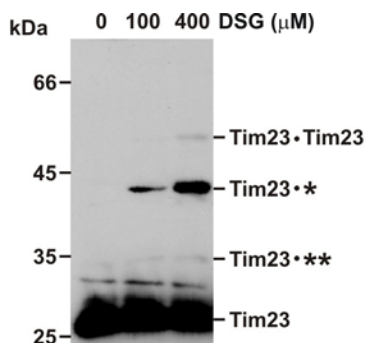


Figure 3.14. Tim23 crosslinking pattern. Mitochondria isolated from wild type cells were incubated with increasing concentrations of DSG and analyzed by SDS-PAGE and immunodecoration with antibodies against N-terminal part of Tim23. The crosslinking products are indicated.

To investigate the environment of Tim23 in mitochondria with different amounts of Tim21, the strain expressing *TIM21* gene from a strong *ADH* promoter was generated. Mitochondria isolated from *wt*, Δ *tim21* and *tim21* \uparrow strains were incubated with DSG and the possible changes in the environment of Tim23 were subsequently observed. Both WT and Δ Tim21 mitochondria gave the same crosslinking pattern of Tim23 indicating that the removal of Tim21 from the TIM23 complex does not lead to significant conformational changes of Tim23. In contrast, overexpression of Tim21 in mitochondria led to a strong increase of Tim23-Tim23 crosslinked dimer and to a drastic decrease of crosslinking adduct of ca. 44 kDa (Figure 3.15).

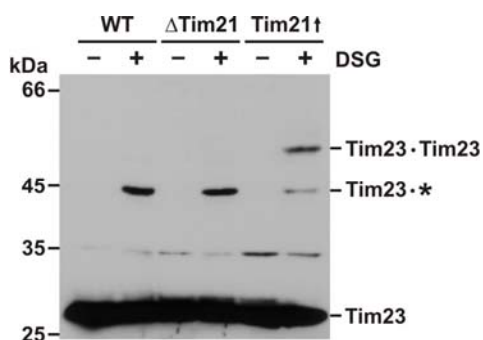


Figure 3.15. Overexpression of Tim21 changes the conformation of the TIM23 complex. Mitochondria isolated from wild type or cells where Tim21 is deleted or overexpressed were incubated with DSG and analyzed by SDS-PAGE followed by immunodecoration with antibodies against Tim23. The crosslinking products are indicated.

Interestingly, while the deletion of Tim21 does not seem to affect the functionality or the structural organization of the translocase, mitochondria isolated from cells expressing Tim21

from the strong promoter contain TIM23 complex in the significantly different conformation to one seen in WT mitochondria.

3.12. Pam17 is the major crosslinking partner of Tim23

The major crosslinking adduct of ca. 44 kDa could, according to its size, correspond to both Tim23-Tim17 and Tim23-Pam17 adducts. It was speculated that the former adduct is more probable, because Tim17 and Tim23 are forming the translocating pore (Pfanner and Geissler, 2001), they are major interacting partners within the complex and their equimolar amounts form a subcomplex (Moro *et al.*, 1999). However, the attempts to confirm this notion were unsuccessful. Therefore, it was tested if the crosslink of ca. 44 kDa is the crosslinking adduct of Tim23 with Pam17. Crosslinking was performed in both WT and mitochondria containing Pam17 with a His₆ tag on the N-terminus (Figure 3.16). Surprisingly, the major crosslinking adduct of ca. 44 kDa was identified as a crosslink of Tim23 to Pam17. Taken into account that the weak crosslinking adduct of ca. 33 kDa is to none of the known components of the TIM23 translocase, Tim23 appears to be crosslinked to neither of its two major known interacting partners, Tim17 and Tim50 under the experimental conditions used. This feature of Tim23, moreover the feature of the proteins from the membrane part of the TIM23 complex, is in contrast to import motor components that are successfully crosslinked among each others.

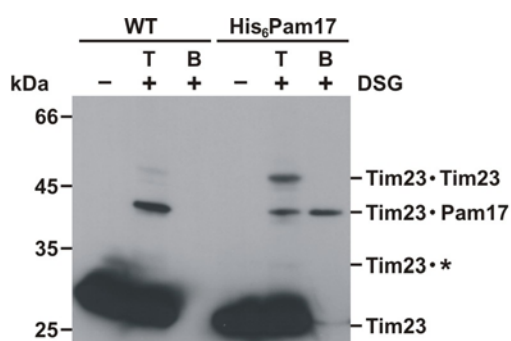


Figure 3.16. Pam17 is the major crosslinking partner of Tim23. Mitochondria isolated from wild type and cells expressing Pam17 with N terminal His₆ tag were incubated with 200μM DSG and incubated with Ni-NTA agarose. After elution from the beads samples were analyzed by SDS-PAGE and immunodecoration with antibodies against Tim23. The crosslinking products are indicated.

To conclude, Pam17 is the major crosslinking partner of Tim23 which is quite an unexpected result concerning the fact that only a minor amount of total Pam17 is present in the TIM23 complex.

3.13. Binding of Tim21 and Pam17 to the TIM23 complex is mutually exclusive

The disappearance of Tim23-Pam17 crosslinking adduct induced by overexpression of Tim21 may either represent the change in position between Pam17 and Tim23 or the overexpression of Tim21 leads to removal of Pam17 from the TIM23 complex. Several observations indicate that the latter possibility is more probable: both Tim21 and Pam17 are subunits of the membrane part of the translocase, they both bind to the Tim17-Tim23 core, but they could not be found in the same complex. To establish if the binding of one of them hampers the binding of another, the effects of the overexpression of these proteins on the assembly of the TIM23 complex were analyzed. Mitochondria containing overexpressed Pam17, Tim21, or both were solubilized in digitonin and immunoprecipitated using the antibodies against Tim16 and Tim17 (Figure 3.17A). Overexpression of Tim21 did not lead to any changes in the stoichiometry of the essential components of the complex. All the essential components were also precipitated in the same amounts in Pam17 \uparrow and Pam17 \uparrow /Tim21 \uparrow mitochondria. However, several observations were made concerning the association of the nonessential components in these mitochondria. Increased levels of Tim21 led to more efficient coprecipitation of Tim21 with both Tim16 and Tim17 antibodies, whereas overexpression of Pam17 did not result in a higher efficiency of its coprecipitation with the rest of the TIM23 translocase. However, in Pam17 \uparrow mitochondria the amount of Tim21 precipitated with the TIM23 complex was significantly reduced. On the other hand, in Tim21 \uparrow mitochondria Pam17 was completely removed from the TIM23 complex observed, whereas in mitochondria with both Pam17 and Tim21 overexpressed, precipitation of Pam17 with the TIM23 complex was again visible, suggesting that increased levels of Pam17 led to the partial removal of the overexpressed Tim21 from the complex.

The same functional connection between Tim21 and Pam17 was observed when these mitochondria were analyzed by Blue Native electrophoresis (Figure 3.17B). The TIM23 complex dissociates into several subcomplexes when analyzed by this method (Chacinska *et al.*, 2003; Dekker *et al.*, 1997; Geissler *et al.*, 2002) and the major portion of Tim21 runs in the complex with Tim17-Tim23 core at ca. 170 kDa (Chacinska *et al.*, 2005; Tamura *et al.*, 2006). The formation of this complex was strongly increased in mitochondria lacking Pam17, whereas it was decreased in mitochondria overexpressing Pam17 when compared to WT situation. On the other hand Pam17 migrates as a ca. 50 kDa subcomplex (van der Laan *et al.*, 2005). Pam17 subcomplex is separate from all the other subcomplexes containing the

components of the TIM23 complex, but appears to be important for the association of Pam17 with the rest of the translocase. The formation of Pam17 subcomplex was greatly impaired in the mitochondria containing overexpressed Tim21 whereas it was promoted in the mitochondria lacking Tim21.

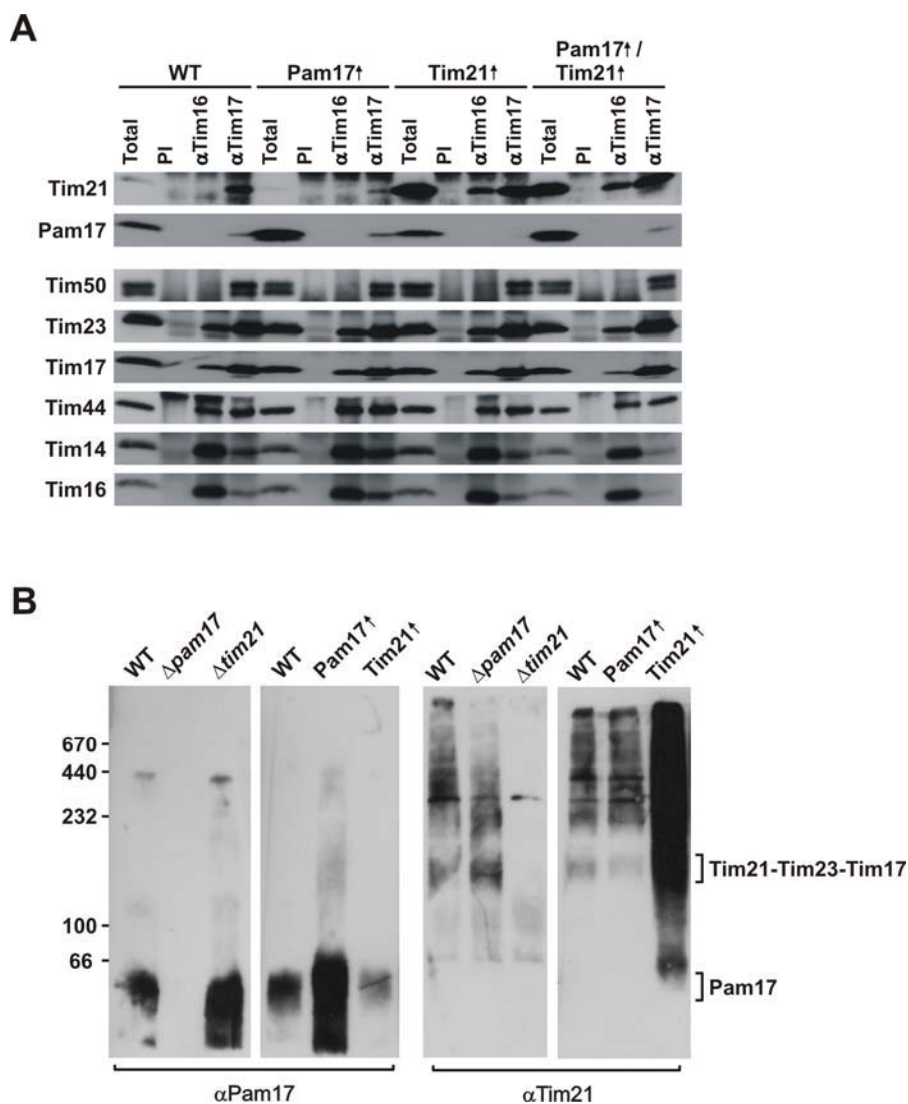


Figure 3.17. Presence of Tim21 and Pam17 in the TIM23 complex is mutually exclusive. (A) Mitochondria were solubilized with digitonin and subjected to immunoprecipitation with the antibodies against Tim16, Tim17 or with the preimmune serum (PI) as a control. Total (20%) and precipitated material were analyzed by SDS-PAGE and immunodecoration with indicated antibodies. **(B)** 50 μg of mitochondria were solubilized in buffer containing 1% digitonin, incubated on ice for 20 min and analyzed by Blue Native Gel electrophoresis (6-16.5% acrylamide gradient gel) and immunodecoration with antibodies against Pam17 and Tim21.

In conclusion, the presence of Tim21 and Pam17 in the TIM23 complex is mutually exclusive. Tim21 has somewhat higher affinity for the translocase, because the increase of its levels in the cell leads to the increased amount of Tim21 that associates with the translocase, which is not the case for Pam17. In addition, increased levels of Tim21 remove Pam17 from

the TIM23 complex completely, whereas upregulation of Pam17 removes Tim21 only partially.

3.14. Overexpression of Pam17 counteracts adverse changes of the TIM23 complex induced by the increased levels of Tim21

To study whether the overexpression of Pam17 counteracts conformational changes of the TIM23 complex induced by the increased levels of Tim21, mitochondria containing overexpressed Pam17, Tim21, or both were subjected to crosslinking with DSG (Figure 3.18). Crosslinking Tim23 in mitochondria with increased levels of Pam17 did not lead to any conformational change of Tim23, in contrast to the overexpression of Tim21 that leads to an increase of Tim23 crosslinked dimer and to a decrease of Tim23-Pam17 adduct. However, increasing the levels of Pam17 in mitochondria with high levels of Tim21 not only restores the Tim23-Pam17 adduct that was lost upon the overexpression of Tim21, but also restores the intensity of the Tim23 crosslinked dimer to the levels seen in WT conditions, indicating that the overexpression of Pam17 counteracts conformational changes induced by the increased levels of Tim21.

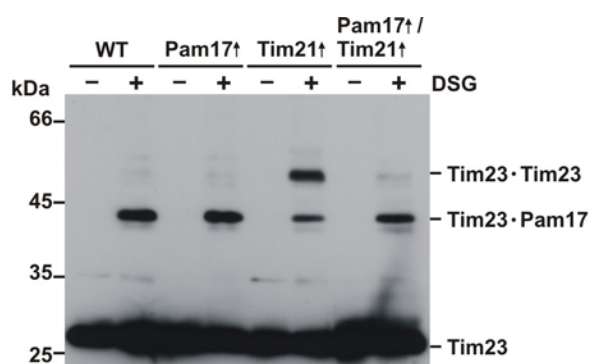


Figure 3.18. Conformational changes induced by overexpression of Tim21 are counteracted by overexpression of Pam17. Mitochondria were subjected to crosslinking with DSG and subsequently analyzed by SDS-PAGE followed by immunodecoration with antibodies against Tim23. The crosslinking products are indicated.

To investigate if the mutually exclusive binding of Tim21 and Pam17 for to the TIM23 complex represents the basis for the functional regulation of the protein import, different preproteins were imported in mitochondria with increased levels of Pam17 and/or Tim21.

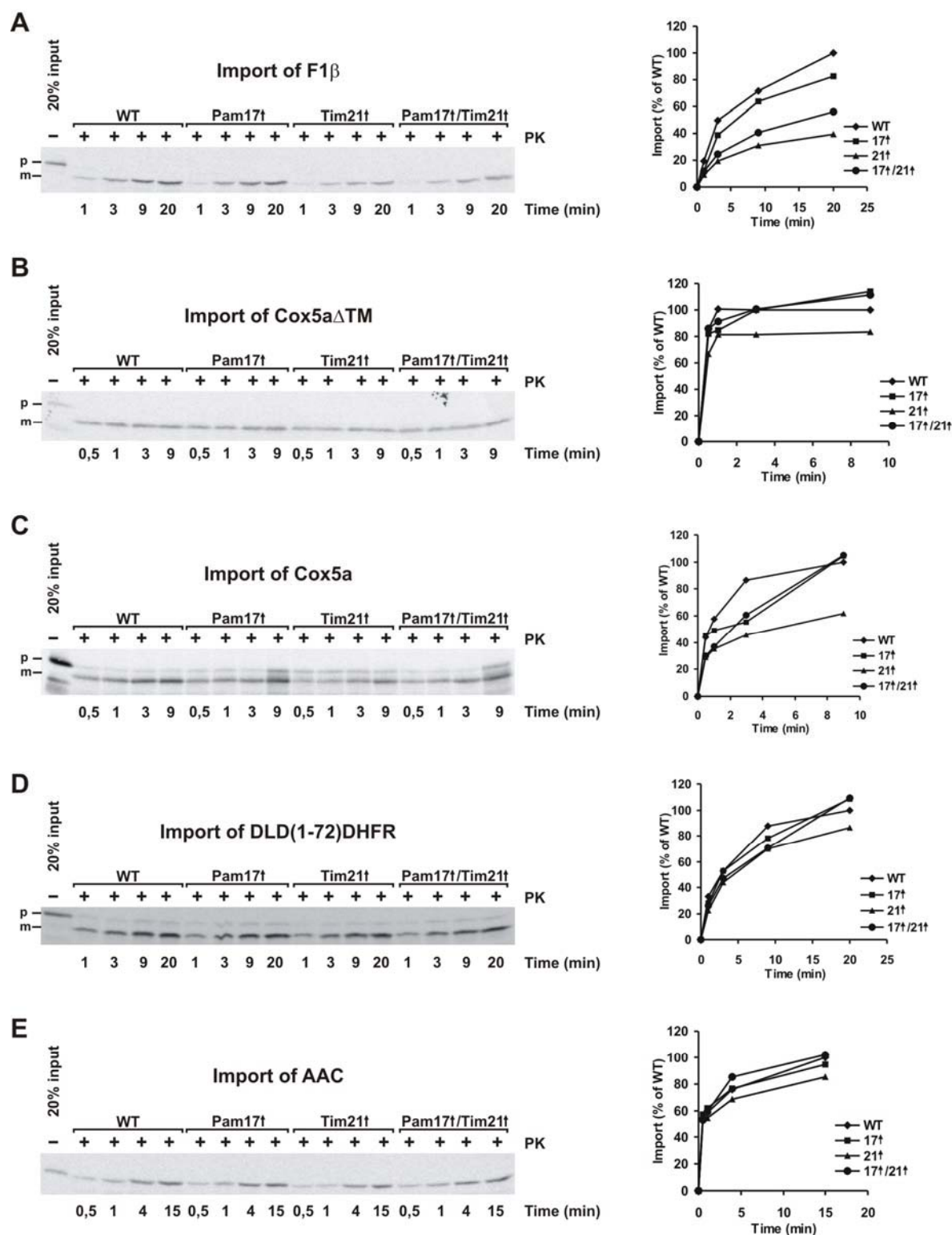


Figure 3.19. Overexpression of Pam17 reduces import defect in Tim21 \uparrow mitochondria. Various [35 S] labeled preproteins: F1 β (A), Cox5a Δ TM (B), Cox5a (C), DLD(1-72)DHFR (D) and AAC (E) were imported into isolated mitochondria followed by protease treatment, SDS-PAGE and autoradiography. The amount of protein imported into WT mitochondria after the last time point was set to 100%.

Increased levels of Pam17 did not affect the import process when any type of preproteins was used. On the other hand, the imports of motor dependent precursors were strongly reduced in Tim21 \uparrow mitochondria. The highest reduction of the import rate was observed in the case of F1 β subunit of the ATP synthase (Figure 3.19A), but the import was also significantly reduced when smaller preproteins that require the presence of the fully functional import motor were used, irrespective of their final destination, i.e. whether they end up in the matrix like Cox5a Δ TM (Figure 3.19B) or they get laterally sorted in the inner mitochondrial membrane like Cox5a (Figure 3.19C). Hence, although the association of the import motor components with the membrane sector is not affected and the stoichiometry of the TIM23 complex remains unchanged in Tim21 \uparrow mitochondria, the import efficiency of motor dependent precursors is reduced. Taken together, these results demonstrate that increased levels of Tim21 disturb the functional state of the translocase in addition to their effect on the conformation of the TIM23 complex.

However, the deficient import of matrix targeted preprotein F1 β was, at least partially, relieved by the additional overexpression of Pam17. Furthermore, when small motor dependent preproteins Cox5a Δ TM and Cox5a were imported in the isolated mitochondria, overexpression of Pam17 complements the import defect of Tim21 \uparrow mitochondria, restoring the import efficiency to the WT levels. In contrast, the import rates of a motor independent preprotein DLD(1-72)DHFR, consisting of D-lactate dehydrogenase fused to mouse DHFR, did not significantly differ between the four different types of mitochondria (Figure 3.19D): This indicates that the overexpression of Tim21 specifically affects only the import processes that include functional import motor. The import of control preprotein AAC, a substrate of the TIM22 translocase, was not affected either (Figures 3.19E).

Thus, the additional overexpression of Pam17 not only restores the conformation of the TIM23 complex, but also its functionality in Tim21 \uparrow mitochondria.

3.15. Deletion of Pam17 leads to a defective import of motor dependent preproteins

To investigate the role of Pam17 in the TIM23 complex, the import of preproteins into isolated mitochondria lacking Pam17 was observed. Different radiolabeled precursors were imported in parallel into the isolated mitochondria from the strains where *TIM21* or both *TIM21* and *PAM17* genes were deleted.

The import of F1 β , the precursor destined for the matrix, was severely affected in Δ Pam17 compared to WT mitochondria (Figure 3.20A). The import efficiency of Cox5a Δ TM, the preprotein that is also targeted to matrix but is much smaller and gets imported by at a higher rate than F1 β , was similarly affected (Figure 3.20B). In addition, the same effect was observed importing Cox5a, the preprotein that is laterally sorted in the inner mitochondrial membrane, but requires the presence of the fully functional import motor (Figure 3.20C). In contrast, the import of DLD(1-72)DHFR, the precursor that is laterally sorted in the inner mitochondrial membrane in a motor independent manner was not affected (Figure 3.20D). Additional deletion of Tim21 in cells already lacking Pam17 had no significant additional effect, neither positive nor negative, on the efficiency of the import process observed in Δ Pam17 mitochondria. As already shown here, import of all tested preproteins did not differ between WT and Δ Tim21 mitochondria. Import of precursor AAC, which does not require the TIM23 translocase was virtually identical in all four types of mitochondria (Figure 3.20E).

In summary, Pam17 is the only member of the membrane part of the complex whose deletion specifically affects only the import of the motor dependent preproteins. Interestingly, import efficiency of motor dependent preproteins in Δ Pam17 mitochondria is reduced in similar manner as in mitochondria isolated from cells where Tim21 was overexpressed.

3.16. Deletion of Pam17 changes the conformation of the TIM23 complex

Reduced efficiency of the import of the motor dependent preproteins was observed for both mitochondria lacking Pam17 and those with very high levels of Tim21. To compare the conformational state of the TIM23 complex in Δ Pam17 and Tim21 \uparrow mitochondria, crosslinking experiments with DSG were performed (Figure 3.21). Increased levels of Tim21 led to a decrease of intensity of the Tim23-Pam17 crosslinking adduct, in accordance with the mutually exclusive binding of Tim21 and Pam17 to the TIM23 complex. More importantly, the appearance of the Tim23 crosslinked dimer in Δ Pam17 mitochondria was of surprisingly similar intensity as the one in Tim21 \uparrow mitochondria, demonstrating that the deletion of Pam17 and the overexpression of Tim21 induce similar conformational changes of the TIM23 translocase.

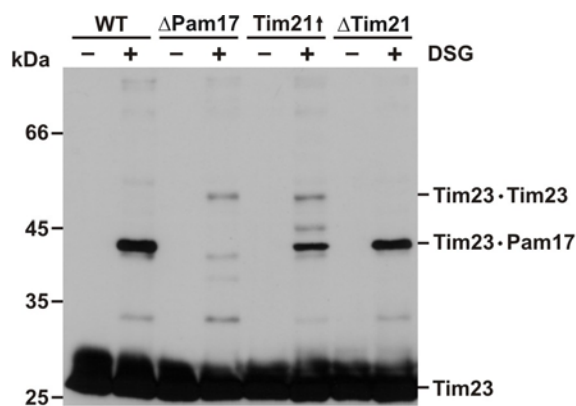


Figure 3.21. Deletion of Pam17 and overexpression of Tim21 induce very similar conformational change of Tim23. Mitochondria were subjected to crosslinking with DSG and subsequently analyzed by SDS-PAGE followed by immunodecoration with antibodies against Tim23. The crosslinking products are indicated.

The conformational change of the TIM23 complex seems to be the reason for defective import of matrix targeted preproteins as the stoichiometry of the essential components of the TIM23 complex remained unaltered in both Tim21 \uparrow and Δ Pam17 mitochondria (Popov-Čeleketić *et al.*). To corroborate this hypothesis, already established crosslinking assays were used to estimate if Pam17 is also involved in specific conformational changes of the import motor. Similarly to Tim23 crosslinking patterns, in Δ Pam17 as well as in Δ Pam17/ Δ Tim21 mitochondria Tim16-Tim16 crosslinks were increased on expense of Tim14-Tim16 adducts after the addition of DSG, whereas the ratio between the two adducts was 1:1 both in WT and Δ Tim21 mitochondria (Figure 3.22). However, this shift towards Tim16-Tim16 adduct represents conformational change along the Tim16-Tim16 interface of the Tim14-Tim16 tetramer, since the stability of this subcomplex was not affected after coimmunoprecipitation and in Tim14 crosslinking adducts (data not shown). Similarly, in mitochondria lacking Pam17 either alone or in combination with Tim21, the crosslinking profile of Tim44 was changed. However, Tim44-mtHsp70 complex was still present when analyzed by coimmunoprecipitation (Popov-Čeleketić *et al.*). Hence, the absence of Pam17 causes a structural reorganization of both the membrane embedded part and the import motor of the TIM23 complex, resulting in the reduced ability of the TIM23 complex to import motor dependent preproteins.

The results from the *in organello* import and crosslinking assays were in accordance with the results obtained *in vivo*. The growth of the strain with a deletion of *PAM17* gene is strongly impaired on any medium, especially when the cells are grown on a non-fermentable medium at elevated temperatures. In contrast, Δ tim21 cells grow even faster than *wt* in these conditions (see also above). However, additional deletion of *TIM21* gene does not improve the growth of Δ pam17 strain (Figure 3.23).

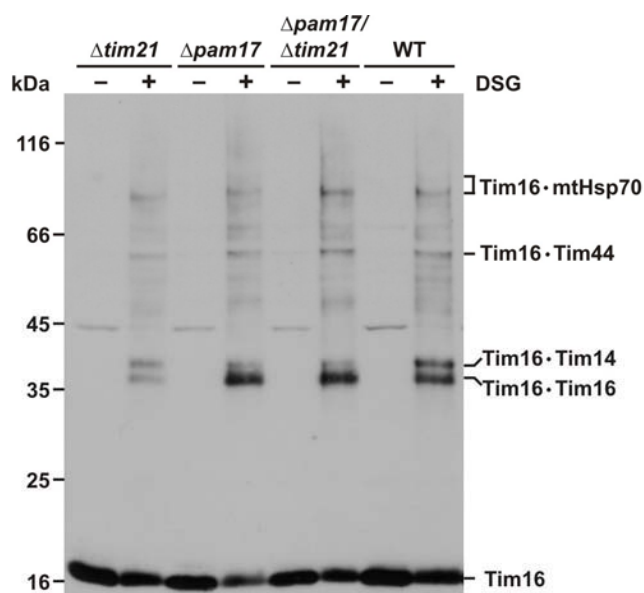


Figure 3.22. The import motor in mitochondria lacking Pam17 assumes altered conformation. Mitochondria were subjected to crosslinking with DSG and subsequently analyzed by SDS-PAGE followed by immunodecoration with antibodies against Tim16. The crosslinking products are indicated.

Additional deletion of *TIM21* gene cannot compensate the phenotype of *Δpam17* strain. On the other hand, overexpression of Pam17 compensates defective import and restores the altered conformation of the TIM23 complex in *Tim21*[↑] mitochondria. These results show on a functional level that the balance of two nonessential components is required for the optimal function of the TIM23 complex.

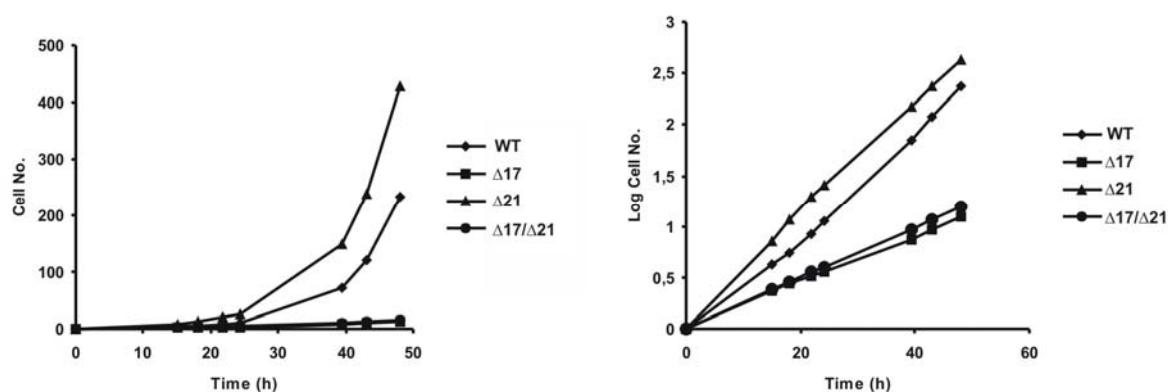


Figure 3.23. Phenotype of *Δpam17* cells can not be relieved by the additional deletion of Tim21. Yeast cells from *wt*, *Δpam17*, *Δtim21* and *Δpam17/Δtim21* strains were grown for 18h in YPGal liquid medium at 30°C, then washed with sterile water and transferred to YPG liquid medium, diluted to $OD_{578}=0,11-0,12$ and grown at 37°C for 48h. Cell growth was measured spectrophotometrically, whereas at time zero cell number was calculated as one. Logarithm of the increasing cell number in the function of growth period is shown on the right.

In summary, the presence of Pam17 is necessary for the optimal conformation of both the import motor and the membrane part of the TIM23 complex. Although Pam17 does not stabilize the assembly of the TIM23 translocase, it seems that Pam17 is involved in adequate

positioning of the import motor towards the membrane part of the complex. However, the activity of Pam17 is under negative regulation of Tim21, which is exhibited by competitive binding of both proteins for the same region of the TIM23 translocase and their balanced presence in the complex is required for its optimal function.

3.17. Analysis of the structural organization of the TIM23 complex during protein translocation

To investigate proposed regulation of the activity and the structural organization of the TIM23 complex during protein translocation in general, a method was developed to trap the complex in defined translocation states. Mitochondria were saturated *in vivo* with preproteins targeted either into the matrix or for the insertion into the inner membrane. To maintain mitochondria saturated preproteins were arrested within the TOM and the TIM23 complexes; the backsliding of the preprotein was prevented by folding of its C-terminal domain while the N-terminus was held by the TIM23 translocase itself. The TIM23 translocase was saturated either with preproteins that are laterally sorted in the inner mitochondrial membrane (L) or with those that are targeted to the matrix (M). Wild type mitochondria with arrested preproteins were analyzed in comparison with those with empty translocases (E) and those isolated under standard conditions (STD) that may still contain some amount of the preproteins in transit (Figure 3.24).

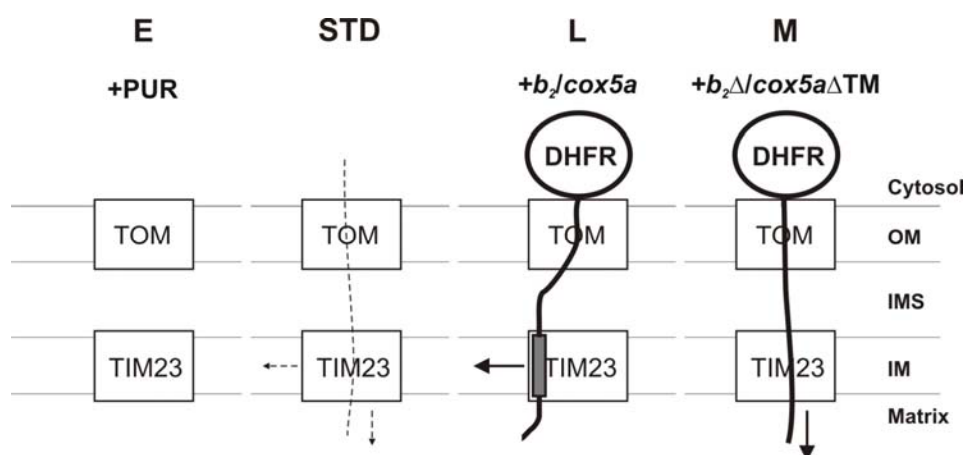


Figure 3.24. Schematic representation of the different states of the TIM23 complex. Mitochondria were isolated from puromycin-treated cells (PUR), from cells grown under standard conditions (STD), and from cells in which the TIM23 complex was saturated with the laterally sorted preprotein (b_2 or $cox5a$) or the matrix targeted preprotein ($b_2\Delta$ or $cox5a\Delta TM$). Both kinds of preproteins were arrested as intermediates that span both TOM and TIM23 complexes due to the stable folding of the dihydrofolate reductase (DHFR) moieties in the cytosol after the addition of aminopterin. OM, outer mitochondrial membrane; IMS, intermembrane space; IM, inner mitochondrial membrane.

Hybrid preproteins with different import pathways were cloned under inducible promoters and used for transformation of *wt* yeast strain YPH499. In the text, the preproteins used for *in vivo* saturation of the TIM23 complex will be written in *italic* font to be distinguished from radiolabeled preproteins used in protein import assays. Two preproteins were generated for *in vivo* saturation of the TIM23 translocase during lateral sorting. The first one, abbreviated as *b₂*, consists of the first 167 amino acid residues of yeast cytochrome *b₂* fused to the full length dihydrofolate reductase (DHFR) from mouse. This preprotein has a matrix targeting signal at its N-terminus followed by a hydrophobic signal which leads to its sorting into the inner membrane in a motor independent manner (Stuart *et al.*, 1994; Voos *et al.*, 1993). The second preprotein, termed *cox5a*, is a hybrid protein of yeast subunit Va of cytochrome c oxidase and DHFR. This preprotein is also laterally sorted in the inner membrane, but it requires the activity of the import motor (Glaser *et al.*, 1990). For the arrest of the complex during translocation of preproteins into the matrix, another two proteins were expressed in *wt* yeast cells. Deletion of 19 amino acid residues of the hydrophobic sorting signal in the *b₂* hybrid preprotein gave rise to *b₂Δ*, a preprotein that is completely translocated into the matrix (Voos *et al.*, 1993). The second preprotein of this type, indicated as *cox5aΔTM*, contains the sequence of *cox5a* preprotein lacking the amino acid residues 101-118 that form a hydrophobic sorting signal in *cox5a* (Glaser *et al.*, 1990). When the expression of these proteins is induced in the presence of folate analogue, aminopterin, the DHFR moieties fold stably in the cytosol, preventing complete import into mitochondria and leading to accumulation of preproteins as intermediates that span and connect both the TOM and the TIM23 complexes (Wienhues *et al.*, 1991). In case of *b₂* and *cox5a*, TIM23 complex is locked in the state of lateral sorting and in the case of *b₂Δ* and *cox5aΔTM* in the state of translocation into the matrix. This way two pairs of saturating preproteins were prepared: *b₂* – *b₂Δ*, and *cox5a* – *cox5aΔTM*, enabling the analysis of both translocation and insertion modes each. In addition, yeast cells were treated with puromycin (+PUR) in order to terminate protein synthesis and, upon the import of truncated polypeptide chains, to leave the TIM23 complex empty. To exclude the possibility of a specific effect of puromycin, yeast cell were, in addition, treated with cycloheximide, a different inhibitor of translation. Mitochondria isolated under standard conditions from cells not treated in any way served as a control.

Upon isolation of mitochondria, the expression levels of hybrid preprotein were evaluated along with the endogenous levels of several mitochondrial proteins (Figure 3.25). Puromycin treatment did not affect the integrity of mitochondria as judged by the evaluation of their protein profiles. Also, the addition of aminopterin and cycloheximide had no effect on

mitochondrial protein profiles (data not shown). All four types of preproteins were expressed in mitochondria as judged by immunodecoration with monoclonal Anti-DHFR antibody. However, as the strongest expression was observed in the case of $b_2\Delta$ preprotein, mitochondria saturated with $b_2 - b_2\Delta$ pair were chosen as the main model system for investigating the behavior of the TIM23 translocase during protein import.

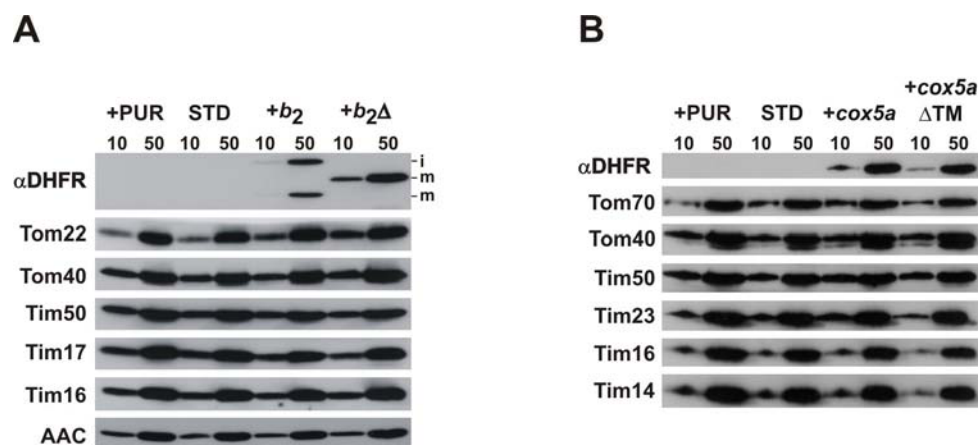


Figure 3.25. Endogenous levels of various proteins in saturated mitochondria. Mitochondria from untreated (STD) and yeast cells treated with puromycin (+PUR) were isolated simultaneously with mitochondria saturated with $b_2 - b_2\Delta$ (A) or $cox5a - cox5a\Delta$ pair (B). 10 and 50 μ g of mitochondria were dissolved in Laemmli buffer and analyzed by SDS-PAGE and immunodecoration with the indicated antibodies.

3.18. Preproteins in transit lead to stronger assembly of the TOM complex

To verify that b_2 and $b_2\Delta$ are indeed arrested within the TOM and the TIM23 complexes, isolated mitochondria were analyzed by BN-PAGE. This method has been previously used to identify the ~600 kDa TOM-TIM23-preprotein supercomplex upon *in vitro* arrest of recombinant $b_2\Delta$ DHFR preprotein (Dekker *et al.*, 1997). *In vivo* saturated mitochondria as well as the empty and the control ones were solubilized in digitonin containing buffer and loaded on a gradient gel. The TOM-TIM23-preprotein supercomplex was observed upon BN-PAGE and immunodecoration with the antibodies against Tom40 in both b_2 and $b_2\Delta$ containing mitochondria suggesting an efficient arrest of both preproteins (Figure 3.26A).

Interestingly, when four times higher amount of mitochondria was used for the same experiment, a band of ca. 100 kDa was visible in both mitochondria isolated from puromycin treated cells and the control ones, but was absent in mitochondria containing arrested preproteins (Figure 3.26B). As this band was previously identified as an assembly intermediate II of the TOM complex (Model *et al.*, 2001), the increased translocation load

appears to induce increased assembly of the TOM complex. The assembly intermediate I of 250 kDa could not be seen due to the strong signal of the assembled TOM complex that covered the range from ca. 200 to ca. 500 kDa.

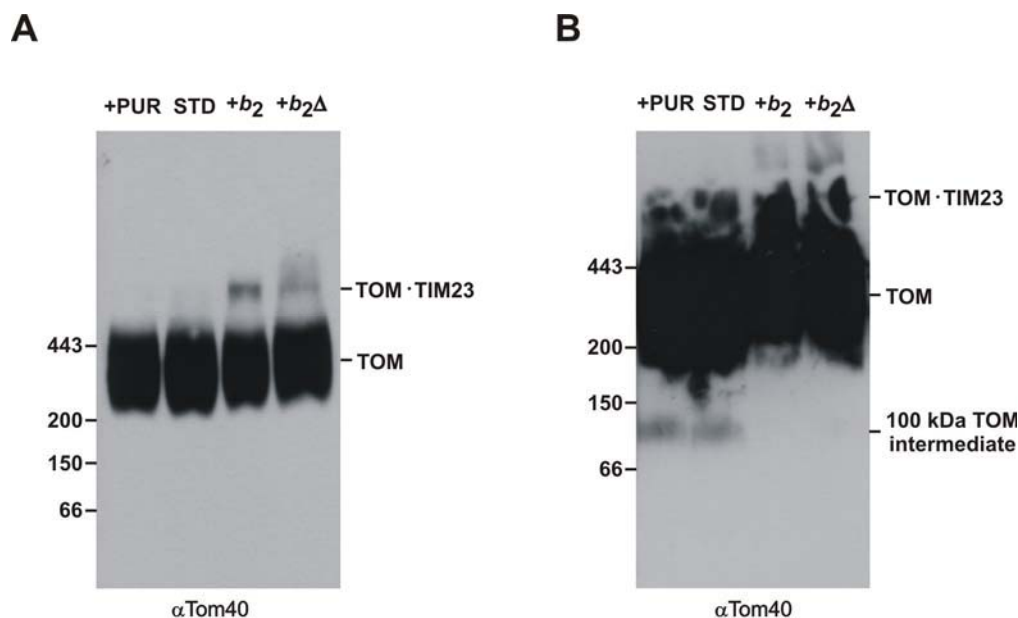


Figure 3.26. Formation of TOM-TIM23-preprotein supercomplex *in vivo*. (A) 25 µg of mitochondria were solubilized in a buffer containing 1% digitonin, incubated on ice for 20 min and analyzed by Blue Native Gel electrophoresis (4-12% acrylamide gradient gel) and immunodecoration with the antibodies against Tom40. (B) 100 µg of mitochondria were solubilized in buffer containing 1% digitonin, incubated on ice for 20 min and analyzed by Blue Native Gel electrophoresis (6-13% acrylamide gradient gel) and immunodecoration with the antibodies against Tom40.

Therefore, both laterally sorted and matrix targeted preproteins can be efficiently arrested between the TOM and the TIM23 translocases *in vivo*, and this system can be used as a tool for the analysis of the mechanistic behavior of protein translocases during the import of preproteins. In addition, the preprotein in transit influence the structural organization of the TOM complex leading to its stronger and/or faster assembly.

3.19. Both laterally sorted and matrix targeted precursors use the same pore in the TIM23 translocase

The nature of the pore of the TIM23 translocase is a matter of dispute. Despite numerous publications the consensus is not achieved in on the following issues: which proteins are exactly forming the pore, what is the size of it and how is it organized. Although the data presented in this work show that TIM23 translocase is a single entity, they do not answer the

question whether TIM23 complex contains a single pore (Truscott *et al.*, 2001) or it is organized in twin-pore structure with cooperate activity (Martinez-Caballero *et al.*, 2007). Hence, if the TIM23 translocase has twin-pore structure one cannot exclude the possibility that one pore may serve for translocation into the matrix while the other may serve for insertion in the inner membrane.

Control mitochondria isolated under standard conditions and mitochondria saturated *in vivo* with b_2 and $b_2\Delta$ preproteins were incubated with [35 S] radiolabeled preproteins targeted either into the matrix ($F_1\beta$) or into the inner membrane [DLD(1-72)DHFR]. In mitochondria with arrested b_2 preprotein the kinetics of imports of both $F_1\beta$ and DLD(1-72)DHFR preproteins was significantly delayed. Even stronger inhibition of import of both types of TIM23 substrates was observed in case of $b_2\Delta$ saturated mitochondria. This can be explained with much higher expression of this preprotein compared to b_2 . In comparison, import of [35 S] radiolabeled AAC, the substrate of TIM22 translocase was only mildly affected likely due to the high number of TOM complex molecules occupied by b_2 or $b_2\Delta$ preproteins (Figure 3.27).

In summary, the majority of the TIM23 complexes are occupied by the arrested preproteins b_2 or $b_2\Delta$. Equal inhibition of both matrix targeted and laterally sorted preproteins additionally suggests that both types of preproteins use the same translocation channel of the TIM23 complex.

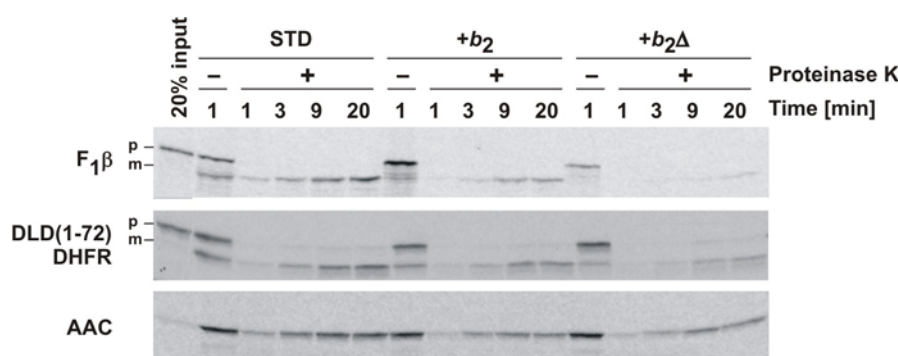


Figure 3.27. Protein import in mitochondria with both types of arrested precursors is blocked. The following [35 S] radiolabeled preproteins: the precursor of β -subunit of F_0F_1 ATPase, $F_1\beta$ (imported into the matrix by the TIM23 complex), a fusion protein of the first 72 amino acid residues of D-lactate dehydrogenase and the full length dihydrofolate reductase from mouse, DLD(1-72)DHFR (inserted into the inner membrane by the TIM23 complex), and precursor of the ATP-ADP carrier, AAC (inserted into the inner membrane by the TIM22 complex) were incubated with isolated mitochondria from cells treated as indicated. Samples were removed after various time periods and treated with (+) or without (-) proteinase K. Mitochondria were reisolated and analysed by SDS-PAGE and autoradiography.

3.20. Changes in stoichiometry of the TIM23 complex during import of preproteins

Coimmunoprecipitation experiments were performed in order to analyze if protein translocation leads to any changes in the stoichiometry of the TIM23 complex. Mitochondria were lysed with digitonin and incubated with the antibodies against Tim16, Tim17 and the preimmune serum prebound to Protein A-Sepharose (Figure 3.28A). No significant difference was observed in the amounts of the essential components: Tim50, Tim23, Tim17, Tim44, Tim14 and Tim16 precipitated from mitochondria in the different states of translocation. Although both preproteins induce the formation of TOM-TIM23-preprotein supercomplex, in the presence of $b_2\Delta$ the supercomplex was more stable, as seen by coprecipitation of Tom40 and Tom22 with the protein constituents of the TIM23 translocase. This suggests that, in addition to higher expression of $b_2\Delta$, the association of preprotein $b_2\Delta$ with the TIM23 complex appears to be tighter than the association of preprotein b_2 .

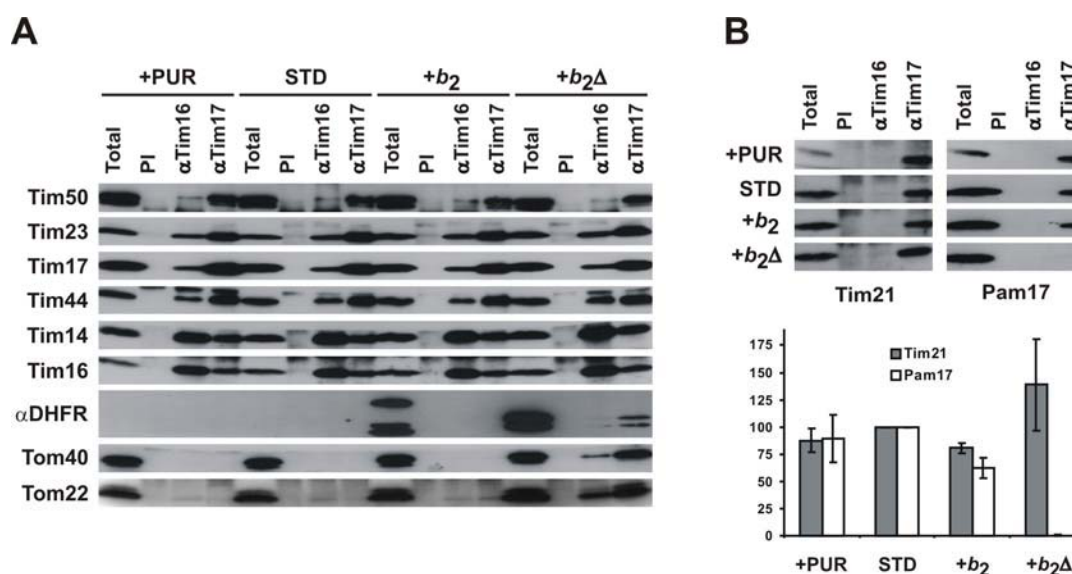


Figure 3.28. The absence of Pam17 from the complex translocating preproteins into the matrix is the only stoichiometrical change within the TIM23 complex in the different modes of preprotein translocation. (A and B) Mitochondria were solubilized with digitonin and incubated with the antibodies against Tim16, Tim17 and the preimmune IgGs (PI) prebound to protein A-sepharose beads. Bound proteins were eluted with Laemmli buffer and analyzed by SDS-PAGE and immunodecoration with the indicated antibodies. Total, 20% of the material used for immunoprecipitations. Amounts of Tim21 and Pam17 precipitated under these conditions were quantified from three independent experiments. Data represent the means \pm standard deviation; precipitation in STD, 100%. Quantification of western blots was performed using ImageMaster software (Amersham Pharmacia).

The association of two nonessential components Tim21 and Pam17 with the rest of the TIM23 translocase was also analyzed (Figure 3.28B). Tim21 was associated with the complex

in all states tested with somewhat reduced presence in the complex saturated with preprotein b_2 . Pam17 was present in the empty complex, while in the complex saturated with preprotein b_2 its presence was reduced. More importantly, it was completely absent in the complex saturated with preprotein $b_2\Delta$. Therefore, Pam17 is involved in preparing the TIM23 complex for the import process. However, once the process is taken off, Pam17 is removed from the complex, apparently by Tim21.

To confirm the opposite behavior of Tim21 and Pam17 in response to the presence of a translocating preprotein, the TOM-TIM23-preprotein supercomplex was purified using His-tag on the arrested recombinant preprotein $b_2\Delta$ DHFR-His₆ and its composition was investigated. Indeed, Tim21 was specifically retained on the Ni-NTA-Agarose beads together with the TIM23 and TOM components. In contrast, Pam17 was absent from the TIM23 complex actively translocating into the matrix also when analyzed *in vitro* (Figure 3.29).

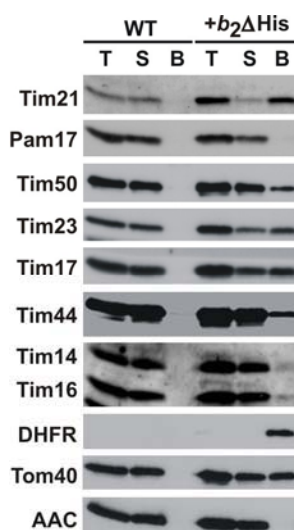


Figure 3.29. Pam17 is not associated with the TIM23 complex during the translocation of matrix targeted precursor *in vitro*. Preprotein $cytb_2(167)\Delta 19$ DHFR-His₆ was recombinantly expressed, purified via His-tag and incubated with wild type mitochondria. Methotrexate was added to arrest the preprotein as an intermediate spanning both TOM and TIM23 complexes. After lysis with digitonin, solubilized material was incubated with Ni-NTA-Agarose beads and bound material eluted with Laemmli buffer containing 300 mM imidazole. Total (T) and bound fractions (B) were analyzed by SDS-PAGE and immunodecoration. Total contains 20% of the material present in the bound fraction.

Taken together, the stoichiometry of the essential constituents of the TIM23 translocase is unaltered in the different states of preprotein translocation, demonstrating that the membrane part and the import motor are associated with each other irrespective of whether the complex is in its resting state or it is translocating different types of preproteins to different mitochondrial subcompartments. However, Pam17 is absent from the complex translocating preproteins into the matrix and less abundant in the complex laterally sorting preproteins in the inner membrane, suggesting that its role is limited on the conformational organization of the complex in import competent state, whereas it is obsolete during the translocation process.

3.21. Conformational changes of the TIM23 translocase during import of preproteins

To investigate if the process of protein translocation is indeed under conformational regulation of the TIM23 translocase already described protein crosslinking assays were used. Chemical crosslinker DSG was added to the isolated intact mitochondria to analyse the environment of Tim23. Crosslinking patterns of Tim23 in mitochondria from control cells and cells treated with puromycin were essentially the same showing that the TIM23 complex is largely empty in mitochondria isolated under standard conditions (Figure 3.30A). Crosslinking experiments with mitochondria isolated from cells treated with cycloheximide gave virtually identical results (data not shown). Arrest of preprotein b_2 , which is sorted into the inner membrane led to a pronounced increase of crosslinking efficiency of two Tim23 molecules and to a decrease of intensity of Tim23-Pam17 adduct. In contrast, Tim23 was not crosslinked to any protein upon arrest of the preprotein $b_2\Delta$ that is targeted to the matrix. The disappearance of Tim23-Pam17 crosslink in $b_2\Delta$ mitochondria is in agreement with the observed removal of Pam17 from the complex during import of the matrix targeted preproteins obtained by immunoprecipitation and pull-down experiments.

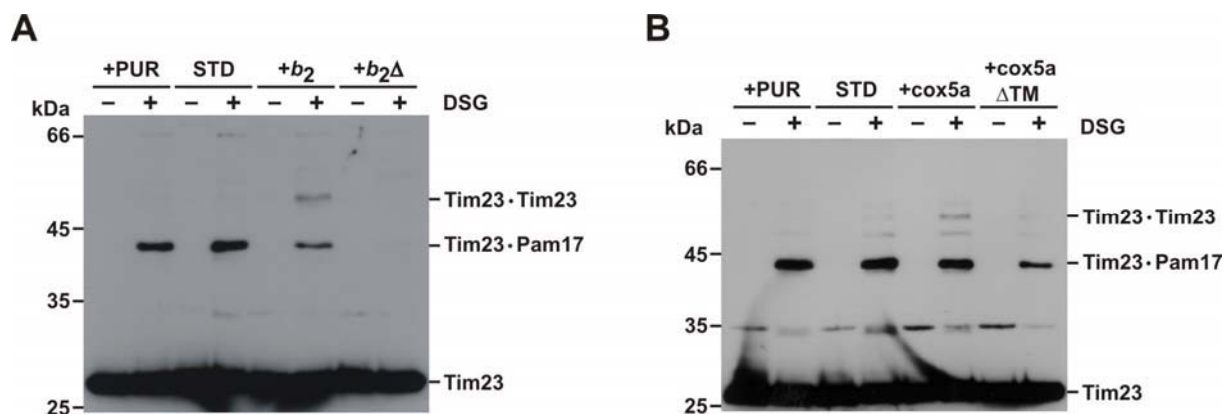


Figure 3.30. Conformational changes of Tim23 in mitochondria saturated with different types of preproteins. (A) Mitochondria isolated from puromycin-treated cells (+PUR), cells grown under standard conditions (STD) and from cells having arrested laterally sorted ($+b_2$) or matrix targeted preprotein ($+b_2\Delta$) were incubated with DSG. Samples were analyzed by SDS-PAGE followed by immunodecoration with the affinity purified antibodies against Tim23. **(B)** As in (A), with a difference that saturating preproteins used were $cox5a$ and $cox5a\Delta TM$. The crosslinking products are indicated.

These various crosslinking patterns of Tim23 may either reflect interactions of a certain preprotein with the complex or may represent different conformations of the complex specific for different modes of translocation. To discriminate between these two possibilities the assay

was repeated with *cox5a* – *cox5a*ΔTM pair. Arrest of these two proteins induced essentially the same changes in the crosslinking patterns of Tim23 as the arrests of *b₂* and *b₂*Δ (Figure 3.30B) showing that the observed changes are genuine differences in the conformation of the complex due to the different translocation modes.

Chemical crosslinker DSG was also used to probe the molecular environment of Tim16 when the translocase is in the empty and the occupied states. There was no significant difference between empty and mitochondria isolated under standard conditions (Figure 3.31). The most prominent difference between empty and mitochondria saturated with preproteins was the reduced crosslinking efficiency to Tim14 in mitochondria arrested with *b₂*Δ, while Tim16 dimer formation remained unaffected. It seems that during the translocation into the matrix conformational changes occur within Tim14-Tim16 tetramer, but these changes are not similar to those previously described in mitochondria depleted of membrane sector components.

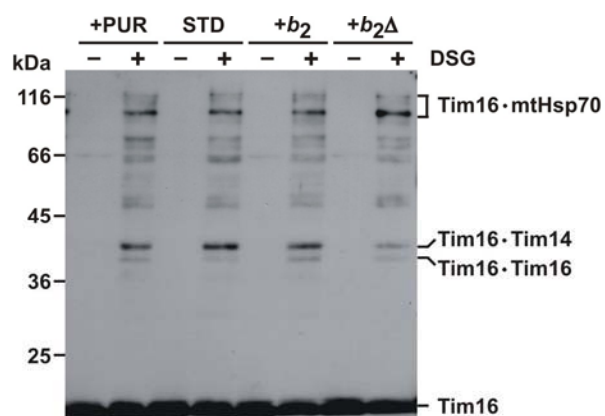


Figure 3.31. Matrix targeted preprotein induces the conformational change of the Tim14-Tim16 subcomplex. Mitochondria were subjected to crosslinking with DSG and subsequently analyzed by SDS-PAGE followed by immunodecoration with antibodies against Tim16. The crosslinking products are indicated.

To study the conformational changes within the import motor of the TIM23 complex during protein import in more detail, the environment of Tim44 was examined by addition of chemical crosslinker disuccinimidyl suberate (DSS). Crosslinking products of Tim44 with mtHsp70, another Tim44, Tim14 and Tim16 did not differ in mitochondria isolated from the cells treated or not with puromycin. The efficiency of crosslinking of Tim44 to mtHsp70 was slightly reduced in mitochondria containing arrested preproteins, especially in the case of *b₂*Δ, as compared to the controls. In mitochondria containing arrested *b₂* or *b₂*Δ the adducts between two Tim44 proteins disappeared and the adducts of Tim44 to Tim14 and Tim16 were dramatically decreased. The very strong crosslinking product of ~80 kDa in mitochondria containing arrested *b₂*Δ represents the crosslink of Tim44 with the preprotein (Figure 3.32A). This was demonstrated by arresting His-tagged *b₂*Δ *in vitro* followed by Ni-NTA-Agarose

pull down of the crosslinking products (Figure 3.32B). Interestingly, when the crosslinking experiments were performed in mitochondria with the second pair of arrested preproteins, Tim44 could be crosslinked to *cox5a* Δ TM, but not to *cox5a* (Figure 3.32C). The product Tim44-*cox5a* Δ TM was not as strong as Tim44-*b*₂ Δ , which could be explained by the lower level of expression of *cox5a* Δ TM compared to *b*₂ Δ . This shows that Tim44 has a high crosslinking potential for the precursors going into the matrix.

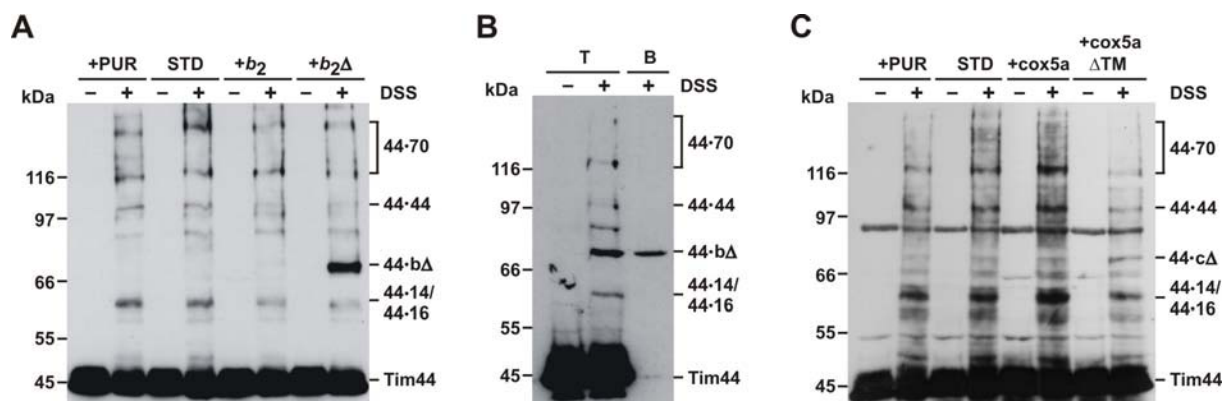


Figure 3.32. Tim44 interacts with preproteins translocated into the matrix. (A) Mitochondria isolated from puromycin-treated cells (+PUR), cells grown under standard conditions (STD) and from cells having arrested laterally sorted (+*b*₂) or matrix targeted preprotein (+*b*₂ Δ) were incubated with DSS. Samples were analyzed by SDS-PAGE followed by immunodecoration with the affinity purified antibodies against Tim23. (B) Recombinant *cytb*₂(167) Δ 19DHFR-His₆ whose DHFR domain was stabilized with methotrexate and NADPH was added to the isolated mitochondria to arrest it as an intermediate crossing both TOM and TIM23 complexes. Samples were then incubated in the presence (+) or absence (-) of DSS. Part of the sample was solubilized in SDS containing buffer and incubated with Ni-NTA-Agarose beads. Totals (T) and material bound to the Ni-NTA-Agarose (B) were analyzed by SDS-PAGE and immunodecoration with antibodies against Tim44. (C) As in (A), with a difference that saturating preproteins used were *cox5a* and. The crosslinking products of Tim44 are indicated as abbreviations: 44 – Tim44, 70 – mtHsp70, 14 – Tim14, 16 – Tim16, bD – *b*₂ Δ , c Δ – *cox5a* Δ TM.

The finding that Tim44 is in contact with the matrix targeted preprotein in transit was in accordance with previously published data (Schneider *et al.*, 1994). The lack of any of its crosslinking adducts with the laterally sorted preprotein may indicate that Tim44, and maybe the other proteins from the import motor, are not in the vicinity of the precursors of this type when they are sorted in the inner membrane. In an attempt to find the interaction between proteins from the import motor and the laterally sorted preprotein in transit, a novel approach was used. Instead of generating TOM-TIM23-preprotein supercomplex, strains with increased levels of several inner membrane proteins, namely Mia40, Tim50 and Tim21, were used (Figure 3.33A). These proteins have the same topology and they are the substrates of the TIM23 translocase, but the lengths of their polypeptide stretches between the presequences and the stop-transfer signals are different. Mia40 has a very short polypeptide stretch of 8

amino acid residues, which corresponds to motor independent preproteins, whereas this stretch is significantly longer in the case of Tim21 (ca. 30 residues) and Tim50 (ca. 70 residues), suggesting that they might need the activity of the import motor to be sorted in the inner membrane.

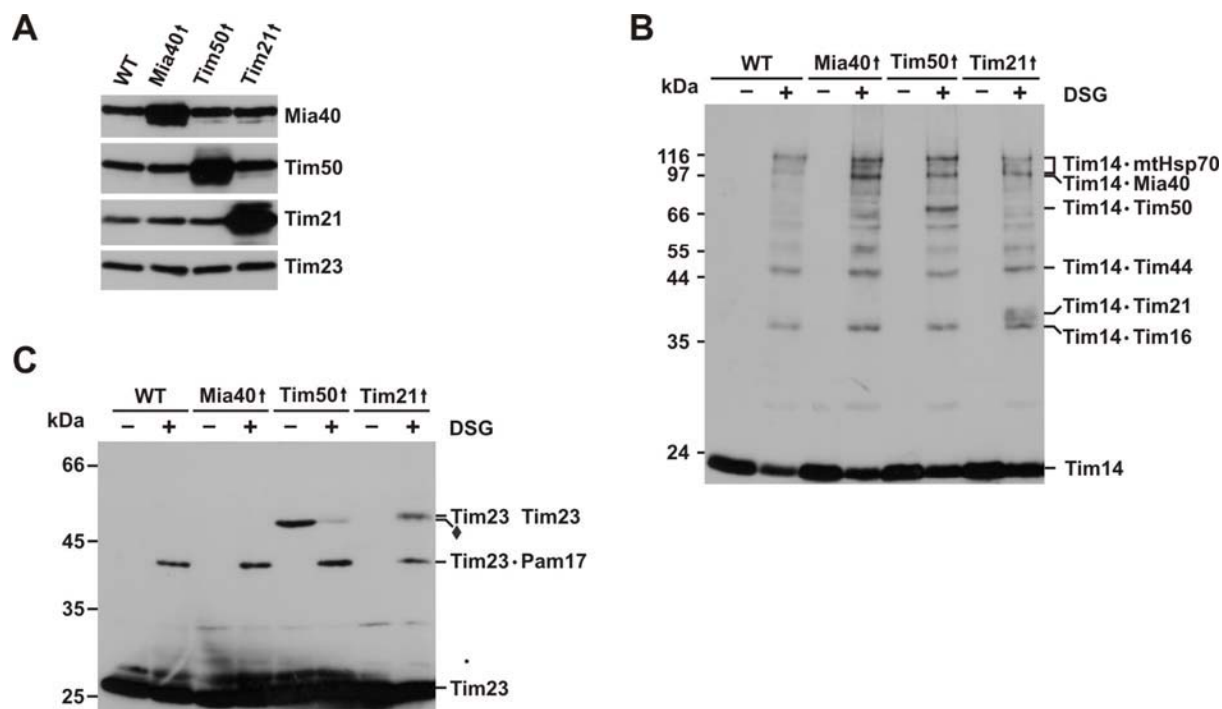


Figure 3.33. Overexpressed precursors of inner membrane proteins are in close vicinity of Tim14. (A) 25 μ g of WT and mitochondria with increased levels of Mia40, Tim50 and Tim21 were dissolved in Laemmli buffer and analyzed by SDS-PAGE and immunodecoration with the indicated antibodies. Mitochondria were incubated with DSG and analyzed by SDS-PAGE followed by immunodecoration with the antibodies against Tim14 (B) and Tim23 (C). The crosslinking products are indicated. The crossreaction of the antibody against Tim23 with Tim50 is labeled with diamond.

When mitochondria isolated from the cells of these strains were subjected to crosslinking with DSG, in addition to already described Tim14 crosslinks with other components of the import motor, new adducts of Tim14 and each of the overexpressed proteins were observed in the corresponding strains (Figure 3.33B), suggesting that in addition to its role as a J protein of the mitochondrial import motor, Tim14 might interact with the laterally sorted preproteins in transit. Although the imports of the investigated inner membrane preproteins are not all dependent on the activity of mtHsp70, these precursors, when overexpressed, were all successfully crosslinked to Tim14. This may suggest that the TIM23 translocase is settled in one conformation during the lateral sorting of preproteins irrespective on the length of the polypeptide stretch between the presequence and the stop-transfer signal. Additionally, Tim14 crosslinking adducts with mtHsp70, Tim44 and Tim16 remained unchanged suggesting that

the import motor seems to be mostly static during opening of the channel and the entrance of the hydrophobic stretch of these proteins in the inner membrane.

As Tim23 crosslinked dimer is a very sensitive indicator of the disrupted translocase, the environment of Tim23 was examined in these mitochondria to exclude the possibility that the overexpression of inner membrane proteins disturbs the conformation of the TIM23 complex (Figure 3.33C). In both Mia40 \uparrow and Tim50 \uparrow mitochondria crosslinking pattern of Tim23 remained the same as in WT mitochondria, showing that the increase of Tim23-Tim23 and the decrease of Tim23-Pam17 adduct induced by overexpression of Tim21 is specific effect of the modulatory role of Tim21 in the TIM23 translocase (see above) and not the artifact of the overexpression of inner membrane proteins. Taken together, the TIM23 complex settles in one conformation during the lateral exit of a preprotein from the complex, irrespective on the preprotein's dependence on the activity of mtHsp70.

To conclude, the TIM23 complex undergoes drastic conformational changes, both in the membrane part and in the import motor, during the import of preproteins. More importantly, different types of preproteins induce different conformations of the TIM23 translocase.

3.22. Tim23 changes its topology during import of preproteins

The N-terminus of Tim23 was observed to be exposed on the surface of the outer membrane and accessible to proteinase K added to intact mitochondria (Donzeau *et al.*, 2000). Since this association of Tim23 with the outer membrane was suggested to be involved in concentrating TIM23 complexes in the inner boundary membrane, the effect of preprotein translocation on the exposure of the N-terminus of Tim23 seemed possible.

After 10 min incubation with proteinase K ca. 5% of Tim23 was accessible to protease added to intact mitochondria isolated from puromycin-treated cells and ca. 10% in control mitochondria (Figure 3.34A). Unlike previously described crosslinking experiments, this assay shows small but experimentally reproducible difference between empty and control mitochondria, suggesting the presence of some residual amount of preproteins in the latter ones. On the other hand, in mitochondria with arrested b_2 roughly 35% of Tim23 was clipped by externally added protease and ca. 45% in mitochondria with arrested $b_2\Delta$. The intactness of mitochondria was not compromised under these conditions as the accessibilities of marker proteins of the outer membrane (Tom70), the intermembrane space (Tim50) and the matrix (Hep1) were not changed. To confirm that the accessibility to protease of Tim23 correlates

with the increased translocation load, mitochondria isolated from puromycin-treated cells were incubated with the increasing amounts of the recombinant purified preprotein $b_2\Delta$ DHFR-His₆. Indeed, addition of increasing amounts of $b_2\Delta$ to mitochondria led to increased insertion of Tim23 into the outer membrane as documented by the increased efficiency of clipping of the N-terminus of Tim23 by added Proteinase K (Figure 3.34B).

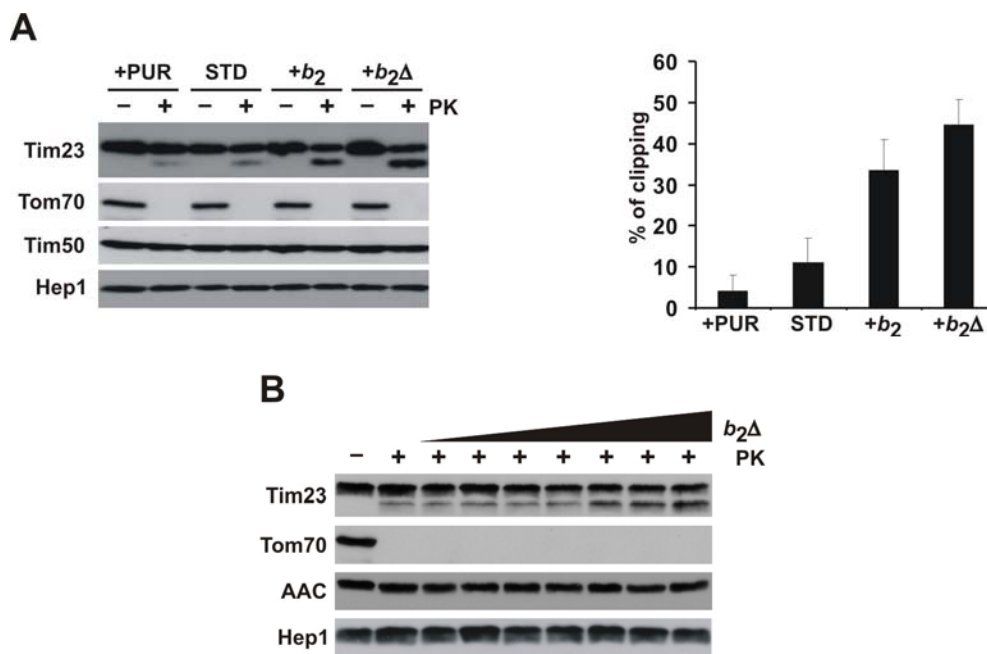


Figure 3.34. During protein import the N-terminus of Tim23 is more exposed on the surface of the outer membrane. (A) Isolated mitochondria were treated with proteinase K (PK) and analyzed by SDS-PAGE followed by immunodecoration with the depicted antibodies. Tim23 was decorated with an antibody against the C-terminal peptide. The percentage of Tim23 clipped under these conditions was quantified and shown with the indicated standard deviation from three independent experiments (right panel). **(B)** Mitochondria isolated from puromycin-treated cells were incubated with increasing amounts of recombinant preprotein *cytb*₂(167)Δ19DHFR-His₆ purified from *E. coli*, treated with PK and analyzed as described under (A).

In summary, presence of the preprotein in transit leads to the change in topology of Tim23 inducing increased exposure of its N-terminus at the mitochondrial surface and accessibility to the added protease.

3.23. The TIM23 translocase is a single entity

Coimmunoprecipitation experiments with solubilized mitochondria containing *in vivo* arrested preproteins have shown that the membrane part and the import motor do not assemble upon demand, but are equally associated when the TIM23 complex is in the different modes of

preprotein translocation. To confirm that the TIM23 complex is a single entity protein interactions in intact mitochondria were analyzed using the crosslinking approach.

The strains where each of the essential subunits of the membrane embedded part of the TIM23 complex was under inducible promoter were grown in the galactose containing medium for several hours prior to isolation of mitochondria. Mitochondria isolated this way: Tim17↓, Tim23↓ and Tim50↓, had more than several fold lower levels of each of these proteins compared to their endogenous levels. The environment of Tim44 in these mitochondria was examined by addition of DSS. Tim44 crosslinking pattern was significantly changed compared to one seen in wt conditions (Figure 3.35A). Although Tim44 interacts with mtHsp70 in the absence of Tim17 and Tim23 both *in vitro* and *in vivo* (Slutsky-Leiderman *et al.*, 2007 and data not shown), in Tim17↓ and Tim23↓ mitochondria crosslinking adducts of Tim44 to mtHsp70 disappeared. In addition, crosslinking adducts of Tim44 with Tim14 and Tim16 underwent minor alterations. These data suggest that only Tim44 bound to the fully functional Tim17-Tim23 core of the translocase adopts a conformation optimal for protein import. On the other hand, depletion of Tim50 did not affect the known crosslinking adducts of Tim44 but instead gave rise to a new one of ~100 kDa. This effect of depletion of Tim50 on the conformation of Tim44 is particularly interesting since no direct interaction of these two proteins was ever observed; so it is either exerted via Tim17-Tim23 core, or these two proteins somehow directly interact.

Decreased levels of Tim50 do not seem to affect the structural organization of Tim14-Tim16 subcomplex. However, depletions of Tim23 and Tim17 strongly increased Tim16-Tim16 crosslinks and slightly reduced Tim16-mtHsp70 crosslinks, whereas no significant changes were observed concerning Tim14-Tim16 crosslinking adduct (Figure 3.35B). Tim14-mtHsp70 crosslinks seemed mildly reduced in Tim17↓ and Tim23↓ mitochondria, while Tim14-Tim16 adduct remains unchanged when observed from Tim14 side (Figure 3.35C). The crosslinking pattern in mitochondria depleted of the essential proteins from the membrane embedded sector suggest a conformational change along the Tim16-Tim16 interface of the Tim14-Tim16 tetramer (Mokranjac *et al.*, 2006) without disruptions in the Tim14-Tim16 dimer formation. This is in agreement with the previous finding that the formation of Tim14-Tim16 heterodimer is not affected by the absence of any other TIM23 component apart from Tim14 and Tim16 themselves (Kozany *et al.*, 2004). Taken together, in addition to structural reorganization of the import motor when one of its components is depleted, this part of the complex changes its conformation also in the case of disruptions within the membrane embedded part of the TIM23 translocase.

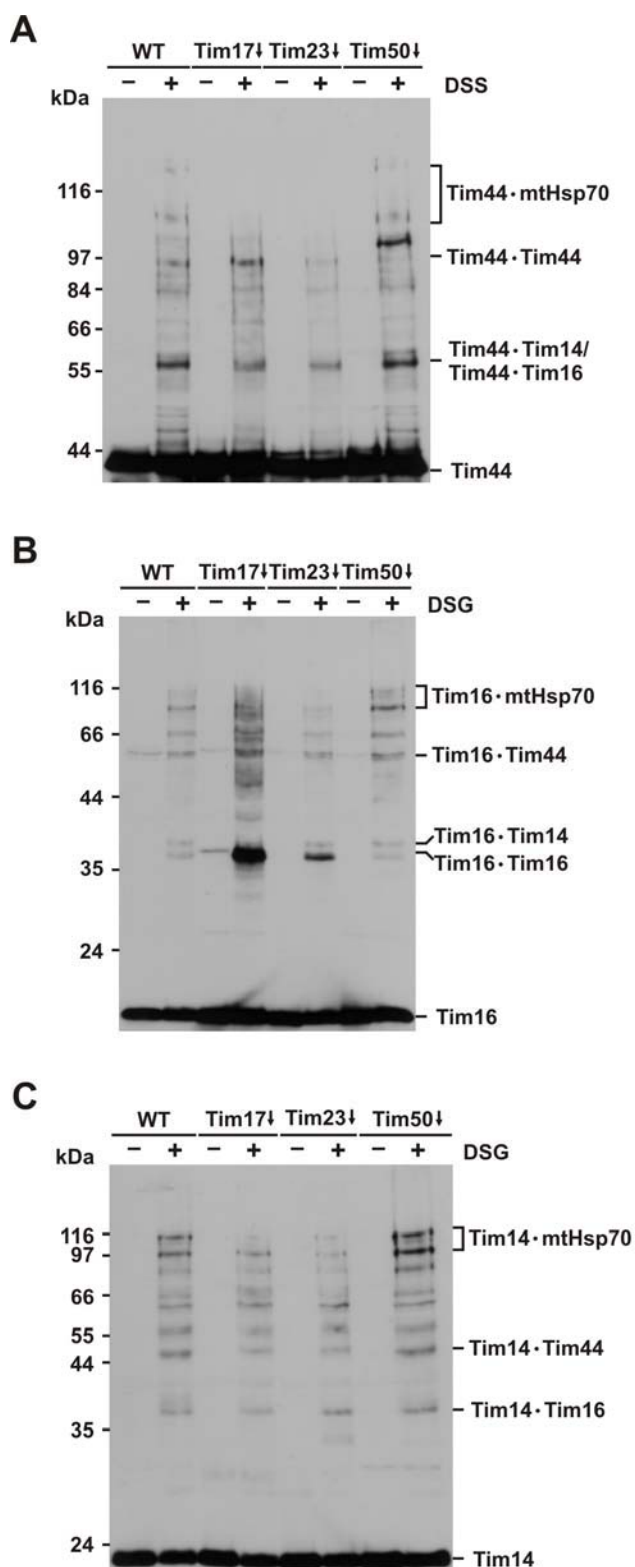


Figure 3.35. Conformational changes of the import motor components induced by disrupted membrane embedded part of the TIM23 complex. Mitochondria isolated from wild type or cells depleted of one of the essential components from the membrane part of the TIM23 complex (Tim17↓, Tim23↓, and Tim50↓) were subjected to crosslinking with disuccinimidyl suberate (DSS) (**A**) or disuccinimidyl glutarate (DSG) (**B and C**) and analyzed by SDS-PAGE followed by immunodecoration with antibodies against Tim44 (**A**), Tim16 (**B**) and Tim14 (**C**). The crosslinking products are indicated.

To analyze the effects of Tim17 and Tim50 on the molecular environment of Tim23, the crosslinking experiment was performed with Tim17↓ and Tim50↓ mitochondria. Depletion of either of the two proteins significantly changed the crosslinking pattern of Tim23 (Figure 3.36A). Crosslinks to Pam17 were reduced upon depletion of Tim50 and barely detectable after depletion of Tim17. In contrast, crosslinking efficiency to the

unidentified protein of 7-8 kDa was substantially increased in mitochondria depleted of Tim50 and also, to a lesser extent, in mitochondria depleted of Tim17. The most drastic change in mitochondria lacking Tim17 was the appearance of an extremely strong crosslinked dimer of Tim23. This adduct was also augmented in mitochondria lacking Tim50 as compared to the wild type, but way less prominent than in Tim17↓ mitochondria. Crosslinking of Tim23 was then performed in mitochondria specifically depleted of Tim44, Tim14 or Tim16 to test if the subunits of the import motor influence the conformation of the membrane embedded sector of the TIM23 translocase. Absence of Tim44 resulted in a significant increase of Tim23 dimerization efficiency and a mild reduction of intensity of the Tim23-Pam17 crosslink. However, the most prominent change in mitochondria lacking Tim44 was a complete absence of the crosslink of ca. 33 kDa, suggesting the possibility that the association of the small 7-8 kDa protein with the TIM23 translocase depends on the presence of Tim44 in the complex. On the other hand, depletion of either Tim14 or Tim16 resulted in the increased intensity of 33 kDa crosslinking adduct. Additionally, depletion of Tim16 increased the Tim23 dimerization to the levels more prominent than the depletion of Tim50 or Tim44 but still less than depletion of Tim17. Interestingly, at longer exposures, a weak crosslink is seen just below Tim23-Pam17 adduct. This may be Tim23-Tim17 crosslink, because it remains unchanged in all tested mitochondria, while it completely disappears in Tim17↓ mitochondria. Taken together, membrane embedded part of the TIM23 translocase appears to be very dynamic as judged by the changing crosslinking pattern of its central component Tim23.

Since depletion of Tim17 leads to a drastic increase of the crosslinking adduct of ca. 54 kDa a truncated version of Tim23 protein lacking its first 50 amino acid residues and having a His₉ tag on its C-terminus was cloned in a single copy plasmid and used for transformations of *wt* YPH499 and *Tim17*↓ yeast cells to confirm this adduct as a Tim23 dimer. Generated strains contained both full length and a His-tagged truncated version of Tim23 protein. Isolated mitochondria were subjected to crosslinking with DSG and subsequently solubilized and loaded on NiNTA-agarose beads. Both types of mitochondria gave additional Tim23-Tim23Δ50His₉ adduct that was retained on the beads, whereas in mitochondria depleted of Tim17 the amount of the eluted adduct was much higher (Figure 3.36B).

In summary, changes in the membrane part of the TIM23 complex result in conformational changes of the import motor and *vice versa* suggesting that two parts of the translocase are tightly coupled and strictly dependent on each other. Therefore, membrane embedded part and

the import motor cannot be observed as two independent complexes, but only as two inseparable parts of the TIM23 complex that is a single entity.

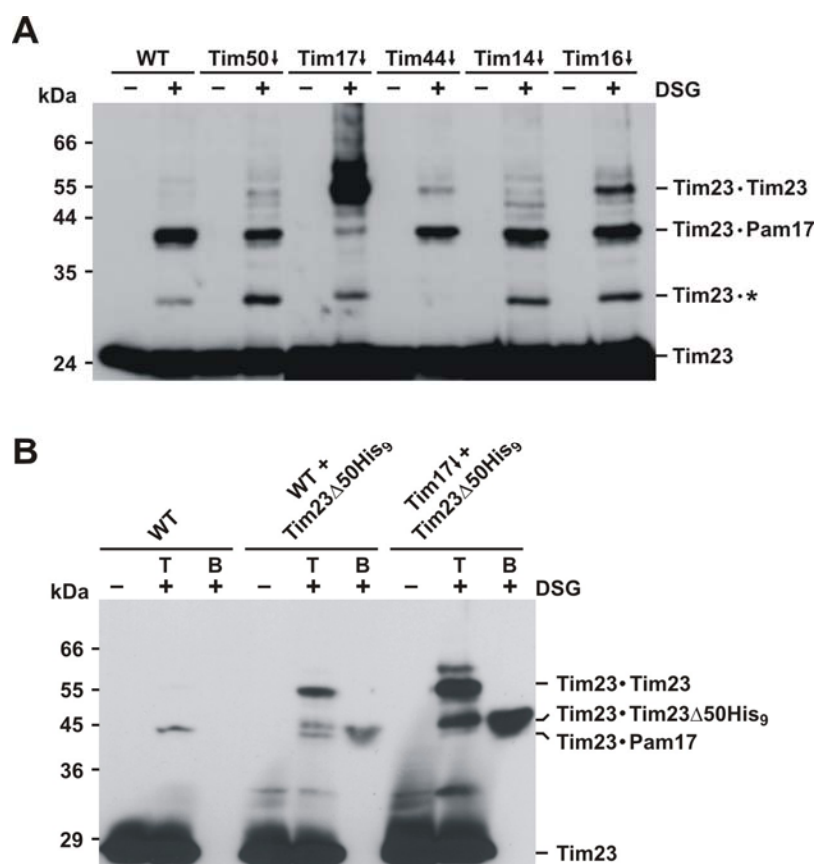


Figure 3.36. Membrane embedded part is sensitive to changes throughout the TIM23 translocase. (A) Mitochondria isolated from wild type or cells depleted of one of the essential TIM23 components (Tim50 \downarrow , Tim17 \downarrow , Tim44 \downarrow , Tim14 \downarrow , and Tim16 \downarrow) were incubated with DSG and analyzed by SDS-PAGE followed by immunodecoration with the antibodies against Tim23. (B) Mitochondria isolated from wild type and cells expressing a version of Tim23 lacking the first 50 amino acid residues and containing the C-terminal His₉ tag either in the wild type or Tim17 \downarrow background were subjected to crosslinking and subsequently incubated with NiNTA Agarose beads. Bound material was eluted with Laemmli buffer containing 300mM imidazole. Samples were analyzed by SDS-PAGE and immunodecoration with antibodies against the N-terminal peptide of Tim23. T, total mitochondria incubated in the absence or presence of DSS; B, material bound to Ni-NTA beads. The crosslinking products are indicated.

3.24. The TIM23 complex reacts to specific mutational alterations of the TOM complex

The import of presequence containing preproteins does not demand only the functional TIM23 translocase, but it also requires the functional TOM complex. New observation that a preprotein in transit influences both the TOM and the TIM23 complexes raised the issue of the nature of the interaction between the two complexes. To test if the altered TOM complex may induce conformational changes within the TIM23 translocase mitochondria isolated from

temperature-sensitive strains generated by mutations in Tom40: 40-2, 40-3 and 40-4 (Kassenbrock *et al.*, 1993) were incubated with DSG and analyzed by SDS-PAGE and subsequent decoration with the affinity purified antibodies against Tim23 (Figure 3.37). Although all three types of mutant mitochondria were isolated from cells grown on 30°C without any shift to non-permissive temperatures, 40-4 mitochondria gave a drastic increase of Tim23 crosslinked dimer, much stronger than Tim23-Pam17 adduct. In 40-3 mitochondria Tim23-Tim23 adduct was also present, though not as intense as in the case of 40-4 ones. In addition, these mitochondria gave increased Tim23-Pam17 adduct and a small crosslinking product of ca. 33 kDa when compared to WT mitochondria. In contrast, the crosslinking pattern of 40-2 mitochondria did not differ significantly from WT mitochondria, suggesting not only that the mutations in the TOM complex induce conformational changes of the TIM23 translocase, but also that the reaction of the TIM23 complex on these mutations appears to be selective and specific.

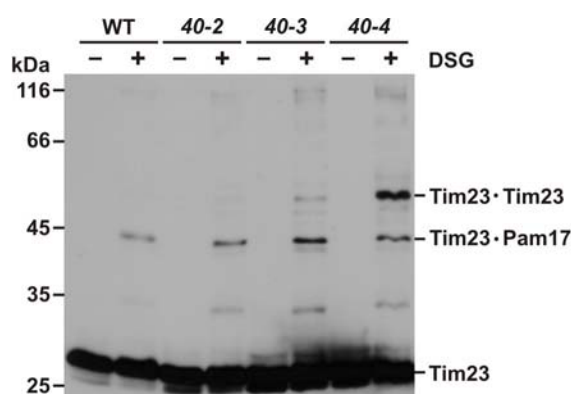


Figure 3.37. Tim23 reacts to mutations in Tom40. Mitochondria were subjected to crosslinking with DSG and subsequently analyzed by SDS-PAGE followed by immunodecoration with antibodies against Tim23. The crosslinking products are indicated.

To get a more detailed insight which type of changes within the TOM complex induce structural reorganization of the TIM23 translocase, mitochondria isolated from cells either lacking one of the TOM complex components or with a specific mutation of one of the components were used in the same crosslinking assay (Figure 3.38). The deletion of Tom70, receptor responsible for recognition of hydrophobic preproteins that mostly use TIM22 complex as the gate for sorting in the inner membrane (Wu and Sha, 2006) had no effect on the crosslinking pattern. In contrast, deletion of Tom20, receptor responsible for recognition of the most presequence containing preproteins that are imported via TIM23 complex (Abe *et al.*, 2000), led to massive structural reorganization of the TIM23 complex. In addition to the increase of the crosslinking product of ca. 33 kDa, in mitochondria lacking Tom20, the intensity of the Tim23-Tim23 adduct was immense, much stronger than the one in 40-4 mitochondria. Such a strong crosslinked dimer was only seen in Tim17↓ mitochondria, but

the difference between Δ Tom20 and Tim17 \downarrow mitochondria is that the deletion of Tom20 apparently has no effect on binding of Pam17 to Tim17-Tim23 core. This indicates that although the deletion of Tom20 and the depletion of Tim17 both induce drastic conformation changes of Tim23, Tom20 has no significant influence on the regulation of the function of the TIM23 complex exhibited by coordinated action of Pam17 and Tim21. The effect observed in Δ Tom20 mitochondria is the first indication that Tim23 communicates with the TOM complex up to the level of the *cis* side receptor. Hence, the TIM23 complex may start entering the optimal conformation for translocation when the preprotein first interacts with Tom20, without even entering the intermembrane space.

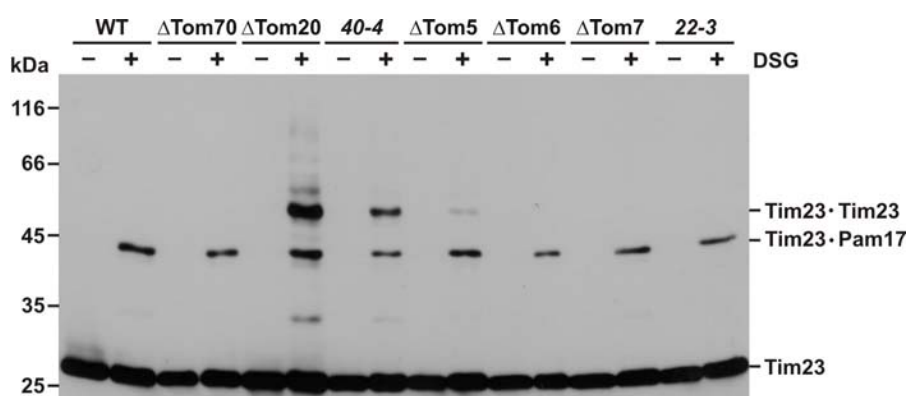


Figure 3.38. Tim23 senses the changes in the TOM complex. Mitochondria were subjected to crosslinking with DSG and subsequently analyzed by SDS-PAGE followed by immunodecoration with antibodies against Tim23. The crosslinking products are indicated.

Experiments with mitochondria isolated from cells in which one of the small Tom proteins was missing have shown that only the deletion of Tom5 affects the conformation of the TIM23 complex, whereas Δ Tom6 and Δ Tom7 had the same pattern as WT mitochondria. This is a very interesting observation, because Tom7 was proposed to constitute *trans* binding site for the incoming presequence (Esaki *et al.*, 2004), together with the C-terminal IMS domain of Tom22 (Bolliger *et al.*, 1995) and IMS exposed residues of Tom40. Accordingly, deletion of IMS exposed domain of Tom22 in 22-3 mitochondria (Moczko *et al.*, 1997) induced no conformational change of the TIM23 complex, which is in agreement with the data obtained with mitochondria lacking Tim21. Taken all these data into account, it seems that either the TIM23 complex does not react at all to adverse changes of the *trans* binding site of the TOM complex, or it may be sensitive only to the changes within Tom40 in the *trans* site. Interestingly, the crosslinking pattern of Tim16 or Tim14 in these mitochondria was not significantly different from the WT conditions (data not shown), indicating that Tim23 is

more sensitive to changes in the environment of the TIM23 complex than the motor components.

To conclude, the TIM23 translocase communicates with its environment in mitochondria. Tim23 acts as a sensor protein perceiving specific mutational alterations of the TOM complex that may affect the function of the TIM23 translocase. Upon receiving this type of signal, the TIM23 translocase selectively reacts by locking in a specific conformation. The conformational changes of the TIM23 translocase induced by specific changes in the outer membrane are similar to those happening during the import of preproteins, but not identical. This is, however, one more indication of the central role of conformational regulation of the TIM23 translocase in the process of protein import in mitochondria.

4. DISCUSSION

The present study describes new findings concerning the structure and the function of the TIM23 translocase. First, a previously unknown component of the TIM23 translocase, Tim21, was identified and characterized. Second, the TIM23 translocase was arrested *in vivo* in different modes of activity. Its ability to sort different classes of preproteins into different mitochondrial subcompartments was found to rely primarily on conformational changes of the essential components of the complex. The nonessential components Tim21 and Pam17 turned out to be responsible for the fine tuning of these conversions. Third, the TIM23 translocase was shown to be a single entity that selectively responds to specific changes in the TOM complex. Finally, a model of the mechanism of the TIM23 translocase is presented.

The first aim of this study was to search for new components of the TIM23 complex of yeast in addition to the described eight essential subunits (Rehling *et al.*, 2004). Mass spectrometric analysis of proteins copurified with yeast Protein A-tagged Tim23 revealed a previously unidentified protein that was named Tim21 according to the established nomenclature (Pfanner *et al.*, 1996). Tim21 is anchored in the inner membrane by a single transmembrane domain, with a small N-terminal segment facing the matrix of mitochondria and a larger C-terminal domain exposed in the intermembrane space (IMS). All homologs identified *in silico* have the same predicted topology. Tim21 is conserved in eukaryotes with the highest level of homology among fungi. Interestingly, high levels of homology are present both in the transmembrane and in the C-terminal IMS domain.

Tim21 is a bona fide constituent of the TIM23 complex, and virtually the total pool of Tim21 in mitochondria was found associated with the TIM23 complex. High amounts of Tim21 could be precipitated with the antibodies against Tim23 and Tim17, the components of the membrane part of the translocase, but low amounts could also be precipitated with antibodies against Tim16, the import motor component. This indicates that Tim21 is present in the complex in which the subunits of both the membrane part and the import motor are present. Tim21 specifically binds to Tim17-Tim23 core of the complex and this interaction is not dependent on the presence of any other essential subunit of the complex. In addition, binding of Tim21 to Tim17-Tim23 core is probably mediated by its transmembrane domain, since the

isolated C-terminal domain of Tim21 interacts with the TIM23 complex with very low affinity. On the other hand, the IMS domain of Tim21 showed a remarkably high affinity for the components of the TOM complex. The interaction of Tim21 with the TOM complex is the first reported direct contact between the proteins from the TOM and the TIM23 complexes. The shortest construct of Tim21 which still interacted with the TOM complex comprised amino acid residues 97 to 225. Further deletion from the C-terminus abolished this interaction. Furthermore, the interaction between Tim21 and the TOM complex is apparently ionic in nature as it was absent in the presence of salt concentration as low as 100 mM. The conservation of the C-terminal domain is therefore crucial for the putative function of Tim21 to physically connect the TIM23 and the TOM complexes. These results are in agreement with the observations made by another group which independently identified Tim21 in yeast and showed that the C-terminal domains of Tim21 and Tom22 directly interact *in vitro* (Chacinska *et al.*, 2005) and with the recently reported structural basis of this interaction (Albrecht *et al.*, 2006).

The importance of the role of Tim21 in tethering the TIM23 and the TOM complexes was scrutinized after the observation that this protein was essential neither for the import of any type of preprotein nor for the assembly of the TIM23 complex. Moreover, the deletion of Tim21 had a positive effect on the growth of yeast cells at elevated temperatures. In contrast to deletion of Tim21, overexpression of Tim21 led to import defect of motor dependent preproteins and to a change of conformation of the TIM23 complex. Both import defect and structural reorganization of the complex were surprisingly similar in mitochondria with increased levels of Tim21 and those lacking Pam17, a recently identified subunit of the TIM23 complex (van der Laan *et al.*, 2005).

Results presented in this study demonstrate a functional interdependence between Tim21 and Pam17 based on the mutually exclusive nature of binding of these two proteins to the Tim17-Tim23 core. It seems that Tim21 has a higher binding affinity for the core of the complex than Pam17. High levels of Tim21 eliminated Pam17 from the complex, whereas increased levels of Pam17 only reduced the amount of Tim21 associated with the complex, but did not remove Tim21 completely under any conditions tested. It is possible, though, that the lower expression of Pam17 compared to Tim21 contributed to this phenomenon. In addition, increased levels of Pam17 in mitochondria did not increase the amount of Pam17 associated with the complex. The opposite situation was seen for Tim21 whose presence in the complex directly correlated with the levels of its overexpression. Crosslinking experiments have shown that Pam17 is necessary for obtaining a conformation of the TIM23 complex optimal for

translocation of preproteins. Mitochondria lacking Pam17 had a reduced import efficiency of preproteins whose import is dependent on the import motor. As Tim21 and Pam17 associate with the TIM23 complex in a mutually exclusive manner, the overexpression of Tim21 removes Pam17 from the complex. This results in a similar import defect for motor dependent preproteins and in the same conformational change of the TIM23 complex as observed for depletion of Pam17. Overexpression of Pam17 in Tim21 overexpressing cells restores both the conformation and the efficiency of import, demonstrating opposite effects of Tim21 and Pam17. Accordingly, Pam17 is able to influence the conformation of the TIM23 complex in cells lacking Tim21 faster than in wild type which enables faster growth of Tim21 depleted cells at elevated temperatures. Taken together, this structural and functional interdependence of Tim21 and Pam17 represents a novel mode of regulation of the activity of the TIM23 translocase.

To analyze the mode of regulation and the behavior of the TIM23 complex during the preprotein translocation in more detail a novel approach was applied, that was based on saturation of the TIM23 complex *in vivo* with different types of preproteins. Trapping the TIM23 complex with arrested preproteins enabled the analysis of the topology, conformation and the composition of the translocase in its empty state and while inserting preproteins into the inner membrane or mediating their translocation into the matrix. Upon arrest of either of the two types of preproteins, the TIM23 complex exhibited strongly reduced import of all types of radiolabeled precursors. This proves that the TIM23 complex cannot be in the translocation and in the insertion mode at the same time. Furthermore, this result also excludes the existence of two separate pools of the TIM23 complexes, one for matrix translocation and one for lateral insertion of preproteins.

How does the TIM23 complex manage to sort preproteins into two different mitochondrial subcompartments? The experiments performed with mitochondria containing homogeneous populations of the TIM23 complex in various states of its function have demonstrated that the translocase actively responds to the incoming precursor proteins. In mitochondria containing the arrested preprotein, the N-terminal segment of Tim23 was exposed at the surface of mitochondria, supporting the view that the N-terminus of Tim23 plays a significant role in the dynamic cooperation between the TOM and the TIM23 complexes during the translocation process (Donzeau *et al.*, 2000). The exposure of the N-terminal segment of Tim23 at the mitochondrial surface correlated with the translocation load, indicating that this represents a response of the TIM23 complex on the incoming preprotein (Figure 4.1). In addition, these experiments showed small but experimentally reproducible difference between empty and

control mitochondria, meaning that during isolation of mitochondria under standard conditions residual amounts of the preproteins in transit remained within the TIM23 translocase.

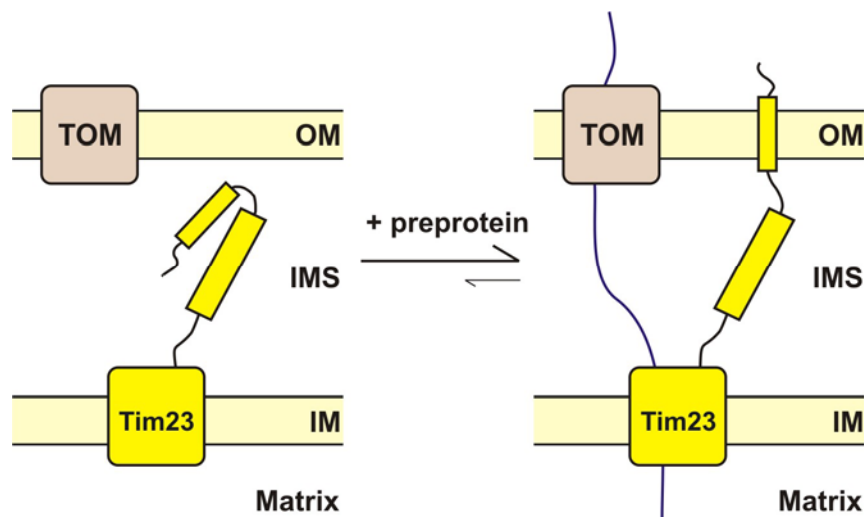


Figure 4.1. Schematic representation of the change of Tim23 topology induced by the presence of the preprotein. See text for details.

Two different types of preproteins demand two different conformations of the TIM23 complex for their unconstrained import. For translocation into the matrix the channel of the translocase opens on the IMS and on the matrix side, but for the insertion of proteins in the inner membrane, the channel has to open laterally to enable the passage of the transmembrane domain of the preprotein into the lipid bilayer (Figure 4.2). The latter process was accompanied by a change in the positioning of the intermembrane space domains of two Tim23 molecules relative to each other leading to increased crosslinking efficiency of Tim23 dimer. In contrast, the weak crosslinked dimer of Tim23 that can be seen with the empty translocase completely disappears during the import of the matrix destined proteins. Thus, the membrane part of the TIM23 complex is in two different conformational end states depending on the type of preprotein the translocase is saturated with.

The preprotein in transit also affected the interaction between Tim44 and mtHsp70. This conformational change was even more conspicuous in the case of matrix targeted preproteins, although the conformational change induced by the presence of laterally sorted preprotein went in the same direction. The conformational changes of the import motor were confirmed when the interposition of two Tim44 molecules and the interaction of Tim44 with Tim14-Tim16 subcomplex were analyzed. The efficiency of the formation of Tim44 crosslinked dimer and Tim44-Tim14/Tim16 adducts was reduced in virtually the same manner for both

types of preproteins. These observations are in accordance with reports that the presequence enters the matrix irrespective of the final destination of the preprotein (Ungermann *et al.*, 1996). Interestingly, Tim44 was efficiently crosslinked to matrix targeted preproteins, suggesting that Tim44 is the initial binding partner of the incoming polypeptide before it is delivered to mtHsp70. Upon the delivery of the preprotein to mtHsp70, the interaction between Tim44 and mtHsp70 is changed and the import motor translocates the preprotein in the matrix using the energy of ATP. If, however, a hydrophobic sorting signal arrives and the activity of energy consuming import motor is not required, the change of interaction between Tim44 and mtHsp70 is less drastic on account of the striking conformational rearrangements of the membrane part of the complex.

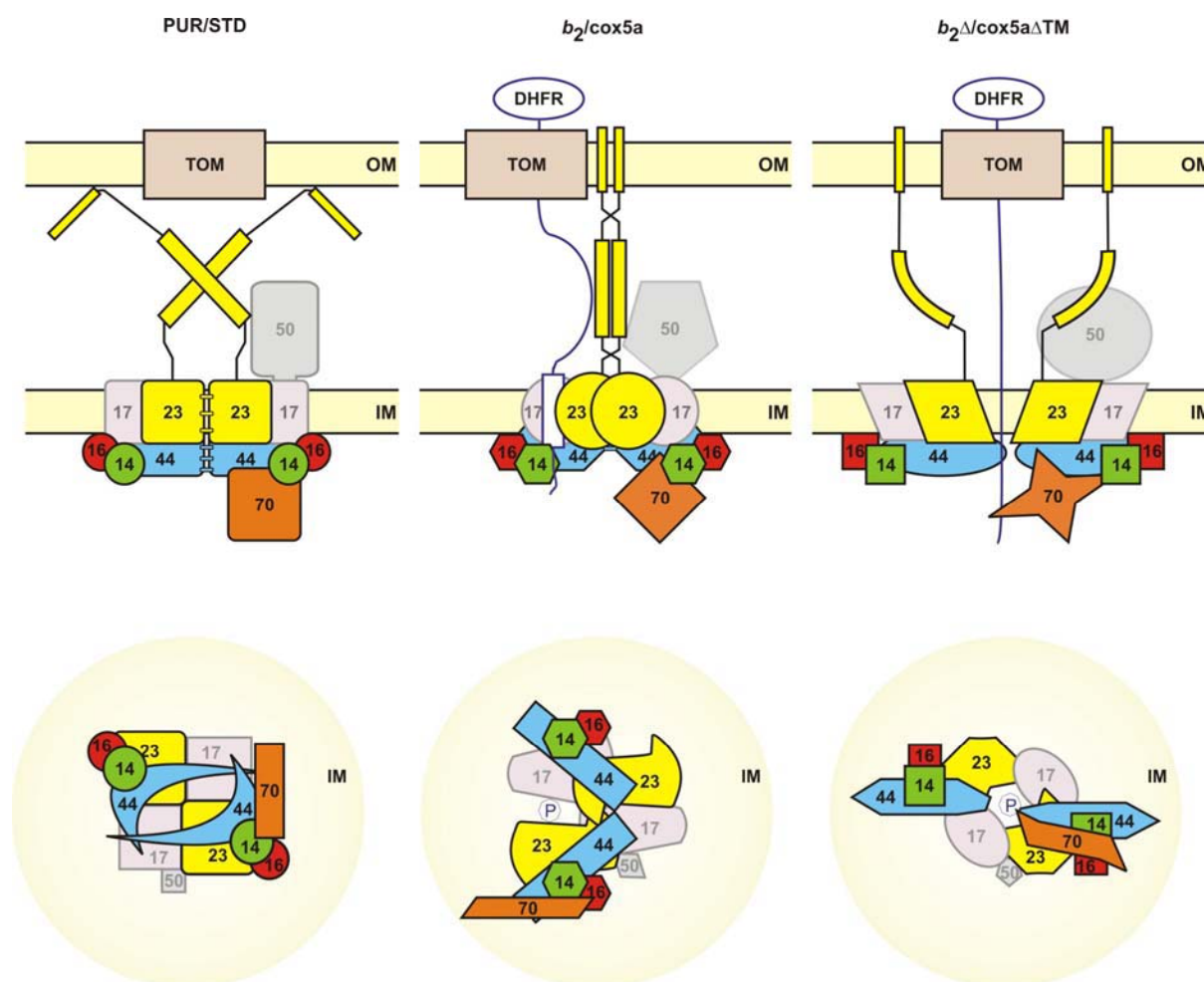


Figure 4.2. Schematic representation of the conformational changes of the essential components of the TIM23 translocase during translocation of different types of preproteins. View from the side (upper panel) and from the matrix (lower panel). In “fade-out” colors are shown components of the TIM23 translocase whose conformational changes were not directly discussed in this study. See text for more details.

The energy saving by the translocase was further confirmed by the conformational changes of the Tim14-Tim16 subcomplex. The stimulatory activity of the J-protein Tim14 on ATP hydrolysis by mtHsp70 is under negative regulation of Tim16, which prevents the idling of the import motor (D'Silva *et al.*, 2005; Li *et al.*, 2004). Transfer of the preprotein from Tim44 to mtHsp70 induced conformational changes of the Tim14-Tim16 subcomplex, relieving the inhibition of Tim14 and stimulating the ATPase activity of mtHsp70. In this process, Tim44 probably undergoes an initial conformational change upon binding of the preprotein and this conformational change is then likely conveyed to the Tim14-Tim16 subcomplex. Thus, translocase goes through a series of reversible conformational states: from import competent state to a state fully saturated with the precursor in transit and then back again to the import competent state, ready to accept a new precursor. That means that there is a dynamic balance of conformational states of the essential subunits of the TIM23 translocase.

The two nonessential subunits Tim21 and Pam17 apparently have a role in fine tuning of activity of the TIM23 translocase is under modulatory role of its. The stoichiometry of the essential proteins remained unaltered in the TIM23 complexes saturated with different preproteins. In contrast, the stoichiometry of the nonessential components was significantly changed. The majority of Tim21 but only minor amounts of total Pam17 present in mitochondria were found associated with the TIM23 complex in its empty state. Pam17 was eliminated from the complex when the TIM23 translocase was saturated with matrix targeted preprotein and partially removed in the case of saturation with laterally sorted preprotein. On the other hand, Tim21 remained associated with the translocase in all three states. The highest amounts of Tim21 were found in the complex when it was saturated with matrix targeted preprotein (Table 4.1).

Table 4.1. The abundance of the nonessential components in the TIM23 translocase in different translocation modes. The amounts of Tim21 and Pam17 found associated with the TIM23 translocase in empty state (PUR) did not differ from their respective amounts associated with the complex in mitochondria isolated under standard conditions (STD). The amounts of components present in the complex trapped with the laterally sorted ($b_2/cox5a$) and matrix targeted precursor proteins ($b_2\Delta/cox5a\Delta TM$) are compared to the situation in PUR/STD mitochondria, not representing the stoichiometric ratio between Tim21 and Pam17.

	PUR/STD	$b_2/cox5a$	$b_2\Delta/cox5a\Delta TM$
Tim21	+++	++	+++++
Pam17	+++	++	—

Hence, Pam17 and Tim21 have opposing roles in the regulation of activity of the TIM23 translocase. When the translocase is in its empty state, Pam17 is present maintaining the import competent conformation of the TIM23 complex. Its association with the complex is controlled by the binding of Tim21. Once the preprotein associates with the translocase, Pam17 is removed while Tim21 remains associated with the complex and possibly binds to regions of the complex liberated by the removal of Pam17. When the preprotein is imported, the TIM23 translocase goes back to the empty state and Pam17 associates again to maintain the optimal conformation of the import competent state.

These results cannot be explained by a recently proposed model according to which the TIM23 complex exists in two forms, one responsible for lateral sorting containing only the membrane part of the complex and one responsible for translocation in the matrix containing both the membrane part and the import motor, but lacking Tim21 (Chacinska *et al.*, 2005). As it is shown here, the preproteins in transit do not affect the assembly of the essential subunits of the translocase. More precisely, the arrest of the preprotein targeted to the matrix did not lead to an increased assembly of the components of the motor and the membrane sector, nor did the presence of a laterally sorted preprotein induce the dissociation of the two parts of the complex, as it was proposed by the abovementioned model. In addition, the stoichiometry of the complex remains the same when the translocase is working at full speed and when it is empty, confirming that the two parts of the complex are associated with each other irrespective of whether the complex is in its resting state or it is translocating different types of preproteins to different mitochondrial subcompartments. In support of the notion that the TIM23 complex is a single entity, the experiments with mitochondria depleted of each of the essential subunits have shown that the membrane part of the complex senses disruptions in the motor part and *vice versa*, demonstrating that these two parts of the translocase are structurally and functionally dependent on each other. Tight coupling of the two parts of the translocase seems to occur in two ways, via direct interaction of Tim14-Tim16 subcomplex with Tim17 and via binding of Tim44 to Tim17-Tim23 core of the complex.

A major reason for arriving at the two strongly contradictory explanations is lying largely on the lack of coisolation of the various import motor components with Protein A tagged Tim21 Pfanner's group observed in their experiments (Chacinska *et al.*, 2005; van der Laan *et al.*, 2005). As shown here placing Protein A tag on Tim21 alters the protein in a way that it acts differently than the wild type form. The Protein A tag has adverse effects on the interaction of Tim21 with various TIM23 components. In a direct comparison of two different tags on Tim21, Protein A-tagged Tim21 was demonstrated to lead to false negative results. This led

also to obvious misclassification of Pam17 as the import motor component (van der Laan *et al.*, 2005). This conclusion is in agreement with a recent report that all the essential subunits of the TIM23 complex can be copurified with FLAG-tagged Tim21 (Tamura *et al.*, 2006). These experimental findings make necessary a change in the nomenclature in the field and the elimination of the term PAM complex (presequence translocase-associated motor) (Bohnert *et al.*, 2007; Koehler, 2004; Pfanner *et al.*, 2004; Rehling *et al.*, 2004). It is obvious that the import motor is not a separate complex, rather a part of an integral TIM23 complex.

On the basis of all these results I present the model of active remodeling of the TIM23 translocase during translocation of different preproteins (Figure 4.3). The import competent or the empty state (**E**) is the only state when the translocase is in the optimal conformation for accepting newly arriving preprotein. The type of the translocating preprotein determines the nature of the conformational change of the TIM23 translocase. The translocase distinguishes between matrix targeted and laterally sorted preproteins. This model implies two conformational states of the TIM23 translocase for the preprotein import, one for laterally sorted (**L**) and one for matrix targeted one (**M**). When the TIM23 translocase is in either of these two conformations it cannot accept new precursor, and it has to go back to E conformation to do so. The arrival of the preprotein with its N-terminal matrix targeting signal (MTS) induces a series of conformational changes in both parts of the complex to allow its passage into the matrix. If no other signal is present in the preprotein, translocation into the matrix will be completed by a number of ATP-driven cycles of the import motor. If, however, a sorting signal is present at some place after the MTS in the preprotein in transit, the translocase undergoes additional conformational changes which lead to lateral insertion of the preprotein or L conformation. In this case, the translocase changes its conformation in E→M→L direction. Some of the laterally sorted preproteins have a sorting signal directly after the presequence and are imported via the TIM23 complex without the help of the import motor. Though it can not be excluded that they also may require a single or a few cycles of the import motor, it is more possible that the translocase changes directly from E to L conformation. Once the preprotein exits the channel (and the TOM complex), the TIM23 translocase will go back directly to the import competent E state. As a consequence, E↔M and E↔L are reversible pathways for the conformational changes of the complex in two opposite directions and M→L pathway is unidirectional.

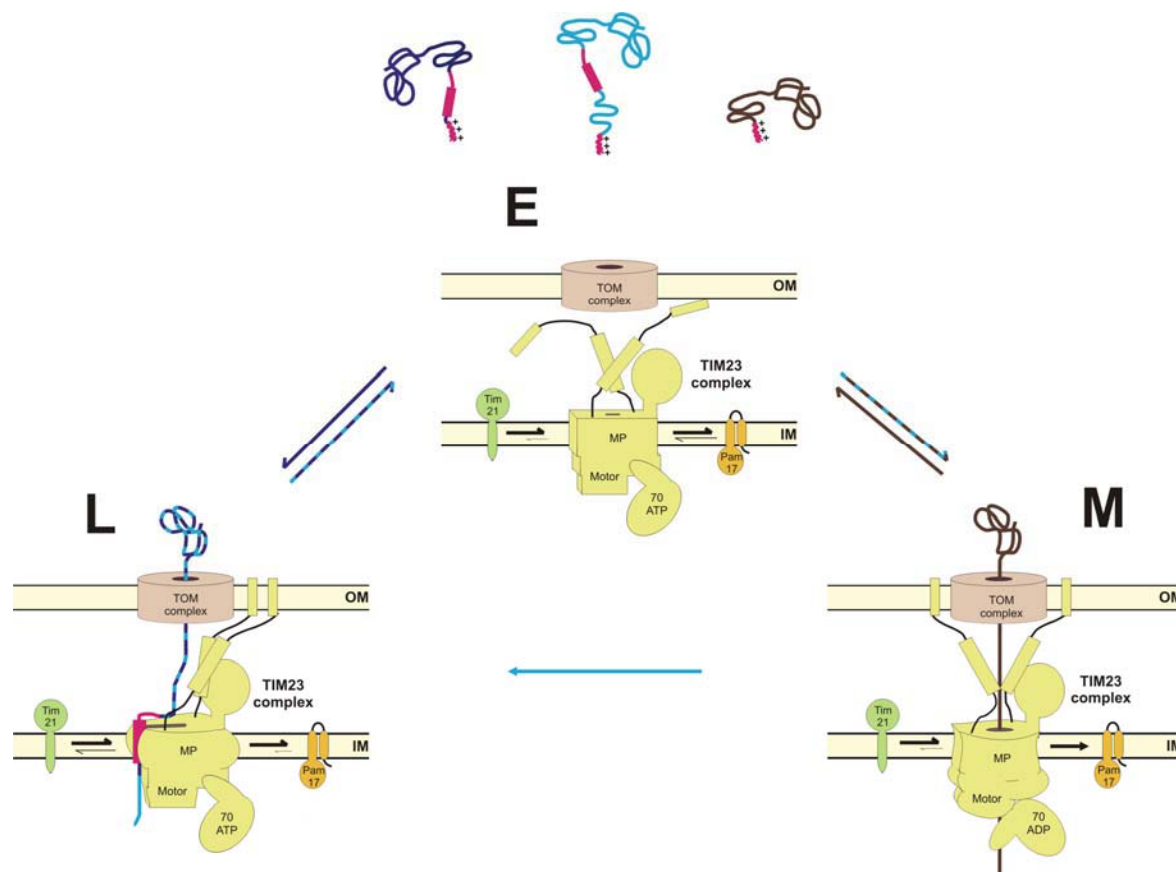


Figure 4.3. Active remodeling of the TIM23 complex during protein translocation. The TIM23 complex imports preproteins that are laterally sorted without the help of the import motor (blue), those that are sorted in a motor dependent manner (cyan) and those targeted to the matrix (brown). The arrows between different translocation states (E, empty; L, lateral sorting; M, matrix translocation) represent different pathways of conformational changes the TIM23 complex undergoes. The colors of these arrows correspond to the type of preprotein that is translocated via the various conformational states. The arrows regarding Pam17 and Tim21 indicate the changes in the association of these proteins with the TIM23 complex. MP, membrane part of the complex. See text for more details.

This model is conceptually different from the model that suggests the existence of two structurally and functionally distinct forms of the TIM23 translocase (Chacinska *et al.*, 2005). The model presented by Chacinska *et al.* provided no explanation as to which signal would cause the switch necessary to release Tim21 and recruit the import motor. The MTS itself evidently cannot be this signal as it is present both in matrix targeted as well as in laterally sorted preproteins. Indeed, it is difficult to envisage such a signal in the above mentioned preproteins which consist of the N-terminal MTS and a passenger protein. Furthermore, the model cannot explain the sorting pathway of a number of laterally sorted preproteins whose import depends on the import motor, because the sorting signal is far apart from the MTS (Gärtner *et al.*, 1995; Stuart *et al.*, 1994; Voos *et al.*, 1993). In contrast, the model presented in this study easily explains the import behavior of all preproteins sorted by the TIM23 translocase. The reasons why the TIM23 translocase reaches the conformational state for

import of laterally sorted preproteins via two postulated pathways lie in the difference in lengths between the MTS and the hydrophobic stop-transfer signal of these preproteins and in the sequences following their transmembrane domains (Table 4.2).

Table 4.2. Laterally sorted preproteins. The length of the segment between the presequence and the stop-transfer signal (*A*) was predicted *in silico*. *B* – experimentally proven import motor dependence of the preprotein.

Name	<i>A</i> (aa)	<i>B</i>	Prediction <i>in silico</i>
Cbp4	1-7	n.a.	HMMTOP and Meier <i>et al.</i> , 2005b
Cox5a	77-82	YES	MitoProt, HMMTOP and Meier <i>et al.</i> , 2005b. Proven to be a motor dependent precursor (Gärtner <i>et al.</i> , 1995).
Cox5b	76-83	n.a.	MitoProt, HMMTOP and Meier <i>et al.</i> , 2005b.
Cytc ₁	14	n.a.	MitoProt, HMMTOP and Meier <i>et al.</i> , 2005b. Two TM domains and possible two different mechanisms for sorting and insertion (Nicholson <i>et al.</i> , 1989).
Cytb ₂	22	YES	MitoProt and HMMTOP. The chimera of first 220 aa of this protein and mouse DHFR on the C-terminus was proven to be a motor independent precursor (Stuart <i>et al.</i> , 1994; Voos <i>et al.</i> , 1993).
Dld1	16	NO	MitoProt, HMMTOP and Meier <i>et al.</i> , 2005b. The chimera DLD(1-72)DHFR is laterally sorted in a motor independent manner (Rojo <i>et al.</i> , 1998).
Hem14	1	n.a.	HMMTOP and Meier <i>et al.</i> , 2005b.
Mia40	8	n.a.	MitoProt, HMMTOP and Meier <i>et al.</i> , 2005b.
Oms1	64	n.a.	MitoProt, HMMTOP and Meier <i>et al.</i> , 2005b.
Sco1	24	n.a.	MitoProt, HMMTOP and Meier <i>et al.</i> , 2005b.
Sco2	39	n.a.	MitoProt, HMMTOP and Meier <i>et al.</i> , 2005b.
She9	256-261	n.a.	MitoProt, HMMTOP and Meier <i>et al.</i> , 2005b.
Tim21	28-31	n.a.	MitoProt and HMMTOP.
Tim50	69-72	n.a.	MitoProt, HMMTOP and Meier <i>et al.</i> , 2005b.
Yme1	187	n.a.	MitoProt, HMMTOP and Meier <i>et al.</i> , 2005b.
Yme2	243	n.a.	MitoProt, HMMTOP and Meier <i>et al.</i> , 2005b.
<i>Cox5a</i> Δ <i>matrix</i>	13-18	NO	<i>MitoProt and HMMTOP. Not a natural precursor. Motor independent version of Cox5a (Gärtner et al., 1995).</i>
<i>Cytb</i> ₂ (167)DHFR	22	NO	<i>MitoProt and HMMTOP. Not a natural precursor. The chimera of first 167 aa of this protein and mouse DHFR on the C-terminus was proven to be a motor independent precursor (Stuart et al., 1994; Voos et al., 1993).</i>

Subunit 5a of cytochrome oxidase (Cox5a) has a stretch of ca. 80 aa between the presequence and the transmembrane domain and is laterally sorted in the inner membrane dependent on the activity of the import motor. When the transmembrane domain is deleted, this protein ends up in the matrix demonstrating that its transmembrane domain is the signal for lateral sorting. However, when a number of residues between the presequence and the TM domain are deleted, shortening this stretch to only 13-18 aa (Cox5aΔ*matrix*), this protein is laterally sorted in the inner membrane without the apparent help of mtHsp70 (Gärtner *et al.*, 1995). Thus, if the stretch between the presequence and the TM domain is long enough to get trapped by mtHsp70, the import of this preprotein will be ATP- and motor-dependent and will

go via E→M→L pathway. If the stretch is short enough, this protein will be sorted directly via E→L pathway. In addition, one must take into account that at least for one of the preproteins the residues after the stop-transfer signal also play a role in the matrix ATP dependence of this preprotein. Preproteins, consisting of 220 or more residues of cytochrome b₂ fused to dihydrofolate reductase, were observed to require matrix ATP, whereas the import of shorter fusion proteins with up to 167 residues of cytochrome b₂ was independent of matrix ATP (Stuart *et al.*, 1994; Voos *et al.*, 1993). The motor dependence of majority of preproteins sorted in the inner membrane has, however, not been investigated.

Another question in this context that requires to be studied is at which time of the translocation process the TIM23 translocase starts changing its conformation. The TIM23 translocase senses the mutational alterations of the TOM complex. The communication between the two complexes seems to be close and several proteins are candidates for mediating this communication. In addition to interactions of Tim21 with the TOM complex interaction and the exposure of the N-terminal segment of Tim23 on the surface of mitochondria, Tim50 interacts with preproteins as soon as they emerge from the outlet of the TOM complex (Yamamoto *et al.*, 2002; Mokranjac *et al.*, 2003a). Interestingly, in the absence of Tim50, Tim23 does not reach the surface of mitochondria (Yamamoto *et al.*, 2002). Thus, at least three components of the TIM23 complex, Tim50, Tim23 and Tim21, are involved in the active cooperation of TOM and TIM23 complexes during the early steps of preprotein translocation via the TIM23 complex. It is possible that other proteins from two complexes that expose domains into the IMS play role in this interaction. The TOM complex is also structurally reorganized during protein translocation, by the entry of a preprotein. In addition, certain mutations in Tom40 disturb only the transfer of preproteins by the TIM23 translocase, whereas the sorting of preproteins into the outer membrane or import of proteins via the TIM22 complex is not affected (Gabriel *et al.*, 2003). Thus, the TIM23 complex may receive information from the outer membrane the moment the preprotein binds to receptors of the TOM complex. The specificity of this communication is further corroborated with results showing drastic conformational change of Tim23 when Tom20, receptor responsible for recognition of the majority of preproteins with the cleavable presequence, was deleted, whereas deletion of Tom70, receptor for most of the preprotein substrates of the TIM22 complex, had no effect on the conformation of Tim23.

The conformational changes of a translocase during the import of different precursors are analyzed here in a systematic fashion. Similar analyses were performed with some other translocases, but these analyses were mainly focused on translocation substrate or on specific

regions of the complex playing a specific role in the process. The approach of locking in specific states and concomitant analysis of the composition, conformation and neighboring relationships of a translocase seems to be a promising approach for elucidating a number of open questions in the field of protein traffic.

5. SUMMARY

The vast majority of mitochondrial proteins are synthesized on cytosolic ribosomes in the form of precursor proteins and subsequently imported into mitochondria through the concerted action of the translocases present in the outer and the inner membrane. Almost all proteins destined to the matrix, the majority of proteins of the inner membrane and a number of proteins residing in the intermembrane space are synthesized with positively charged N-terminal matrix targeting sequences (MTS). The TIM23 complex (*translocase of the inner membrane*) mediates translocation of MTS-containing precursor proteins across or their insertion into the mitochondrial inner membrane in a membrane potential and ATP-dependent manner. The TIM23 complex consists of eight essential subunits that can be assigned to two operationally defined parts: the membrane embedded protein conducting channel with the receptor and the import motor associated with the channel at the matrix side of the inner membrane. The present study was undertaken to gain insight into the dynamics of the TIM23 translocase during import of different types of preproteins.

To investigate whether the TIM23 translocase contains components in addition to the ones described so far, the complex was purified by affinity chromatography using a yeast strain which was constructed to express Protein A-tagged Tim23 and analyzed by mass spectrometry. A previously uncharacterized protein was identified and termed Tim21. It is the first subunit of the TIM23 complex that was found not to be essential for viability of yeast cells. Tim21 is anchored in the mitochondrial inner membrane by a single transmembrane domain exposing the C-terminal domain into the intermembrane space. The C-terminal domain shows high affinity for the TOM complex. The transmembrane domain of Tim21 is conserved and is likely responsible for binding of Tim21 to the Tim17-Tim23 core of the TIM23 complex. Tim21 competes for binding to the membrane part of the complex with another newly identified nonessential subunit, Pam17. Deletion of Pam17 was found to induce a change of the conformation of the TIM23 complex that led to a constrained import of the motor dependent precursor proteins.

The TIM23 translocase switches between translocation mode that facilitates import of proteins into the matrix and insertion mode that allows lateral sorting of proteins into the lipid

bilayer. To study the nature of this process a novel approach was applied by which homogenous populations of the TIM23 complex trapped in different translocation states could be accumulated. The composition, the conformation and the topology of the TIM23 complex trapped in different states of translocation of precursor proteins were analyzed. The essential components of the membrane part and of the import motor were found in one complex. They were present at the same ratio irrespective of the state of activity of the translocase. The TIM23 translocase adopted different conformations in its various states of activity: when it was empty, when it inserted preproteins into the inner membrane and when it translocated preproteins targeted to the matrix. Furthermore, increased translocation load induced increased exposure of the N-terminal segment of Tim23 on the surface of mitochondria. This shows the involvement of this segment in the interplay between the outer membrane and the TIM23 complex during translocation of preproteins. The interconversion of the TIM23 translocase between the functional states occurs primarily by conformational changes of the essential components, whereas Tim21 and Pam17 are responsible for the fine tuning of these processes. A hypothesis that describes the behavior of the TIM23 translocase is presented.

6. LITERATURE

Abe, Y., Shodai, T., Muto, T., Mihara, K., Torii, H., Nishikawa, S., Endo, T., and Kohda, D. (2000). Structural basis of presequence recognition by the mitochondrial protein import receptor Tom20. *Cell* *100*, 551-560.

Ahting, U., Thieffry, M., Engelhardt, H., Hegerl, R., Neupert, W., and Nussberger, S. (2001). Tom40, the pore-forming component of the protein-conducting TOM channel in the outer membrane of mitochondria. *J. Cell Biol.* *153*, 1151-1160.

Ahting, U., Thun, C., Hegerl, R., Typke, D., Nargang, F.E., Neupert, W., and Nussberger, S. (1999). The TOM core complex: the general protein import pore of the outer membrane of mitochondria. *J. Cell Biol.* *147*, 959-968.

Ainavarapu, S.R., Li, L., Badilla, C.L., and Fernandez, J.M. (2005). Ligand binding modulates the mechanical stability of dihydrofolate reductase. *Biophys. J.* *89*, 3337-3344.

Albrecht, R., Rehling, P., Chacinska, A., Brix, J., Cadamuro, S.A., Volkmer, R., Guiard, B., Pfanner, N., and Zeth, K. (2006). The Tim21 binding domain connects the preprotein translocases of both mitochondrial membranes. *EMBO Rep.* *7*, 1233-1238.

Allen, S., Balabanidou, V., Sideris, D.P., Lisowsky, T., and Tokatlidis, K. (2005). Erv1 mediates the Mia40-dependent protein import pathway and provides a functional link to the respiratory chain by shuttling electrons to cytochrome c. *J. Mol. Biol.* *353*, 937-944.

Bauer, M.F., Sirrenberg, C., Neupert, W., and Brunner, M. (1996). Role of Tim23 as voltage sensor and presequence receptor in protein import into mitochondria. *Cell* *87*, 33-41.

Beasley, E.M., Muller, S., and Schatz, G. (1993). The signal that sorts yeast cytochrome b2 to the mitochondrial intermembrane space contains three distinct functional regions. *EMBO J.* *12*, 2303-2311.

Berks, B.C., Sargent, F., De Leeuw, E., Hinsley, A.P., Stanley, N.R., Jack, R.L., Buchanan, G., and Palmer, T. (2000). A novel protein transport system involved in the biogenesis of bacterial electron transfer chains. *Biochim. Biophys. Acta* *1459*, 325-330.

Blobel, G. (1980). Intracellular protein topogenesis. *Proc. Natl. Acad. Sci. USA* *77*, 1496-1500.

Bohnert, M., Pfanner, N., and van der Laan, M. (2007). A dynamic machinery for import of mitochondrial precursor proteins. *FEBS Lett.* *581*, 2802-2810.

Bolliger, L., Junne, T., Schatz, G., and Lithgow, T. (1995). Acidic receptor domains on both sides of the outer membrane mediate translocation of precursor proteins into yeast mitochondria. *EMBO J.* *14*, 6318-6326.

Borst, P., and Grivell, L.A. (1978). The mitochondrial genome of yeast. *Cell* *15*, 705-723.

Bradford, M.M. (1976). A rapid and sensitive method for quantitation of microgram quantities of protein utilising the principle of protein-dye binding. *Anal. Biochem.* *72*, 248-254.

Braun, H.P., Emmermann, M., Kruff, V., and Schmitz, U.K. (1992). The general mitochondrial processing peptidase from potato is an integral part of cytochrome c reductase of the respiratory chain. *EMBO J.* *11*, 3219-3227.

Breitfeld, P.P., Casanova, J.E., Simister, N.E., Ross, S.A., McKinnon, W.C., and Mostov, K.E. (1989). Sorting signals. *Curr. Opin. Cell Biol.* *1*, 617-623.

- Burri, L., Vascotto, K., Fredersdorf, S., Tiedt, R., Hall, M.N., and Lithgow, T. (2004). Zim17, a novel zinc finger protein essential for protein import into mitochondria. *J. Biol. Chem.* *279*, 50243-50249.
- Casadaban, M.J., and Cohen, S.N. (1980). Analysis of gene control signals by DNA fusion and cloning in *Escherichia coli*. *J. Mol. Biol.* *138*, 179-207.
- Chacinska, A., Lind, M., Frazier, A.E., Dudek, J., Meisinger, C., Geissler, A., Sickmann, A., Meyer, H.E., Truscott, K.N., Guiard, B., *et al.* (2005). Mitochondrial presequence translocase: switching between TOM tethering and motor recruitment involves Tim21 and Tim17. *Cell* *120*, 817-829.
- Chacinska, A., Pfannschmidt, S., Wiedemann, N., Kozjak, V., Sanjuan Szklarz, L.K., Schulze-Specking, A., Truscott, K.N., Guiard, B., Meisinger, C., and Pfanner, N. (2004). Essential role of Mia40 in import and assembly of mitochondrial intermembrane space proteins. *EMBO J.* *23*, 3735-3746.
- Chacinska, A., Rehling, P., Guiard, B., Frazier, A.E., Schulze-Specking, A., Pfanner, N., Voos, W., and Meisinger, C. (2003). Mitochondrial translocation contact sites: separation of dynamic and stabilizing elements in formation of a TOM-TIM-preprotein supercomplex. *EMBO J.* *22*, 5370-5381.
- Cline, K., and Mori, H. (2001). Thylakoid Δ pH-dependent precursor proteins bind to a cpTatC-Hcf106 complex before Tha4-dependent transport. *J. Cell Biol.* *154*, 719-729.
- Coppock, D.L., and Thorpe, C. (2006). Multidomain flavin-dependent sulfhydryl oxidases. *Antioxid. Redox Signal.* *8*, 300-311.
- Court, D.A., Nargang, F.E., Steiner, H., Hodges, R.S., Neupert, W., and Lill, R. (1996). Role of the intermembrane-space domain of the preprotein receptor Tom22 in protein import into mitochondria. *Mol. Cell Biol.* *16*, 4035-4042.
- Curran, S.P., Leuenberger, D., Leverich, E.P., Hwang, D.K., Beverly, K.N., and Koehler, C.M. (2004). The role of Hot13p and redox chemistry in the mitochondrial TIM22 import pathway. *J. Biol. Chem.* *279*, 43744-43751.
- D'Silva, P.D., Schilke, B., Walter, W., Andrew, A., and Craig, E.A. (2003). J protein cochaperone of the mitochondrial inner membrane required for protein import into the mitochondrial matrix. *Proc. Natl. Acad. Sci. USA* *100*, 13839-13844.
- D'Silva, P.R., Schilke, B., Walter, W., and Craig, E.A. (2005). Role of Pam16's degenerate J domain in protein import across the mitochondrial inner membrane. *Proc. Natl. Acad. Sci. USA* *102*, 12419-12424.
- Davis, A.J., Alder, N.N., Jensen, R.E., and Johnson, A.E. (2007). The Tim9p/10p and Tim8p/13p complexes bind to specific sites on Tim23p during mitochondrial protein import. *Mol. Biol. Cell* *18*, 475-486.
- Davis, A.J., Sepuri, N.B., Holder, J., Johnson, A.E., and Jensen, R.E. (2000). Two intermembrane space TIM complexes interact with different domains of Tim23p during its import into mitochondria. *J. Cell Biol.* *150*, 1271-1282.
- De Los Rios, P., Ben-Zvi, A., Slutsky, O., Azem, A., and Goloubinoff, P. (2006). Hsp70 chaperones accelerate protein translocation and the unfolding of stable protein aggregates by entropic pulling. *Proc. Natl. Acad. Sci. USA* *103*, 6166-6171.
- Dekker, P.J., Martin, F., Maarse, A.C., Bomer, U., Muller, H., Guiard, B., Meijer, M., Rassow, J., and Pfanner, N. (1997). The Tim core complex defines the number of mitochondrial translocation contact sites and can hold arrested preproteins in the absence of matrix Hsp70-Tim44. *EMBO J.* *16*, 5408-5419.
- Dekker, P.J., Ryan, M.T., Brix, J., Muller, H., Honlinger, A., and Pfanner, N. (1998). Preprotein translocase of the outer mitochondrial membrane: molecular dissection and assembly of the general import pore complex. *Mol. Cell Biol.* *18*, 6515-6524.
- Diekert, K., Kispal, G., Guiard, B., and Lill, R. (1999). An internal targeting signal directing proteins into the mitochondrial intermembrane space. *Proc. Natl. Acad. Sci. U S A* *96*, 11752-11757.

- Dietmeier, K., Honlinger, A., Bomer, U., Dekker, P.J., Eckerskorn, C., Lottspeich, F., Kubrich, M., and Pfanner, N. (1997). Tom5 functionally links mitochondrial preprotein receptors to the general import pore. *Nature* 388, 195-200.
- Dimmer, K.S., Fritz, S., Fuchs, F., Messerschmitt, M., Weinbach, N., Neupert, W., and Westermann, B. (2002). Genetic basis of mitochondrial function and morphology in *Saccharomyces cerevisiae*. *Mol. Biol. Cell* 13, 847-853.
- Donzeau, M., Kaldi, K., Adam, A., Paschen, S., Wanner, G., Guiard, B., Bauer, M.F., Neupert, W., and Brunner, M. (2000). Tim23 links the inner and outer mitochondrial membranes. *Cell* 101, 401-412.
- Dower, W.J., Miller, J.F., and Ragsdale, C.W. (1988). High efficiency transformation of *E. coli* by high voltage electroporation. *Nucleic Acids Res.* 16, 6127-6145.
- Eilers, M., and Schatz, G. (1986). Binding of a specific ligand inhibits import of a purified precursor protein into mitochondria. *Nature* 322, 228-232.
- Emtage, J.L., and Jensen, R.E. (1993). MAS6 encodes an essential inner membrane component of the yeast mitochondrial protein import pathway. *J. Cell Biol.* 122, 1003-1012.
- Endres, M., Neupert, W., and Brunner, M. (1999). Transport of the ADP/ATP carrier of mitochondria from the TOM complex to the TIM22.54 complex. *EMBO J.* 18, 3214-3221.
- Esaki, M., Kanamori, T., Nishikawa, S.I., Shin, I., Schultz, P.G., and Endo, T. (2003). Tom40 protein import channel binds to non-native proteins and prevents their aggregation. *Nat. Struct. Biol.* 10, 988-994.
- Esaki, M., Shimizu, H., Ono, T., Yamamoto, H., Kanamori, T., Nishikawa, S., and Endo, T. (2004). Mitochondrial protein import. Requirement of presequence elements and tom components for precursor binding to the TOM complex. *J. Biol. Chem.* 279, 45701-45707.
- Fölsch, H., Guiard, B., Neupert, W., and Stuart, R.A. (1996). Internal targeting signal of the BCS1 protein: a novel mechanism of import into mitochondria. *EMBO J.* 15, 479-487.
- Fölsch, H., Gaume, B., Neupert, W., Brunner, M., and Stuart, R.A. (1998). C- to N-terminal translocation of preproteins into mitochondria. *EMBO J.* 17, 6508-6515.
- Frazier, A.E., Dudek, J., Guiard, B., Voos, W., Li, Y., Lind, M., Meisinger, C., Geissler, A., Sickmann, A., Meyer, H.E., *et al.* (2004). Pam16 has an essential role in the mitochondrial protein import motor. *Nat. Struct. Mol. Biol.* 11, 226-233.
- Frazier, A.E., Taylor, R.D., Mick, D.U., Warscheid, B., Stoepel, N., Meyer, H.E., Ryan, M.T., Guiard, B., and Rehling, P. (2006). Mdm38 interacts with ribosomes and is a component of the mitochondrial protein export machinery. *J. Cell Biol.* 172, 553-564.
- Funes, S., Nargang, F.E., Neupert, W., and Herrmann, J.M. (2004). The Oxa2 protein of *Neurospora crassa* plays a critical role in the biogenesis of cytochrome oxidase and defines a ubiquitous subbranch of the Oxa1/YidC/Alb3 protein family. *Mol. Biol. Cell* 15, 1853-1861.
- Gabriel, K., Egan, B., and Lithgow, T. (2003). Tom40, the import channel of the mitochondrial outer membrane, plays an active role in sorting imported proteins. *EMBO J.* 22, 2380-2386.
- Gallas, M.R., Dienhart, M.K., Stuart, R.A., and Long, R.M. (2006). Characterization of Mmp37p, a *Saccharomyces cerevisiae* mitochondrial matrix protein with a role in mitochondrial protein import. *Mol. Biol. Cell* 17, 4051-4062.
- Gärtner, F., Voos, W., Querol, A., Miller, B.R., Craig, E.A., Cumsy, M.G., and Pfanner, N. (1995). Mitochondrial import of subunit Va of cytochrome c oxidase characterized with yeast mutants - Independence from receptors, but requirement for matrix hsp70 translocase function. *J. Biol. Chem.* 270, 3788-3795.
- Geissler, A., Chacinska, A., Truscott, K.N., Wiedemann, N., Brandner, K., Sickmann, A., Meyer, H.E., Meisinger, C., Pfanner, N., and Rehling, P. (2002). The mitochondrial presequence translocase: an essential role of Tim50 in directing preproteins to the import channel. *Cell* 111, 507-518.

- Gentle, I., Gabriel, K., Beech, P., Waller, R., and Lithgow, T. (2004). The Omp85 family of proteins is essential for outer membrane biogenesis in mitochondria and bacteria. *J. Cell Biol.* *164*, 19-24.
- Gietz, D., St Jean, A., Woods, R.A., and Schiestl, R.H. (1992). Improved method for high efficiency transformation of intact yeast cells. *Nucleic Acids Res.* *20*, 1425.
- Glaser, S.M., Miller, B.R., and Cumsky, M.G. (1990). Removal of a hydrophobic domain within the mature portion of a mitochondrial inner membrane protein causes its mislocalization to the matrix. *Mol. Cell Biol.* *10*, 1873-1881.
- Glick, B.S., Beasley, E.M., and Schatz, G. (1992a). Protein sorting in mitochondria. *Trends Biochem. Sci.* *17*, 453-459.
- Glick, B.S., Brandt, A., Cunningham, K., Muller, S., Hallberg, R.L., and Schatz, G. (1992b). Cytochromes c1 and b2 are sorted to the intermembrane space of yeast mitochondria by a stop-transfer mechanism. *Cell* *69*, 809-822.
- Gould, S.J., and Collins, C.S. (2002). Opinion: peroxisomal-protein import: is it really that complex? *Nat. Rev. Mol. Cell Biol.* *3*, 382-389.
- Grivell, L.A., Artal-Sanz, M., Hakkaart, G., de Jong, L., Nijtmans, L.G., van Oosterum, K., Siep, M., and van der Spek, H. (1999). Mitochondrial assembly in yeast. *FEBS Lett.* *452*, 57-60.
- Habib, S.J., Waizenegger, T., Lech, M., Neupert, W., and Rapaport, D. (2005). Assembly of the TOB complex of mitochondria. *J. Biol. Chem.* *280*, 6434-6440.
- Habib, S.J., Neupert, W., and Rapaport, D. (2007a). Analysis and prediction of mitochondrial targeting signals. *Methods Cell Biol.* *80*, 761-781.
- Habib, S.J., Waizenegger, T., Niewianda, A., Paschen, S.A., Neupert, W., and Rapaport, D. (2007b). The N-terminal domain of Tob55 has a receptor-like function in the biogenesis of mitochondrial beta-barrel proteins. *J. Cell Biol.* *176*, 77-88.
- Hammen, P.K., Gorenstein, D.G., and Weiner, K. (1996). Amphiphilicity determines binding properties of three mitochondrial presequences to lipid surface. *Biochemistry* *35*, 3772-3781.
- Harlow, E., and Lane, D. (1988). *Antibodies: A Laboratory Manual* (Cold Spring Harbor; NY, Cold Spring Harbor Laboratory Press).
- Hell, K., Neupert, W., and Stuart, R.A. (2001). Oxa1p acts as a general membrane insertion machinery for proteins encoded by mitochondrial DNA. *EMBO J.* *20*, 1281-1288.
- Herlan, M., Vogel, F., Bornhøvd, C., Neupert, W., and Reichert, A.S. (2003). Processing of Mgm1 by the rhomboid-type protease Pcp1 is required for maintenance of mitochondrial morphology and of mitochondrial DNA. *J. Biol. Chem.* *278*, 27781-27788.
- Herrmann, J.M., Fölsch, H., Neupert, W., and Stuart, R.A. (1994). Isolation of yeast mitochondria and study of mitochondrial protein translation. In *Cell Biology: A Laboratory Handbook*, J.E. Celis, ed. (San Diego, Academic Press), pp. 538-544.
- Herrmann, J.M., and Hell, K. (2005). Chopped, trapped or tacked - protein translocation into the IMS of mitochondria. *Trends Biochem. Sci.* *30*, 205-211.
- Hofhaus, G., Lee, J.E., Tews, I., Rosenberg, B., and Lisowsky, T. (2003). The N-terminal cysteine pair of yeast sulfhydryl oxidase Erv1p is essential for in vivo activity and interacts with the primary redox centre. *Eur. J. Biochem. / FEBS* *270*, 1528-1535.
- Hofmann, S., Rothbauer, U., Muhlenbein, N., Baiker, K., Hell, K., and Bauer, M.F. (2005). Functional and mutational characterization of human MIA40 acting during import into the mitochondrial intermembrane space. *J. Mol. Biol.* *353*, 517-528.
- Hoppins, S.C., and Nargang, F.E. (2004). The Tim8-Tim13 complex of *Neurospora crassa* functions in the assembly of proteins into both mitochondrial membranes. *J. Biol. Chem.* *279*, 12396-12405.
- Horwich, A. (1990). Protein import into mitochondria and peroxisomes. *Curr. Opin. Cell Biol.* *2*, 625-633.

- Iosefson, O., Levy, R., Marom, M., Slutsky-Leiderman, O., and Azem, A. (2007). The Pam18/Tim14-Pam16/Tim16 complex of the mitochondrial translocation motor: the formation of a stable complex from marginally stable proteins. *Protein Sci.* *16*, 316-322.
- Ishikawa, D., Yamamoto, H., Tamura, Y., Moritoh, K., and Endo, T. (2004). Two novel proteins in the mitochondrial outer membrane mediate beta-barrel protein assembly. *J. Cell Biol.* *166*, 621-627.
- Jarvis, J.A., Ryan, M.T., Hoogenraad, N.J., Craik, D.J., and Hoj, R.B. (1995). Solution structure of the acetylated and noncleavable mitochondrial targeting signal of rat chaperonin 10. *J. Biol. Chem.* *270*, 1323-1331.
- Jia, L., Dienhart, M., Schramp, M., McCauley, M., Hell, K., and Stuart, R.A. (2003). Yeast Oxa1 interacts with mitochondrial ribosomes: the importance of the C-terminal region of Oxa1. *EMBO J.* *22*, 6438-6447.
- Johnson, A.E., and van Waes, M.A. (1999). The translocon: a dynamic gateway at the ER membrane. *Annu. Rev. Cell Dev. Biol.* *15*, 799-842.
- Josyula, R., Jin, Z., Fu, Z., and Sha, B. (2006). Crystal structure of yeast mitochondrial peripheral membrane protein Tim44p C-terminal domain. *J. Mol. Biol.* *359*, 798-804.
- Kaldi, K., Bauer, M.F., Sirrenberg, C., Neupert, W., and Brunner, M. (1998). Biogenesis of Tim23 and Tim17, integral components of the TIM machinery for matrix-targeted preproteins. *EMBO J.* *17*, 1569-1576.
- Karniely, S., Regev-Rudzki, N., and Pines, O. (2006). The presequence of fumarase is exposed to the cytosol during import into mitochondria. *J. Mol. Biol.* *358*, 396-405.
- Kassenbrock, C.K., Cao, W., and Douglas, M.G. (1993). Genetic and biochemical characterization of ISP6, a small mitochondrial outer membrane protein associated with the protein translocation complex. *EMBO J.* *12*, 3023-3034.
- Khyse-Anderson, J. (1984). Electrophoretic transfer of multiple gels: a simple apparatus without buffer tank for rapid transfer of proteins from polyacrylamide to nitrocellulose. *J. Biochem. Biophys. Methods* *10*, 203-207.
- King, M.C., Lusk, C.P., and Blobel, G. (2006). Karyopherin-mediated import of integral inner nuclear membrane proteins. *Nature* *442*, 1003-1007.
- Knop, M., Siegers, K., Pereira, G., Zachariae, W., Winsor, B., Nasmyth, K., and Schiebel, E. (1999). Epitope tagging of yeast genes using a PCR-based strategy: more tags and improved practical routines. *Yeast* *15*, 963-972.
- Knudsen, K.A. (1985). Proteins transferred to nitrocellulose for use as immunogens. *Anal. Biochem.* *147*, 285-288.
- Koehler, C.M. (2004). New developments in mitochondrial assembly. *Annu. Rev. Cell Dev. Biol.* *20*, 309-335.
- Koehler, C.M., Merchant, S., and Schatz, G. (1999). How membrane proteins travel across the mitochondrial intermembrane space. *Trends Biochem. Sci.* *24*, 428-432.
- Komiya, T., Rospert, S., Koehler, C., Looser, R., Schatz, G., and Mihara, K. (1998). Interaction of mitochondrial targeting signals with acidic receptor domains along the protein import pathway: evidence for the 'acid chain' hypothesis. *EMBO J.* *17*, 3886-3898.
- Kovermann, P., Truscott, K.N., Guiard, B., Rehling, P., Sepuri, N.B., Muller, H., Jensen, R.E., Wagner, R., and Pfanner, N. (2002). Tim22, the essential core of the mitochondrial protein insertion complex, forms a voltage-activated and signal-gated channel. *Mol. Cell* *9*, 363-373.
- Kozany, C., Mokranjac, D., Sichting, M., Neupert, W., and Hell, K. (2004). The J domain-related cochaperone Tim16 is a constituent of the mitochondrial TIM23 preprotein translocase. *Nat. Struct. Mol. Biol.* *11*, 234-241.

- Kozjak, V., Wiedemann, N., Milenkovic, D., Lohaus, C., Meyer, H.E., Guiard, B., Meisinger, C., and Pfanner, N. (2003). An essential role of Sam50 in the protein sorting and assembly machinery of the mitochondrial outer membrane. *J. Biol. Chem.* 278, 48520-48523.
- Kuhn, A., Stuart, R., Henry, R., and Dalbey, R.E. (2003). The Alb3/Oxa1/YidC protein family: membrane-localized chaperones facilitating membrane protein insertion? *Trends Cell Biol.* 13, 510-516.
- Kunkele, K.P., Juin, P., Pompa, C., Nargang, F.E., Henry, J.P., Neupert, W., Lill, R., and Thieffry, M. (1998). The isolated complex of the translocase of the outer membrane of mitochondria. Characterization of the cation-selective and voltage-gated preprotein-conducting pore. *J. Biol. Chem.* 273, 31032-31039.
- Laemmli, U.K. (1970). Cleavage of structural proteins during the assembly of the head of bacteriophage T4. *Nature* 227, 680-685.
- Lee, C.M., Sedman, J., Neupert, W., and Stuart, R.A. (1999). The DNA helicase, Hmi1p, is transported into mitochondria by a C-terminal cleavable targeting signal. *J. Biol. Chem.* 274, 20937-20942.
- Li, Y., Dudek, J., Guiard, B., Pfanner, N., Rehling, P., and Voos, W. (2004). The presequence translocase-associated protein import motor of mitochondria. Pam16 functions in an antagonistic manner to Pam18. *J. Biol. Chem.* 279, 38047-38054.
- Lilley, B.N., and Ploegh, H.L. (2004). A membrane protein required for dislocation of misfolded proteins from the ER. *Nature* 429, 834-840.
- Lithgow, T., Glick, B.S., and Schatz, G. (1995). The protein import receptor of mitochondria. *Trends Biochem. Sci.* 20, 98-101.
- Liu, Q., D'Silva, P., Walter, W., Marszalek, J., and Craig, E.A. (2003). Regulated cycling of mitochondrial Hsp70 at the protein import channel. *Science* 300, 139-141.
- Lutz, T., Neupert, W., and Herrmann, J.M. (2003). Import of small Tim proteins into the mitochondrial intermembrane space. *EMBO J.* 22, 4400-4408.
- Manting, E.H., and Driessen, A.J. (2000). *Escherichia coli* translocase: the unravelling of a molecular machine. *Mol. Microbiol.* 37, 226-238.
- Marc, P., Margeot, A., Devaux, F., Blugeon, C., Corral-Debrinski, M., and Jacq, C. (2002). Genome-wide analysis of mRNAs targeted to yeast mitochondria. *EMBO Rep.* 3, 159-164.
- Margulis, L. (1970). Aerobiosis and the mitochondrion. *Origin of Eukaryotic Cells; Evidence and Research Implications for a Theory of the Origin and Evolution of Microbial, Plant, and Animal Cells on the Precambrian Earth.* Yale University Press, New Haven, CT. 178-207.
- Martinez-Caballero, S., Grigoriev, S.M., Herrmann, J.M., Campo, M.L., and Kinnally, K.W. (2007). Tim17p regulates the twin pore structure and voltage gating of the mitochondrial protein import complex TIM23. *J. Biol. Chem.* 282, 3584-3593.
- Matouschek, A., Pfanner, N., and Voos, W. (2000). Protein unfolding by mitochondria. The Hsp70 import motor. *EMBO Rep.* 1, 404-410.
- Mayer, A., Neupert, W., and Lill, R. (1995). Mitochondrial protein import: Reversible binding of the presequence at the trans side of the outer membrane drives partial translocation and unfolding. *Cell* 80, 127-137.
- Meier, S., Neupert, W., and Herrmann, J.M. (2005a). Conserved N-terminal negative charges in the Tim17 subunit of the TIM23 translocase play a critical role in the import of preproteins into mitochondria. *J. Biol. Chem.* 280, 7777-7785.
- Meier, S., Neupert, W., and Herrmann, J.M. (2005b). Proline residues of transmembrane domains determine the sorting of inner membrane proteins in mitochondria. *J. Cell Biol.* 170, 881-888.

- Meinecke, M., Wagner, R., Kovermann, P., Guiard, B., Mick, D.U., Hutu, D.P., Voos, W., Truscott, K.N., Chacinska, A., Pfanner, N., *et al.* (2006). Tim50 maintains the permeability barrier of the mitochondrial inner membrane. *Science* 312, 1523-1526.
- Meisinger, C., Pfannschmidt, S., Rissler, M., Milenkovic, D., Becker, T., Stojanovski, D., Youngman, M.J., Jensen, R.E., Chacinska, A., Guiard, B., *et al.* (2007). The morphology proteins Mdm12/Mmm1 function in the major beta-barrel assembly pathway of mitochondria. *EMBO J.* 26, 2229-2239.
- Meisinger, C., Rissler, M., Chacinska, A., Szklarz, L.K., Milenkovic, D., Kozjak, V., Schonfisch, B., Lohaus, C., Meyer, H.E., Yaffe, M.P., *et al.* (2004). The mitochondrial morphology protein Mdm10 functions in assembly of the preprotein translocase of the outer membrane. *Dev. Cell* 7, 61-71.
- Meisinger, C., Wiedemann, N., Rissler, M., Strub, A., Milenkovic, D., Schonfisch, B., Muller, H., Kozjak, V., and Pfanner, N. (2006). Mitochondrial protein sorting: differentiation of beta-barrel assembly by Tom7-mediated segregation of Mdm10. *J. Biol. Chem.* 281, 22819-22826.
- Melcak, I., Hoelz, A., and Blobel, G. (2007). Structure of Nup58/45 suggests flexible nuclear pore diameter by intermolecular sliding. *Science* 315, 1729-1732.
- Melton DA, K.P., Rebagliati MR, Maniatis T, Zinn K, and Green MR, (1984). Efficient in vitro synthesis of biologically active mRNA and RNA hybridization probes from plasmids containing a bacteriophage SP6 promoter. *Nucleic Acids Res.* 12, 7035-7056.
- Mesecke, N., Terziyska, N., Kozany, C., Baumann, F., Neupert, W., Hell, K., and Herrmann, J.M. (2005). A disulfide relay system in the intermembrane space of mitochondria that mediates protein import. *Cell* 121, 1059-1069.
- Mihara, K., and Omura, T. (1996). Cytoplasmic chaperones in precursor targeting to mitochondria - the role of MSF and hsp70. *Trends Cell Biol.* 6, 104-108.
- Milenkovic, D., Kozjak, V., Wiedemann, N., Lohaus, C., Meyer, H.E., Guiard, B., Pfanner, N., and Meisinger, C. (2004). Sam35 of the mitochondrial protein sorting and assembly machinery is a peripheral outer membrane protein essential for cell viability. *J. Biol. Chem.* 279, 22781-22785.
- Moczko, M., Bomer, U., Kubrich, M., Zufall, N., Honlinger, A., and Pfanner, N. (1997). The intermembrane space domain of mitochondrial Tom22 functions as a trans binding site for preproteins with N-terminal targeting sequences. *Mol. Cell Biol.* 17, 6574-6584.
- Model, K., Meisinger, C., Prinz, T., Wiedemann, N., Truscott, K.N., Pfanner, N., and Ryan, M.T. (2001). Multistep assembly of the protein import channel of the mitochondrial outer membrane. *Nat. Struct. Biol.* 8, 361-370.
- Mokranjac, D., Bourenkov, G., Hell, K., Neupert, W., and Groll, M. (2006). Structure and function of Tim14 and Tim16, the J and J-like components of the mitochondrial protein import motor. *EMBO J.* 25, 4675-4685.
- Mokranjac, D., Paschen, S.A., Kozany, C., Prokisch, H., Hoppins, S.C., Nargang, F.E., Neupert, W., and Hell, K. (2003a). Tim50, a novel component of the TIM23 preprotein translocase of mitochondria. *EMBO J.* 22, 816-825.
- Mokranjac, D., Sichtung, M., Neupert, W., and Hell, K. (2003b). Tim14, a novel key component of the import motor of the TIM23 protein translocase of mitochondria. *EMBO J.* 22, 4945-4956.
- Mokranjac, D., Sichtung, M., Popov-Čeleketić, D., Berg, A., Hell, K., and Neupert, W. (2005). The import motor of the yeast mitochondrial TIM23 preprotein translocase contains two different J proteins, Tim14 and Mdj2. *J. Biol. Chem.* 280, 31608-31614.
- Mori, H., and Cline, K. (2001). Post-translational protein translocation into thylakoids by the Sec and DeltapH-dependent pathways. *Biochim. Biophys. Acta* 1541, 80-90.
- Moro, F., Sirrenberg, C., Schneider, H.C., Neupert, W., and Brunner, M. (1999). The TIM17.23 preprotein translocase of mitochondria: composition and function in protein transport into the matrix. *EMBO J.* 18, 3667-3675.

- Naoe, M., Ohwa, Y., Ishikawa, D., Ohshima, C., Nishikawa, S., Yamamoto, H., and Endo, T. (2004). Identification of Tim40 that mediates protein sorting to the mitochondrial intermembrane space. *J. Biol. Chem.* *279*, 47815-47821.
- Neupert, W. (1997). Protein import into mitochondria. *Annu. Rev. Biochem.* *66*, 863-917.
- Neupert, W., and Brunner, M. (2002). The protein import motor of mitochondria. *Nat. Rev. Mol. Cell Biol.* *3*, 555-565.
- Neupert, W., and Herrmann, J.M. (2007). Translocation of proteins into mitochondria. *Annu. Rev. Biochem.* *76*, 723-749.
- Nicholson, D.W., Stuart, R.A., and Neupert, W. (1989). Biogenesis of cytochrome c1. Role of cytochrome c1 heme lyase and of the two proteolytic processing steps during import into mitochondria. *J. Biol. Chem.* *264*, 10156-10168.
- Okamoto, K., Brinker, A., Paschen, S.A., Moarefi, I., Hayer-Hartl, M., Neupert, W., and Brunner, M. (2002). The protein import motor of mitochondria: a targeted molecular ratchet driving unfolding and translocation. *EMBO J.* *21*, 3659-3671.
- Osborne, A.R., Rapoport, T.A., and van den Berg, B. (2005). Protein translocation by the Sec61/SecY channel. *Annu. Rev. Cell Dev. Biol.* *21*, 529-550.
- Ott, M., Prestele, M., Bauerschmitt, H., Funes, S., Bonnefoy, N., and Herrmann, J.M. (2006). Mba1, a membrane-associated ribosome receptor in mitochondria. *EMBO J.* *25*, 1603-1610.
- Paschen, S.A., and Neupert, W. (2001). Protein import into mitochondria. *IUBMB Life* *52*, 101-112.
- Paschen, S.A., Rothbauer, U., Kaldi, K., Bauer, M.F., Neupert, W., and Brunner, M. (2000). The role of the TIM8-13 complex in the import of Tim23 into mitochondria. *EMBO J.* *19*, 6392-6400.
- Paschen, S.A., Waizenegger, T., Stan, T., Preuss, M., Cyrklaff, M., Hell, K., Rapoport, D., and Neupert, W. (2003). Evolutionary conservation of biogenesis of beta-barrel membrane proteins. *Nature* *426*, 862-866.
- Pfanner, N., Douglas, M.G., Endo, T., Hoogenraad, N.J., Jensen, R.E., Meijer, M., Neupert, W., Schatz, G., Schmitz, U.K., and Shore, G.C. (1996). Uniform nomenclature for the protein transport machinery of the mitochondrial membranes. *Trends Biochem. Sci.* *21*, 51-52.
- Pfanner, N., and Geissler, A. (2001). Versatility of the mitochondrial protein import machinery. *Nat. Rev. Mol. Cell Biol.* *2*, 339-349.
- Pfanner, N., Hoeben, P., Tropschug, M., and Neupert, W. (1987). The carboxyl-terminal two-thirds of the ADP/ATP carrier polypeptide contains sufficient information to direct translocation into mitochondria. *J. Biol. Chem.* *262*, 14851-14854.
- Pfanner, N., Wiedemann, N., Meisinger, C., and Lithgow, T. (2004). Assembling the mitochondrial outer membrane. *Nat. Struct. Mol. Biol.* *11*, 1044-1048.
- Popov-Čeleketić, D., Mapa, K., Neupert, W., Mokranjac, D. Active remodeling of the TIM23 complex during translocation of preproteins into mitochondria. *In submission*.
- Preuss, M., Leonhard, K., Hell, K., Stuart, R.A., Neupert, W., and Herrmann, J.M. (2001). Mba1, a novel component of the mitochondrial protein export machinery of the yeast *Saccharomyces cerevisiae*. *J. Cell Biol.* *153*, 1085-1096.
- Ramage, L., Junne, T., Hahne, K., Lithgow, T., and Schatz, G. (1993). Functional cooperation of mitochondrial protein import receptors in yeast. *EMBO J.* *12*, 4115-4123.
- Rapaport, D. (2003). Finding the right organelle. Targeting signals in mitochondrial outer-membrane proteins. *EMBO Rep.* *4*, 948-952.
- Rapaport, D., Mayer, A., Neupert, W., and Lill, R. (1998). cis and trans sites of the TOM complex of mitochondria in unfolding and initial translocation of preproteins. *J. Biol. Chem.* *273*, 8806-8813.

- Rapaport, D., and Neupert, W. (1999). Biogenesis of Tom40, core component of the TOM complex of mitochondria. *J. Cell Biol.* *146*, 321-331.
- Rapaport, D., Neupert, W., and Lill, R. (1997). Mitochondrial protein import. Tom40 plays a major role in targeting and translocation of preproteins by forming a specific binding site for the presequence. *J. Biol. Chem.* *272*, 18725-18731.
- Rassow, J., Guiard, B., Wienhues, U., Herzog, V., Hartl, F.U., and Neupert, W. (1989). Translocation arrest by reversible folding of a precursor protein imported into mitochondria. A means to quantitate translocation contact sites. *J. Cell Biol.* *109*, 1421-1428.
- Rassow, J., Harmey, M.A., Muller, H.A., Neupert, W., and Tropschug, M. (1990). Nucleotide sequence of a full-length cDNA coding for the mitochondrial precursor protein of the beta-subunit of F1-ATPase from *Neurospora crassa*. *Nucleic Acids Res.* *18*, 4922.
- Regev-Rudzki, N., Karniely, S., Ben-Haim, N.N., and Pines, O. (2005). Yeast aconitase in two locations and two metabolic pathways: seeing small amounts is believing. *Mol. Biol. Cell* *16*, 4163-4171.
- Rehling, P., Brandner, K., and Pfanner, N. (2004). Mitochondrial import and the twin-pore translocase. *Nat. Rev. Mol. Cell Biol.* *5*, 519-530.
- Rehling, P., Model, K., Brandner, K., Kovermann, P., Sickmann, A., Meyer, H.E., Kuhlbrandt, W., Wagner, R., Truscott, K.N., and Pfanner, N. (2003). Protein insertion into the mitochondrial inner membrane by a twin-pore translocase. *Science* *299*, 1747-1751.
- Roise, D., and Schatz, G. (1988). Mitochondrial presequences. *J. Biol. Chem.* *263*, 4509-4511.
- Rojo, E.E., Guiard, B., Neupert, W., and Stuart, R.A. (1998). Sorting of D-lactate dehydrogenase to the inner membrane of mitochondria. Analysis of topogenic signal and energetic requirements. *J. Biol. Chem.* *273*, 8040-8047.
- Ryan, K.R., Leung, R.S., and Jensen, R.E. (1998). Characterization of the mitochondrial inner membrane translocase complex: the Tim23p hydrophobic domain interacts with Tim17p but not with other Tim23p molecules. *Mol. Cell Biol.* *18*, 178-187.
- Ryan, K.R., Menold, M.M., Garrett, S., and Jensen, R.E. (1994). SMS1, a high-copy suppressor of the yeast mas6 mutant, encodes an essential inner membrane protein required for mitochondrial protein import. *Mol Biol Cell* *5*, 529-538.
- Sambrook, J., Fritsch, E.F., and Maniatis, T. (1989). *Molecular Cloning: A Laboratory Manual* 2nd ed., (Cold Spring Harbor, N.Y., Cold Spring Laboratory Press).
- Sanchez-Pulido, L., Devos, D., Genevrois, S., Vicente, M., and Valencia, A. (2003). POTRA: a conserved domain in the FtsQ family and a class of beta-barrel outer membrane proteins. *Trends Biochem. Sci.* *28*, 523-526.
- Sato, T., Esaki, M., Fernandez, J.M., and Endo, T. (2005). Comparison of the protein-unfolding pathways between mitochondrial protein import and atomic-force microscopy measurements. *Proc. Natl. Acad. Sci. USA* *102*, 17999-18004.
- Schagger, H., Cramer, W.A., and von Jagow, G. (1994). Analysis of molecular masses and oligomeric states of protein complexes by blue native electrophoresis and isolation of membrane protein complexes by two-dimensional native electrophoresis. *Anal. Biochem.* *217*, 220-230.
- Schatz, G., and Dobberstein, B. (1996). Common principles of protein translocation across membranes. *Science* *271*, 1519-1526.
- Schleiff, E., Silvius, J.R., and Shore, G.C. (1999). Direct membrane insertion of voltage-dependent anion-selective channel protein catalyzed by mitochondrial Tom20. *J. Cell Biol.* *145*, 973-978.
- Schleiff, E., and Soll, J. (2005). Membrane protein insertion: mixing eukaryotic and prokaryotic concepts. *EMBO Rep.* *6*, 1023-1027.

- Schmitt, S., Ahting, U., Eichacker, L., Granvogl, B., Go, N.E., Nargang, F.E., Neupert, W., and Nussberger, S. (2005). Role of Tom5 in maintaining the structural stability of the TOM complex of mitochondria. *J. Biol. Chem.* *280*, 14499-14506.
- Schneider, H.C., Berthold, J., Bauer, M.F., Dietmeier, K., Guiard, B., Brunner, M., and Neupert, W. (1994). Mitochondrial Hsp70/MIM44 complex facilitates protein import. *Nature* *371*, 768-774.
- Schnell, D.J., and Hebert, D.N. (2003). Protein translocons: multifunctional mediators of protein translocation across membranes. *Cell* *112*, 491-505.
- Schulz, G.E. (2000). beta-Barrel membrane proteins. *Curr. Opin. Struct. Biol.* *10*, 443-447.
- Schwartz, M.P., and Matouschek, A. (1999). The dimensions of the protein import channels in the outer and inner mitochondrial membranes. *Proc. Natl. Acad. Sci. U S A* *96*, 13086-13090.
- Sherman, E.L., Go, N.E., and Nargang, F.E. (2005). Functions of the small proteins in the TOM complex of *Neurospora crassa*. *Mol. Biol. Cell* *16*, 4172-4182.
- Sherman, E.L., Taylor, R.D., Go, N.E., and Nargang, F.E. (2006). Effect of mutations in Tom40 on stability of the translocase of the outer mitochondrial membrane (TOM) complex, assembly of Tom40, and import of mitochondrial preproteins. *J. Biol. Chem.* *281*, 22554-22565.
- Sichting, M., Mokranjac, D., Azem, A., Neupert, W., and Hell, K. (2005). Maintenance of structure and function of mitochondrial Hsp70 chaperones requires the chaperone Hep1. *EMBO J.* *24*, 1046-1056.
- Sickmann, A., Reinders, J., Wagner, Y., Joppich, C., Zahedi, R., Meyer, H.E., Schonfisch, B., Perschil, I., Chacinska, A., Guiard, B., *et al.* (2003). The proteome of *Saccharomyces cerevisiae* mitochondria. *Proc. Natl. Acad. Sci. USA* *100*, 13207-13212.
- Sikorski, R.S., and Hieter, P. (1989). A system of shuttle vectors and yeast host strains designed for efficient manipulation of DNA in *Saccharomyces cerevisiae*. *Genetics* *122*, 19-27.
- Slutsky-Leiderman, O., Marom, M., Iosefson, O., Levy, R., Maoz, S., and Azem, A. (2007). The interplay between components of the mitochondrial protein translocation motor studied using purified components. *J. Biol. Chem. Epub. Sep.* *19*.
- Soll, J., and Schleiff, E. (2004). Protein import into chloroplasts. *Nat. Rev. Mol. Cell. Biol.* *5*, 198-208.
- Souza, R.L., Green-Willms, N.S., Fox, T.D., Tzagoloff, A., and Nobrega, F.G. (2000). Cloning and characterization of COX18, a *Saccharomyces cerevisiae* PET gene required for the assembly of cytochrome oxidase. *J. Biol. Chem.* *275*, 14898-14902.
- Stuart, R. (2002). Insertion of proteins into the inner membrane of mitochondria: the role of the Oxa1 complex. *Biochim. Biophys. Acta* *1592*, 79.
- Stuart, R.A., Gruhler, A., van der Klei, I., Guiard, B., Koll, H., and Neupert, W. (1994). The requirement of matrix ATP for the import of precursor proteins into the mitochondrial matrix and intermembrane space. *Eur. J. Biochem. / FEBS* *220*, 9-18.
- Szyrach, G., Ott, M., Bonnefoy, N., Neupert, W., and Herrmann, J.M. (2003). Ribosome binding to the Oxa1 complex facilitates co-translational protein insertion in mitochondria. *EMBO J.* *22*, 6448-6457.
- Tamm, L.K., Arora, A., and Kleinschmidt, J.H. (2001). Structure and assembly of beta-barrel membrane proteins. *J. Biol. Chem.* *276*, 32399-32402.
- Tamura, Y., Harada, Y., Yamano, K., Watanabe, K., Ishikawa, D., Ohshima, C., Nishikawa, S., Yamamoto, H., and Endo, T. (2006). Identification of Tam41 maintaining integrity of the TIM23 protein translocator complex in mitochondria. *J. Cell Biol.* *174*, 631-637.
- Taylor, S.W., Fahy, E., and Ghosh, S.S. (2003). Global organellar proteomics. *Trends Biotech.* *21*, 82-88.

- Terziyska, N., Grumbt, B., Bien, M., Neupert, W., Herrmann, J.M., and Hell, K. (2007). The sulfhydryl oxidase Erv1 is a substrate of the Mia40-dependent protein translocation pathway. *FEBS Lett.* *581*, 1098-1102.
- Terziyska, N., Lutz, T., Kozany, C., Mokranjac, D., Mesecke, N., Neupert, W., Herrmann, J.M., and Hell, K. (2005). Mia40, a novel factor for protein import into the intermembrane space of mitochondria is able to bind metal ions. *FEBS Lett.* *579*, 179-184.
- Truscott, K.N., Kovermann, P., Geissler, A., Merlin, A., Meijer, M., Driessen, A.J., Rassow, J., Pfanner, N., and Wagner, R. (2001). A presequence- and voltage-sensitive channel of the mitochondrial preprotein translocase formed by Tim23. *Nat. Struct. Biol.* *8*, 1074-1082.
- Truscott, K.N., Voos, W., Frazier, A.E., Lind, M., Li, Y., Geissler, A., Dudek, J., Muller, H., Sickmann, A., Meyer, H.E., *et al.* (2003). A J-protein is an essential subunit of the presequence translocase-associated protein import motor of mitochondria. *J. Cell Biol.* *163*, 707-713.
- Tzagoloff, A., and Myers, A.M. (1986). Genetics of mitochondrial biogenesis. *Annu. Rev. Biochem.* *55*, 249-285.
- Ungermann, C., Guiard, B., Neupert, W., and Cyr, D.M. (1996). The delta psi- and Hsp70/MIM44-dependent reaction cycle driving early steps of protein import into mitochondria. *EMBO J.* *15*, 735-744.
- Ungermann, C., Neupert, W., and Cyr, D.M. (1994). The role of Hsp70 in conferring unidirectionality on protein translocation into mitochondria. *Science* *266*, 1250-1253.
- van der Laan, M., Chacinska, A., Lind, M., Perschil, I., Sickmann, A., Meyer, H.E., Guiard, B., Meisinger, C., Pfanner, N., and Rehling, P. (2005). Pam17 is required for architecture and translocation activity of the mitochondrial protein import motor. *Mol. Cell Biol.* *25*, 7449-7458.
- van Loon, A.P., Brandli, A.W., and Schatz, G. (1986). The presequences of two imported mitochondrial proteins contain information for intracellular and intramitochondrial sorting. *Cell* *44*, 801-812.
- van Wilpe, S., Ryan, M.T., Hill, K., Maarse, A.C., Meisinger, C., Brix, J., Dekker, P.J., Moczko, M., Wagner, R., Meijer, M., *et al.* (1999). Tom22 is a multifunctional organizer of the mitochondrial preprotein translocase. *Nature* *401*, 485-489.
- Vasiljev, A., Ahting, U., Nargang, F.E., Go, N.E., Habib, S.J., Kozany, C., Panneels, V., Sinning, I., Prokisch, H., Neupert, W., *et al.* (2004). Reconstituted TOM core complex and Tim9/Tim10 complex of mitochondria are sufficient for translocation of the ADP/ATP carrier across membranes. *Mol. Biol. Cell* *15*, 1445-1458.
- Vestweber, D., and Schatz, G. (1989). DNA-protein conjugates can enter mitochondria via the protein import pathway. *Nature* *338*, 170-172.
- Von Heijne, G. (1990). Protein targeting signals. *Curr. Opin. Cell Biol.* *2*, 604-608.
- Voos, W., Gambill, B.D., Guiard, B., Pfanner, N., and Craig, E.A. (1993). Presequence and mature part of preproteins strongly influence the dependence of mitochondrial protein import on heat shock protein 70 in the matrix. *J. Cell Biol.* *123*, 119-126.
- Voulhoux, R., Bos, M.P., Geurtsen, J., Mols, M., and Tommassen, J. (2003). Role of a highly conserved bacterial protein in outer membrane protein assembly. *Science* *299*, 262-265.
- Wach, A., Brachat, A., Alberti-Segui, C., Rebischung, C., and Philippsen, P. (1997). Heterologous HIS3 marker and GFP reporter modules for PCR-targeting in *Saccharomyces cerevisiae*. *Yeast* *13*, 1065-1075.
- Waizenegger, T., Habib, S.J., Lech, M., Mokranjac, D., Paschen, S.A., Hell, K., Neupert, W., and Rapaport, D. (2004). Tob38, a novel essential component in the biogenesis of beta-barrel proteins of mitochondria. *EMBO Rep.* *5*, 704-709.
- Waizenegger, T., Schmitt, S., Zivkovic, J., Neupert, W., and Rapaport, D. (2005). Mim1, a protein required for the assembly of the TOM complex of mitochondria. *EMBO Rep.* *6*, 57-62.

- Walter, P., and Lingappa, V.R. (1986). Mechanism of protein translocation across the endoplasmic reticulum membrane. *Annu. Rev. Cell Biol.* 2, 499-516.
- Waltner, M., and Weiner, H. (1995). Conversion of a nonprocessed mitochondrial precursor protein into one that is processed by the mitochondrial processing peptidase. *J. Biol. Chem.* 270, 26311-26317.
- Webb, C.T., Gorman, M.A., Lazarou, M., Ryan, M.T., and Gulbis, J.M. (2006). Crystal structure of the mitochondrial chaperone TIM9.10 reveals a six-bladed alpha-propeller. *Mol. Cell* 21, 123-133.
- Werhahn, W., and Braun, H.P. (2002). Biochemical dissection of the mitochondrial proteome from *Arabidopsis thaliana* by three-dimensional gel electrophoresis. *Electrophoresis* 23, 640-646.
- Westermann, B., and Neupert, W. (1997). Mdj2p, a novel DnaJ homolog in the mitochondrial inner membrane of the yeast *Saccharomyces cerevisiae*. *J. Mol. Biol.* 272, 477-483.
- Westermann, B., Prip-Buus, C., Neupert, W., and Schwarz, E. (1995). The role of the GrpE homologue, Mge1p, in mediating protein import and protein folding in mitochondria. *EMBO J.* 14, 3452-3460.
- Wiedemann, N., Kozjak, V., Chacinska, A., Schonfisch, B., Rospert, S., Ryan, M.T., Pfanner, N., and Meisinger, C. (2003). Machinery for protein sorting and assembly in the mitochondrial outer membrane. *Nature* 424, 565-571.
- Wiedemann, N., Truscott, K.N., Pfannschmidt, S., Guiard, B., Meisinger, C., and Pfanner, N. (2004). Biogenesis of the protein import channel Tom40 of the mitochondrial outer membrane: intermembrane space components are involved in an early stage of the assembly pathway. *J. Biol. Chem.* 279, 18188-18194.
- Wienhues, U., Becker, K., Schleyer, M., Guiard, B., Tropschug, M., Horwich, A.L., Pfanner, N., and Neupert, W. (1991). Protein folding causes an arrest of preprotein translocation into mitochondria in vivo. *J. Cell Biol.* 115, 1601-1609.
- Wimley, W.C. (2003). The versatile beta-barrel membrane protein. *Curr. Opin. Struct. Biol.* 13, 404-411.
- Wu, T., Malinverni, J., Ruiz, N., Kim, S., Silhavy, T.J., and Kahne, D. (2005). Identification of a multicomponent complex required for outer membrane biogenesis in *Escherichia coli*. *Cell* 121, 235-245.
- Wu, Y., and Sha, B. (2006). Crystal structure of yeast mitochondrial outer membrane translocon member Tom70p. *Nat. Struct. Mol. Biol.* 13, 589-593.
- Yamamoto, H., Esaki, M., Kanamori, T., Tamura, Y., Nishikawa, S., and Endo, T. (2002). Tim50 is a subunit of the TIM23 complex that links protein translocation across the outer and inner mitochondrial membranes. *Cell* 111, 519-528.
- Yamamoto, H., Momose, T., Yatsukawa, Y., Ohshima, C., Ishikawa, D., Sato, T., Tamura, Y., Ohwa, Y., and Endo, T. (2005). Identification of a novel member of yeast mitochondrial Hsp70-associated motor and chaperone proteins that facilitates protein translocation across the inner membrane. *FEBS Lett.* 579, 507-511.
- Ye, Y., Shibata, Y., Kikkert, M., van Voorden, S., Wiertz, E., and Rapoport, T.A. (2005). Inaugural Article: Recruitment of the p97 ATPase and ubiquitin ligases to the site of retrotranslocation at the endoplasmic reticulum membrane. *Proc. Natl. Acad. Sci. USA* 102, 14132-14138.
- Ye, Y., Shibata, Y., Yun, C., Ron, D., and Rapoport, T.A. (2004). A membrane protein complex mediates retro-translocation from the ER lumen into the cytosol. *Nature* 429, 841-847.
- Young, J.C., Hoogenraad, N.J., and Hartl, F.U. (2003). Molecular chaperones Hsp90 and Hsp70 deliver preproteins to the mitochondrial import receptor Tom70. *Cell* 112, 41-50.

ABBREVIATIONS

α	antibody
AAC	ADP/ATP carrier
Ab	antibody
ADP	adenosine diphosphate
<i>A. gossypii</i>	<i>Ashbiya gossypii</i>
Amp	ampicillin
APS	ammonium peroxodisulfate
APT	aminopterin
ATP	adenosine triphosphate
ATPase	adenosine triphosphatase
b_2	cytochrome b_2
b_2	precursor protein for <i>in vivo</i> saturation of the TIM23 complex consisting of the N-terminal 167 amino acid residues of yeast cytochrome b_2 fused to mouse full length DHFR
$b_2\Delta$	precursor protein for <i>in vivo</i> saturation of the TIM23 complex consisting of the N-terminal 167 amino acid residues of yeast cytochrome b_2 with deletion of the hydrophobic sorting signal fused to mouse full length DHFR
BN-PAGE	blue native polyacrylamide gel electrophoresis
BSA	bovine serum albumin
C-	carboxy-
<i>C. albicans</i>	<i>Candida albicans</i>
CBB	coomassie brilliant blue
cDNA	complementary DNA
<i>C. elegans</i>	<i>Caenorhabditis elegans</i>
CNBr	cyanogen bromide
Cox5a	precursor to yeast cytochrome c oxidase subunit Va
<i>cox5a</i>	precursor protein for <i>in vivo</i> saturation of the TIM23 complex consisting of yeast subunit Va of cytochrome c oxidase and mouse full length DHFR
<i>cox5a</i> Δ TM	precursor protein for <i>in vivo</i> saturation of the TIM23 complex consisting of yeast subunit Va of cytochrome c oxidase and mouse full length DHFR with deletion of the hydrophobic sorting signal
CV	column volume
DFDNB	1,5-difluoro-2,4-dinitrobenzene
DHFR	dihydrofolate reductase
DMSO	dimethylsulfoxid
DNA	deoxyribonucleic acid
dNTP	deoxyribonucleoside triphosphate
DLD	D-lactate dehydrogenase
<i>D. melanogaster</i>	<i>Drosophila melanogaster</i>
DSG	disuccinimidyl glutarate
DSS	disuccinimidyl suberate
DTT	dithiotreitol
$\Delta\Psi$	membrane potential
<i>E. coli</i>	<i>Escherichia coli</i>

EDTA	ethylenediamine tetraacetate
F1 β	F1 β subunit of the ATP synthase
gDNA	genomic DNA
GIP	general import pore
HA	Haemagglutinin
HEPES	N-2 hydroxyl piperazine-N'-2-ethane sulphonic acid
His	histidine
<i>H. sapiens</i>	<i>Homo sapiens</i>
Hsp	heat shock protein
IgG	immunoglobuline G
IM	inner membrane
Imp	inner membrane peptidase
IMS	intermembrane space
IPTG	isopropyl- β ,D-thiogalactopyranoside
KAN	kanamycin
kDa	kilodalton
LB	Luria Bertani
MBP	maltose binding protein
MOPS	N-morpholinopropane sulphonic acid
MPP	mitochondrial processing peptidase
MTS	matrix targeting signal
MTX	methotrexate
N-	amino-
<i>N. crassa</i>	<i>Neurospora crassa</i>
NADH	nicotine amide adenine dinucleotide
NADPH	nicotine amide adenine dinucleotide phosphate
Ni-NTA	nickel-nitrilo triacetic acid
NMR	nuclear magnetic resonance
OD _x	optical density at x nm
OM	outer membrane
Oxa	oxidase assembly
PAGE	polyacrylamide gel electrophoresis
PAS	protein A-Sepharose
PCR	polymerase chain reaction
PEG	polyethylene glycol
PI	preimmune serum
PK	proteinase K
PMSF	phenylmethylsulfonyl fluoride
Preprotein	precursor protein
ProtA	Protein A
PUR	mitochondria isolated from puromycin treated cells
PVDF	polyvinylidene difluoride
RNA	ribonucleic acid
RNasin	ribonuclease inhibitor
RT	room temperature
<i>S. cerevisiae</i>	<i>Saccharomyces cerevisiae</i>
SDS	sodium dodecyl sulfate
STD	mitochondria isolated under standard conditions
TBS	TRIS buffered saline
TCA	trichloroacetic acid
TEMED	N,N,N',N'-tetramethylene diamine

TIM	translocase of the inner mitochondrial membrane
TOB	translocase of outer membrane β -barrel proteins
TOM	translocase of the outer mitochondrial membrane
Tris	tris-(hydroxymethyl)-aminomethane
TX-100	Triton X-100
v/v	volume per volume
<i>X. tropicalis</i>	<i>Xenopus tropicalis</i>
w/v	weight per volume
WT	wild type

Publications resulting from this thesis

Popov-Čeleketić, D., Mapa, K., Neupert, W., Mokranjac, D. Active remodeling of the TIM23 complex during translocation of preproteins into mitochondria. *In submission*.

Mokranjac, D.*, Popov-Čeleketić, D.*, Hell, K., and Neupert, W. (2005). Role of Tim21 in mitochondrial translocation contact sites. *J. Biol. Chem.* 280, 23437-23440.

*These authors equally contributed to this publication.

Mokranjac, D., Sichtung, M., Popov-Čeleketić, D., Berg, A., Hell, K., and Neupert, W. (2005). The import motor of the yeast mitochondrial TIM23 preprotein translocase contains two different J proteins, Tim14 and Mdj2. *J. Biol. Chem.* 280, 31608-31614.

ACKNOWLEDGEMENTS

Rruner riv and this is the end my only friend at least of this PhD work so thank you all who were there when necessary first and foremost Prof. Walter Neupert for accepting me in his lab putting up with me for all these years and actively working on the formation of my scientific mindframe while resisting almost irresistible temptation of firing someone opposite in some of his scientific ethical and political points of view and accepting the confrontation of homo faber vs homo ludens even if that meant almost drowning in the cold mountain river and I would also like to thank Prof. Jürgen Soll for kindly accepting to act as my mentor at the Faculty of Biology Ludwig-Maximilians-Universität in Munich where it is intended for me to defend this thesis stuck in the position I would hardly get into without the help of Helga Döge and Christine Werner who were clearing all the bureaucratic obstacles along the way my direct supervisor Dejana Mokranjac made big contribution to the completion of this thesis from the first crosslinking experiments in the spring of 2004 to formatting of this text in the fall 2007 especially during identification of Tim21 with huge amounts of scientific and other discussions in between yes we never lacked the words that I also shared with Kai Hell who was my first group leader and who has always had this beautiful feature of letting students develop their ideas while playing devil's advocate in my understanding of how a supervisor should treat his students both Dejana and Kai equally contributed whereas my bench mate Koyeli Mapa was the reason why silence was the heart of music sharing with me the good experiments the bad results and the ugly problems we were encountering during the LEM project which would not be successfully finished in its final form without her experiments with Pam17 donating important pieces of the puzzle that I finally articulated as the LEM model based on experiments I performed with mitochondria most of the time prepared by Marica Malešić and various buffers solutions and sera prepared mostly by Heiko Germeroth who is above all a decent human being like all other colleagues from the Neupert lab to whom I owe one huge thank you my droogy Igor for sharing interesting brainburning obscure part of science with me Andreja for the discussions and frantic friendship three girls Barbara Nadia and Silvia each for the special reasons Shukry my fitness trainer and spiritual guide sometimes Zdenka for taking special care as well as others who made this journey more interesting Doron Thomas Stephane Carsten Christian Iris Max Marcel my family my father Djordje who made me fly to Turkey and all my friends Bane Lana Mala Mića Žarko Areti Talija Marko and many more from Belgrade Munich and all four corners of the world thank you.

My deepest gratitude goes to my mother Dušica and my grandmother Smilja for the unconditional love and support and my grandfather Čedomir who was the main responsible for building my character.

This work is dedicated to my wife Jelena and our son who will be born soon. Bez vas ništa ne bi imalo smisla.

D.

Munich, 4. 11. 2007

Curriculum Vitae

Dušan Popov-Čeleketić

- 27.02.1977 Born in Belgrade, Serbia
- 1984-1992 Elementary school "Radoje Domanović", Belgrade
- 1992-1996 X Belgrade Gimnasium "Mihailo Pupin", Belgrade
- 1996-2002 Studies of Biochemistry at the Faculty of Chemistry, University of Belgrade
- 2002-2004 Research Assistant in the Institute of Nuclear Sciences "Vinča", Belgrade
- 2004-2007 PhD research in the laboratory of Prof. Dr. Dr. Walter Neupert at the Adolf-Butenandt-Institut für Physiologische Chemie, Ludwig-Maximilians-Universität München